PHOSPHORUS DYNAMICS IN SHELF SEAS

Thesis submitted in accordance with the requirements of the University of Liverpool for the degree of Doctor in Philosophy

By

Clare Elizabeth Davis

Department of Earth and Ocean Sciences

University of Liverpool

June 2012

ABSTRACT

Phosphorus dynamics in shelf seas

Clare E. Davis

Shelf seas are highly productive regions of the world's ocean. Contributing 16 - 30 % to global ocean carbon fixation while representing a mere 7 % of the area, their importance in the carbon cycle is disproportionate to their size. This high productivity has economical significance, supporting over 90 % of global fishery yields (Pauly et al., 2002). Shelf seas are also physically dynamic regions. On an annual cycle, the water column in shelf seas is fully mixed in winter and thermally stratified in summer in deeper regions, with enhanced mixing along the shelf edge. In addition, shelf seas act as a buffer between the land and coastal seas, and the open ocean. However, the processes that transform nutrients within the shelf sea are poorly understood. More so, the role of physical processes in both transporting nutrients, as well as their interaction with the biological processes that govern nutrient concentrations and partitioning are currently unresolved.

Here, nutrient dynamics, with a specific focus on phosphorus, were assessed within the Celtic Sea, part of the northwest European shelf. The distribution and partitioning of phosphorus between the particulate (PPhos) and dissolved organic (DOP) and inorganic (DIP) phases was determined over various temporal and spatial scales. The concentration of labile DOP (phosphomonoesters, PME) and its rate of turnover were determined using enzyme rate assays. The microbes involved in PME hydrolysis were identified using enzyme labelled fluorescence techniques. The influence of physical processes, including spring-neap tidal cycle, mixing over topography and storm enhanced mixing on the vertical distribution of phosphorus in the water column were also assessed.

DOP accumulated in the surface layer of the thermally stratified shelf waters and at the shelf edge. DOP production was enhanced at the shelf edge and during storm events due to enhanced mixing and fluxes of phosphate, which were rapidly shunted into the DOP pool through enhanced primary production. However, during mixing there was a counteracting downward flux of DOP exported to the bottom waters. Profiles

of PME concentrations revealed a relatively labile component to bottom layer DOP, which had turnover times in the order of days.

Comparison of observations in the Celtic Sea and Porcupine Bank region demonstrated that the accumulation of DOP on the shelf and at the shelf edge relative to the adjacent slope and oceanic regions is a persistent feature of the western European continental margin. Through a number of shelf-edge exchange processes, including wind mixing on short time scales, tidal mixing on fortnightly timescales and seasonal winter mixing, the Celtic Sea was identified as a potential source of DOP to the North Atlantic, where production is thought to be phosphorus limited (Mather et al., 2008).

I certify that the work described in this thesis is my own except where otherwise stated and has not previously been submitted for any degree at this or any other University.

Clare E. Davis

ACKNOWLEDGEMENTS

I would like to start by thanking my family; Mum, Dad, Katherine and Chris for their enduring love, support and encouragement during the deceptively long past 'few' years.

I am indebted to my supervisors, Claire, George and Jonathan who have been as supportive as they are knowledgeable. Claire this thesis would not have been possible without you. It has been quite a long, eventful and occasionally trying time. I'm thankful and surprised that your patience and faith in me haven't faltered (that I know of). You have always acted in my best interests and continually gave up your valuable time to help me. It has always been, and still is, very much appreciated. Thank you for humouring my predicted hand-in dates, or at least pretending to – and thanks for the diary, I plan to start using it any day now!

Despite the much appreciated help from my supervisors, I am also very grateful to Matthew Palmer and Jo Hopkins of NOCL, Linda Gilpin of Napier University, Anna Hickman of Essex University and Anouska Panton of the University of Liverpool for their help, data and much more. Thank you to Anu and Carmel for their support and guidance with lab work and their saint-like patience when I contaminated/broke equipment. I would also like to thank all the lecturers in the Ocean Sciences department, particularly Harry for his unfaltering support since supervising me during my undergraduate days.

Another massive thank you must go to Paula. You have been like a fourth supervisor these past years. I am certain that without your help I would never have got this far. Your wisdom with finances and forms, and your friendship have saved me from falling at various hurdles more often than I can say.

I would like to thank all of my friends for the continued support, tolerance, pep-talks, and distractions they have offered over recent years, particularly during the tougher times. Special thanks go to Nelson, Kat, Sarah, Ed, Nick, Holly and Fiona for always having the right words at the right time, and failing that, having the right drink. Thanks to my PhD colleagues Nuala, Nick and Lucy who I feel very fortunate to also call friends. And especially Charlotte, there are so many things I am grateful to you for, I just hope you already know. You are all science idols in my eyes. And huge thanks to Joe and Amelia for adopting me. I love you guys, you're my best friends and I would be lost without you all of you. Oopsy daisy, I almost forgot Caz.

I would never have got this far without tea.

DEDICATION

I would like to dedicate my thesis to two dearly loved and greatly missed people: my granny Yorkie and my good friend Phil.

Phil, I know you would have been proud that I managed to stay at university for almost a decade and equally impressed that I actually did some work while I was there.

CONTENTS

TABLE OF CONTENTS

LIST OF FIGURES

LIST OF TABLES

1. INTRODUCTION

1. Introduction

Shelf seas act as a natural buffer between terrestrial and oceanic systems. Their high productivity makes them economically important through supporting fisheries and they also play an important biogeochemical role in the global carbon cycle.

The Celtic Sea forms part of the extensive northwest European shelf sea. As winter N:P ratios are below Redfield ratio (14; Hydes et al., 2004) and are lower than those found at the shelf break (15.9; Gowen et al., 2008), production in the Celtic Sea is presumed to be nitrogen limited, thus previous studies in this region have largely focused on inorganic nitrogen dynamics. Few studies have taken account of organic nutrients or phosphorus which is in excess of nitrogen relative to the Redfield ratio (Redfield et al., 1963). However, like nitrogen, phosphorus (P) is also an essential macronutrient. Phosphorus is delivered to shelf seas via rivers and winter recharge and is regenerated internally through particulate and dissolved organic remineralisation.

Shelf sea exchange is an important export pathway of terrestrial and coastally derived carbon. With high phosphorus inputs to a nitrogen limited system, could the Celtic Sea also potentially act as a source of phosphorus to the North Atlantic, where production is considered phosphorus-limited (Mather et al., 2008)? To answer this question a greater understanding of shelf sea processes and phosphorus dynamics in the Celtic Sea is required.

1.1. An introduction to shelf seas

1.1.1. Shelf sea processes and physical mixing

Continental shelf seas are shallow regions of the global ocean, typically in close proximity to land and not exceeding 200m water depth. In terms of ocean carbon storage, their importance is disproportionate to their size. Extrapolated from North Sea data, coastal regions and shelf seas account for 16-30 % of total ocean uptake of anthropogenic CO_2 (Thomas et al., 2004). The key concept behind this efficient carbon drawdown is known as 'shelf sea pumping'. This consists of a number of different mechanisms, including generous nutrient loading and efficient use, but the most significant is seasonal stratification of deeper regions of shelf seas accompanied by a subsurface chlorophyll maximum (SCM; e.g. Sharples et al., 2001).

Stratification occurs when solar driven thermal buoyancy forcing at the surface, which favours stratification, overcomes tidally driven stirring and mixing processes caused by interaction with the bed. In regions of shelf seas where water depth is sufficient, thermal stratification dominates during the spring-autumn period. At the onset and breakdown of stratification, phytoplankton blooms occur in response to the alleviation of light limitation and the supply of new nutrients from below the thermocline, respectively. In the intervening period, subsurface chlorophyll maxima (SCM) associated with the thermocline contribute significantly to new production throughout summer stratification (e.g. Rippeth, 2005; Rippeth et al., 2009). Over the course of the stratified period, the SCM can contribute an equivalent carbon drawdown as the spring bloom. The SCM is sustained by a diapycnal source of nutrients from the deep water below the thermocline and is often closely associated with the nutricline (Sharples et al., 2001a; Sharples, 2008). The mechanisms responsible for the variability of this nutrient flux are complex and are still not fully understood. However, many studies agree that internal tide dissipation and inertial oscillation-induced shear stresses are important processes.

Internal tides

Dissipation of tidal energy can enhance the upward inorganic nutrient flux across the thermocline with a phase lag of the order of hours (Sharples et al., 2001). Another important aspect of mixing in shelf seas is that of internal tides. Internal tidal waves can be initiated when a stratified tidal flow encounters a sudden irregularity in bottom topography, i.e. a hydraulic force (Sharples and Tett, 1994). The result, if linear, is an internal wave travelling along the pycnocline with a wavelength of the order of 10 km. Alternatively, if the response is non-linear, packets of high frequency solitons with wavelengths of the order of 1 km may propagate away from the source. Such internal waves occur at the continental shelf break and can potentially enhance vertical mixing 10-100 km inshore of the shelf break (Rippeth, 2005). In these regions, internal tides are the dominant mechanism driving diapycnal nutrient fluxes across the thermocline (Sharples et al, 2001).

Spring tidal currents can be significantly stronger than those of neap tides, increasing the potential energy available for mixing by as much as eight times. As such, spring-neap modulation of stratification and mixing is an important consideration, particularly when predicting the onset of stratification. For example, spring tidal currents may enhance mixing sufficiently to delay the onset of stratification until the following neap tide. The timing of the spring bloom may therefore vary which can have significant implications for various trophic levels in the food web. Indeed, there is a notable spring-neap modulation of internal tidal waves within the main stratified region of the Celtic Sea where topographic features, such as Jones Bank, can initiate internal tidal waves during spring tides. Accompanying this is a spring-neap modulation of export from the thermocline, as stronger tidal currents during spring tides act to enhance entrainment from the thermocline to the deep water relative to neap tides (Sharples et al., 2001; Sharples, 2008).

Inertial oscillations

Baroclinic near-inertial oscillations or inertial currents generally refer to circular motions of currents in the surface mixed layer. The trigger mechanism is an abrupt change in wind direction and the result is an

enhancement of shear at the thermocline as the bottom water will not be moving in the same manner. Such oscillations dissipate over a period of a few days, during which time they can contribute significantly to turbulent mixing across the thermocline (depending on their initial magnitude; Rippeth, 2005; Rippeth et al., 2009). Such wind-induced changes in turbulence are important in weakening the thermocline barrier to the vertical flux of nutrients from deep water (Sharples and Tett, 1994). Like internal tides their strength varies across the shelf sea environment, but unlike internal tides, which have a reasonably predictable nature, inertial oscillations are episodic.

Simpson et al. (1996) identified a midwater source of turbulent kinetic energy (TKE) in stratified regions and suggested that this was the reason models were underestimating tidal energy dissipation in stratified shelf seas (Simpson et al., 1996). It is now thought that a combination of the decay of internal tides and near-inertial oscillation-induced shear instabilities at the thermocline may account for this midwater source of TKE and enhanced dissipation. The result is stratified turbulence within the water column (Simpson et al. 1996).

1.1.2. Nutrient fluxes across the thermocline

Turbulent mixing of nutrients across the thermocline in seasonally stratified zones of shelf seas enhances the shelf sea pump and CO_2 storage. As already discussed, the SCM is maintained by diapycnal mixing of nutrients across the thermocline, which is often coincident with the nutricline. Sharples et al. (2001) calculated the vertical flux of nitrate in the Western English Channel as:

$$nitrate\ flux = -K_z\left(\frac{\Delta N}{\Delta z}\right)\ [mmol\ N\ m^{-2}\ s^{-1}],$$

where ΔN is the difference between surface and bottom mixed layer NO_3^- concentrations, Δz is the thickness of the nitracline (maximum gradient in concentration), and K_z is the vertical eddy viscosity which can be obtained from free-fall turbulent profile data, such as that obtained by Fast Light

Yoyo (FLY) free fall instrument or Vertical Micro- structure Profiler (VMP) microstructure profilers (Sharples et al., 2001). As diapycnal mixing of nitrate into the surface waters is in essence a 'new' nutrient source (Dugdale and Goering, 1967), production at the SCM resulting from this flux is therefore 'new' production and a positive carbon drawdown mechanism (e.g. Rippeth et al., 2009).

Intuitively, a downward flux of surface mixed layer and thermocline water must counter the upward flux of deep water and inorganic nutrients (e.g. Vidal et al., 1999). This flux is the primary export of carbon from the photic zone to the deep water where it contributes to ocean carbon storage (Rippeth, 2005). In the open ocean, the time-averaged exported quantities of organic matter are typically of similar order to the vertical upward inorganic nutrient flux (Eppley and Peterson, 1979). However, the intricacies of dissolved organic matter export will be discussed further in a later section.

1.1.3. Phytoplankton in the subsurface chlorophyll maximum (SCM)

Subsurface chlorophyll maxima are associated with the thermocline and nutricline in shelf seas. This concentration of primary producers is thought to arise through enhanced phytoplankton survival. Turbulence in the thermocline is minimal in comparison to the water column en masse. As such, phytoplankton in the thermocline are less likely to be entrained into the nutrient-depleted wind-mixed surface layer or the nutrient-rich but light-deficient tidally-mixed bottom water (Ross and Sharples, 2007). At the thermocline the diapycnal nutrient flux from deep combined with the positioning at adequate light levels for photosynthesis allows phytoplankton to survive and grow successfully (Sharples et al., 2001).

A study in the Celtic Sea found the nutrient flux across the thermocline was steady enough to allow *in situ* phytoplankton growth in layers relative to different light and nutrient niches. *Synechococcus* dominate SCM biomass and typically occupy the upper levels of the chlorophyll maxima, with increasing abundance of picoeukaryotes with depth through the SCM (Hickman et al., 2009). Thus, there is selection resulting in taxonomic composition adaptation (Hobson and Lorenzen, 1972; Moore et al., 2009).

Vertically within the water column structure, phytoplankton may acclimate to varying light availability to enhance their competitive photosynthetic edge and improve their chances of survival (Moore et al., 2006). As a result of photoacclimation of species within the thermocline, it is highly possible that the chlorophyll maximum is distinct and occurs at a different depth to the phytoplankton biomass maxima (Fennel and Boss, 2003). In regions of such low turbulence, motile species, such as dinoflagellates and sometimes coccolithophores, are more adept to compete with non-motile phytoplankton species that would otherwise be more successful competitors for nutrients in more turbulent environments (Ross and Sharples, 2007).

Zooplankton grazing in shelf seas is seasonally variable. During summer stratification, grazing is focused on the SCM while at the onset of stratification breakdown, grazing is concentrated in the surface mixed layer. Studies seem to suggest a dominance of microzooplankton (Hobson and Lorenzen, 1972). This may also relate to the dominant zooplankton species and the stage of life cycle of the dominant grazing group (Townsend et al., 1984). In well-mixed water columns in the Irish Sea zooplankton diel migration is apparent, while during times of stratification and the formation of SCM, zooplankton are closely associated with the chlorophyll maxima and do not appear to migrate from that pycnocline (Scrope-Howe and Jones, 1986). If zooplankton grazing is concentrated at the SCM during the summer, then dissolved and particulate matter flux to below the thermocline may be enhanced due to release from sloppy feeding, entrainment during migration and faecal pellet particle aggregation and sinking (Carlson, 2002). The level of degradation that organic matter has undergone before export will influence the efficiency of the shelf sea pump in terms of carbon drawdown (aged organic matter is typically C-rich relative to nitrogen and phosphorus). Relatively fresh organic matter would suffice as a source of nitrogen and phosphorus, as well as carbon, and thus may be a suitable substrate choice for bacteria and enhance bacterial production and remineralisation. Alternatively, the organic matter may be mixed back into the thermocline before degradation where it may fuel primary production (Hopkinson and Vallino, 2005).

1.2. Dissolved organic matter (DOM)

Dissolved organic matter (DOM) is a relatively broad term applied to a large group of dissolved organic molecules that are produced throughout the food web. DOM is primarily comprised of dissolved organic carbon (DOC), nitrogen (DON) and phosphorus (DOP; Sarmiento and Gruber, 2006). For example the DOC pool includes compounds such as carbohydrates; the DON pool includes compounds such as urea and dissolved combined amino acids; and the DOP pool includes compounds such as DNA, phosphoesters and phospholipids. DOM constitutes one of the largest carbon reservoirs in the ocean, contributing 80-90% of total organic matter in marine environments (Kepkay, 1994). With a typical C:N:P ratio of 300:25:1, oceanic DOM can prove a very efficient export of organic carbon from the surface waters to the deep ocean (Hopkinson et al., 1997; Hopkinson and Vallino, 2005).

DOM is a substrate for heterotrophic bacterial growth and can also be accessed by autotrophs after hydrolysis facilitated by associated ectoenzymes to meet nutritional requirements when inorganic nutrients are depleted. DOM released by phytoplankton is rapidly assimilated by bacteria, which in turn are grazed by heterotrophic flagellates. The subsequent grazing of flagellates by microzooplankton results in further release of DOM and inorganic nutrients and the microbial loop is completed (Azam et al., 1983). Generally, it is refractory (i.e. chemically stable and resistant to further degradation) DOM which cannot be accessed by microbes that is exported to the deep ocean interior and acts as a carbon sink. It is important to consider biogeochemical processes when assessing carbon export from productive surface waters as they inherently affect the lability and thus the reactivity and bioavailability of DOM (Carlson, 2002). The following discussion of processes affecting DOM cycling will be directed towards shelf seas and coastal environments where appropriate.

1.2.1. Origins of DOM

Dissolved organic matter is biologically derived and produced in the euphotic zone with net production resulting from a decoupling of *in situ*

production and consumption (Hopkinson et al., 1997). Such a decoupling is common during bloom events and has been observed during the summer in the Baltic Sea (Zweifel et al., 1995), the Northwest Mediterranean (Copin-Montegut and Avril, 1993), and the Sargasso Sea (Carlson et al., 1994) and after a spring bloom in South Ross Sea (Carlson et al., 2000). Given its biological origins, the production of DOM is strongly regulated by primary production. The main sources of DOM in the ocean are extracellular phytoplankton production (active overflow related to photosynthetic rate or passive diffusion related to phytoplankton biomass), DOM production induced by zooplankton grazing (prey fragmentation/sloppy feeding, excretion and diffusion), cell lysis and viral lysis, bacterial lysis, solubilisation of particles (through bacterial ectoenzyme concentration on aggregate surfaces) and bacterially derived DOM (direct release as hydrolytic enzymes or transformation of HMW DOM to LMW DOM; Carlson, 2002). DOM produced *in situ* by plankton is usually labile when fresh (Azam et al., 1983). Both models and experimental data suggest that zooplankton grazing processes are the most significant source of DOM (e.g. Nagata, 2000).

Mesocosm experiments with Norwegian fjord water investigated variations in DOM production under various nutrient regimes with either mixed phytoplankton communities or diatom-dominated communities (Conan et al., 2007). New DOC was found to accumulate in all regimes at a rate of 22-33% of POC production, with much higher absolute values associated with diatom communities. DON production was greatly dependent on N availability (as NO_3^-, NO_2^- and NH_4^+), thus leading to N depleted, P-rich DOM accumulating under N-limitation. New DOP production was independent of nutrient availability in diatom communities and tracked DIP availability in mixed community (Conan et al., 2007). DOM is also produced bacterially, and through viral lysis and grazing. Bacterial degradation can result in DOM of a more refractory nature through alteration of molecular structure so that the biological origins are no longer recognisable so that DOM is no longer susceptible to enzymatic hydrolysis (Ogawa et al., 2001). DOC production has also been observed to be independent of nutrient regime in a New Caledonia lagoon, but reactivity was influenced by phytoplankton and bacterioplankton community composition (Mari et al., 2007).

Terrestrial DOM has been found to contribute to marine DOM particularly in shelf seas and is delivered via rivers. Thus it is not surprising that in the Northern Adriatic a summertime increase in colloidal (>1 kDa) DOM and biorefractory compounds followed river discharge (Pettine et al., 1999). Similar relationships were found in the East China Sea (Hung et al., 2003). Lignin is a commonly used biomarker of terrestrially derived DOM and often behaves conservatively in the marine environment because of its relatively refractory nature (Moran et al., 1991). Although many studies indicate that the majority of terrestrial DOM is retained in estuaries and does not reach shelf seas (Dafner et al., 2007), there are others that suggest that terrestrial DOM and POM may be transported in nepheloid layers across continental shelves (Bianchi et al., 1997), which may account for the presence of lignin and dissolved humics in the Atlantic and Pacific contributing 0.7-2.4% of total DOM (Opsahl and Benner, 1997). Terrestrial DOM has a residence time of 21-132 years and thus can be turned over faster than some marine DOM (Opsahl and Benner, 1997). The proportion of DOM transported to open ocean environments from continental shelves depends on DOM turnover time versus water mass residence time on the shelf (Carlson et al., 2000; Hung et al., 2003). In many instances, the contribution of terrestrial DOM to the marine pool has been estimated to be negligible (e.g. <0.2% of bulk DOM; Moran et al., 1991), however within certain DOM fractions, for example dissolved organic phosphorus, the bioavailable fraction supplied to coastal regions by estuaries may be substantial (Monbet et al., 2009).

1.2.2. DOM lability

The bioavailability of organic matter and the resultant transfer through trophic levels are strongly influenced by chemical composition and molecular size class (Amon and Benner, 1996). Dissolved organic matter lability can vary greatly and is commonly divided into 3 pools, namely labile (turnover times of minutes to days), semilabile (weeks to years), and refractory (decades to millennia) pools (Ducklow, 2000). Given its rapid turnover by the microbial community, labile DOM concentrations are typically low (Carlson, 2002). This is reflected by higher remineralisation rates in shelf waters than in adjacent oceanic waters, presumed to be related to lability (Hung et al., 2003). Refractory DOM constitutes the

'background' DOM concentrations and is the major contributor to bulk DOM below the euphotic zone. In the productive euphotic zone, where DOM production may exceed consumption, the semi-labile pool may exceed refractory concentrations (Carlson and Ducklow, 1995).

Biological processes affecting lability

The residence time of DOM within a certain water body appears to have a strong influence over lability. For example, in a New Caledonia lagoon, DOC reactivity decreased with residence time as the semi-enclosed nature of the lagoon allowed accumulation and ageing of DOM as a result of bacterial degradation (Mari et al., 2007). Similarly at a northwest Iberian upwelling system, labile DOM accumulated in surface waters during relaxation periods in upwelling. Deepwater DOM upwelled to the surface was largely refractory and was diluted by labile DOM advected from the adjacent continental shelf region (Alvarez-Salgado et al., 1999).

Bacterial degradation is a significant biological pathway for the production of refractory DOM. High molecular weight (HMW) based bacterial growth indicates a strong dependency on phytoplankton-derived DOM (Amon and Benner, 1996). As part of this, non-specific enzyme reactions can play a significant role in producing refractory DOM of small molecular size as the original structure is lost and enzymatic recognition and further degradation is no longer possible. Bacterial conversion of labile DOM to refractory compounds can occur in less than 48 hours, with the product persisting for timescales of years (Ogawa et al., 2001). Bacterial diagenetic processes are a crucial part of the DOM reactivity and molecular size continuum. Evidence shows that the bioreactive proportion of HMW DOM is greater than that of LMW in many different aquatic environments. The understanding is that molecular weight decreases as a result of diagenetic processes, thus each degradation product is less reactive and smaller than its precursor and also less susceptible to further degradation. This continuum explains why 80% of deep ocean refractory DOM is LMW and fresh DOM found in surface waters is often HMW (Amon and Benner, 1996; Kaiser and Benner, 2009). Colloidal organic matter is also more resistant to bacterial degradation as its size class places it between two different transport uptake pathways;

Brownian motion for small colloidal particles and turbulent shear for larger particles (Kepkay, 1994).

The majority of organic export is in the particulate fraction with about 80% of OM export as particulates and 20% dissolved. However, the stoichiometry of DOM is generally much more carbon rich than that of POM; with labile DOM having a typical C:N:P ratio of 199:20:1 and refractory DOM of 3511:202:1. Hence, for a given amount of N or P added to surface waters, a potential 62% or 88% more DOC, respectively, can be exported by DOM than Redfield ratios of 106:16:1 would suggest (Hopkinson and Vallino, 2005).

Abiotic processes affecting lability

Dissolved organic matter can be degraded abiotically through photodegradation (e.g. Moran and Zepp, 1997). Photochemical decomposition reactions convert light absorbing DOM fractions into biologically labile products such as, carbon gases, unidentified bleached organics, N and P rich compounds (NH_4^+ and PO_4^{3-}), and LMW organics such as carbonyl compounds (Moran and Zepp, 1997). Photochemical reactions can also produce structurally complex LMW compounds that are highly resistant to degradation (Benner and Biddanda, 1998). Photochemistry has been linked to enhanced secondary microbial community productivity through the assimilation of photoproducts such as LMW carbon compounds and DIN (Miller and Moran, 1997). Conversely, Benner and Biddanda (1998) found a 75% reduction in bacterial production when surface water DOM was exposed to sunlight, while exposure of deep water DOM gave a 40% enhancement in bacterial production (Benner and Biddanda, 1998).

Photodegradation of DOM is potentially significant during seasonally stratified surface waters of continental shelf seas. Sunlight exposure can result in relatively high losses of DOM from coastal environments over short time scales, through direct loss of carbon photoproducts and through the repeated stimulation of biological degradation (Miller and Moran, 1997). DOM photodegradation in a continental shelf system during one full day of exposure in summer resulted in degradation products equivalent to over

20% of bacterial carbon demand and 30% of bacterial nitrogen demand. When extrapolated to the world surface ocean, this gives an annual supply of $1x10^{15}$g C and $0.15x10^{15}$g N (Moran and Zepp, 1997).

1.2.3. DOM consumption

DOM can be assumed to be removed from the water in one of two ways: 1) transformation of DOM to particulate organic matter, and 2) remineralisation back to its inorganic constituents. These pathways can be facilitated by both biotic and abiotic mechanisms. The primary biotic sink of DOM in the ocean is free living heterotrophic bacteria, although eukaryotes also account for some DOM removal (Pomeroy, 1974). Bacterial processes are often positively correlated with POC (Shiah et al., 2000) and DOM at high concentration is remineralised more rapidly than at low concentrations (Hopkinson et al., 1997). Bacterioplankton can also take up labile carbon e.g. as glucose and DFAA luxuriously to sequester limiting nutrients (Carlson and Ducklow, 1996). In the case of DOM utilisation as a C or N source, phosphorus may be regenerated as DIP given that fresh DOP is preferentially utilised within the DOM pool (Benitez-Nelson and Buesseler, 1999; Lonborg et al., 2009); this is also apparent from depth profiles of DOM (Hung et al., 2003). It is this preferential remineralisation of phosphorus and nitrogen and the resultant high C:N:P ratio that leads to the efficient export of DOC from the surface ocean when turnover times exceed water residence times at the surface (Hopkinson et al., 1997).

Prokaryotes can assimilate LMW DOM via permeases and HWM DOM after partial remineralisation involving enzymes. Eukaryotes can also directly assimilate labile fractions of LMW DOM and, in low light or low nutrient conditions, can assimilate larger DOM compounds through phagotrophy and osmotrophy. In general, biotic processes remove the more labile DOM (Carlson, 2002). Phototransformation is a major abiotic DOM sink that is capable of removing more refractory DOM. This can either result in direct photochemical mineralisation of DOM or incomplete photodegradation of HMW DOM to bioavailable LMW DOM, dramatically reducing turnover times of these compounds (discussed above; Moran and Zepp, 1997). Sorption of

DOM onto sinking particles also acts as an abiotic process removing DOM from the surface ocean (Carlson, 2002).

Mixing of DOM below the thermocline is an important export process that acts to remove DOM from the euphotic zone. Vidal et al. (1999) found in the Central Atlantic that there was a strong microzooplankton-respiration sink of DOM at the thermocline that acted as a buffer between the relatively weak gradient-driven downward flux of DOM and the much stronger upward flux of DOM from intermediate waters below. The downward flux of DOM comprised mostly refractory HMW, C-rich DOM which may only become available for microbial consumption in the presence of external N and P sources below the thermocline. DOP export relative to production is much less than that of DON suggesting that phosphorus is more efficiently recycling and retained in the euphotic zone (Vidal et al., 1999). Thus, while export below the thermocline is a common sink of C-rich refractory DOM there is also a potential source of DOM through turbulent diffusion of deepwater into the euphotic zone. Seasonal deep mixing drives fluxes of DOC-enriched surface waters below the thermocline. This DOC flux was found by Carlson et al. (1994) to consist of ~ 33 % freshly produced DOC and ~ 66 % residual DOC, which was produced during the previous spring and escaped winter remineralisation.

1.2.4. Sedimentary organic matter

In the Celtic Sea, continental shelf sediments are typically coarse grained sands with low organic matter content. However, in shallow environments such as these organic matter is continuously supplied to sediments through wave pumping and POM deposited after bloom events may be periodically buried as a result of sand ripple migration (Shum and Sundby, 1996). Typically there are low burial efficiencies of organic matter in shelf seas due to oxic mineralisation (Lohse et al., 1998) and resuspension by tidal and storm mixing (Jones et al., 1998).

1.3. Phosphorus, dissolved organic phosphorus (DOP) and alkaline phosphatase

1.3.1. Biological role of phosphorus

Phosphorus is a macronutrient that is essential to all life (e.g. Benitez-Nelson, 2000; Karl and Bjorkman, 2002; Paytan and McLaughlin, 2007) due to its involvement in DNA, RNA and phospholipids and ATP. Deoxyribonucleic acid (DNA) is the double helical structure that stores all the genetic information of cells. DNA transcription synthesises ribonucleic acid (RNA) allowing for the subsequent translation and synthesis of proteins according to the genetic coding. Adenosine Triphosphate (ATP) is the principal free-energy donor in most cellular energy-requiring processes and is essential for many functional processes such as active transport across cell membranes and the synthesis of macromolecules. Phospholipids are a major component of cell membranes. Other important cellular processes also involve phosphorus including phosphorolysis, which is the cleavage of a bond by orthophosphate and is an important part of initialising or suppressing enzyme expression and synthesis including phosphatases (Cembella et al., 1984).

1.3.2. Phosphorus limitation

Nutrient limitation can refer to restricted growth rates of phytoplankton present in an environment, or limitation of net primary production (allowing for potential community shifts under varying nutrient regimes), or net ecosystem production limitation (Howarth, 1988). The second definition, limitation with respect to net primary production, is commonly applied in marine research and thus is used here.

Marine nutrient stoichiometry (C:N:P ratio) is commonly used to identify the limiting nutrient of particular systems. Typically, dissolved ratios of inorganic nutrients are used to identify which nutrient is in deficit according to deviation from the Redfield ratio of C_{106}:N_{16}:P (Redfield et al., 1963). However, cellular N:P ratios of culture phytoplankton species can vary vastly and so using a fixed ratio such as 16N:1P perhaps offers an oversimplification in assessing nutrient limitation. The ratio may also vary within species as a function of growth rate, light cycles and nutrient source

and 16:1 is rather an approximate average value (Cembella et al., 1984; Webber and Deutsch, 2010). A review by Arrigo (2005) found 'survivalist' microbial communities had a higher N:P demand, while 'bloomers' had a low N:P demand, requiring relatively more phosphorus than Redfield for growth machinery. It was only 'generalist' phytoplankton communities that required near Redfield nutrient ratios (Arrigo, 2005). With respect to primary production through phytoplankton growth and production, carbon is generally assumed to be available and thus macronutrient limitation generally refers to inorganic N:P.

The global nitrogen budget is controlled by biological processes such as nitrogen fixation and denitrification, while the global phosphorus budget is controlled by geological processes (Gruber and Sarmiento, 1997; Froelich et al., 1982). Recent studies indicate that realistically phosphorus residence times in the ocean are of the order of 10 000-30 000 years (Benitez-Nelson, 2000) rather than 80 000 years as previously suggested (e.g. Froelich et al., 1982). In either case, these values greatly exceed estimates for the residence time of nitrogen in the ocean which is of the order of a few thousands of years (Gruber, 2008).

Freshwater ecosystems, such as rivers and lakes, are typically phosphorus limited with high nitrogen to phosphorus ratios due to the influence of nitrogen fixation and the loss of phosphorus through binding to iron oxyhydroxides (e.g. Dodds et al., 1998; Nurnberg, 1996; Benitez-Nelson, 2000). Tyrrell (1999) constructed a simple model of macronutrient ratios and ocean primary production. The results of his study indicated that nitrogen is the proximal limiting nutrient in that it limits growth locally and over biological timescales, while phosphorus is the ultimate limiting nutrient, i.e. basin scale over geological time. This is the result of nitrogen fixers being able to outcompete other phytoplankton in low nitrogen environments, while a sustained increase in river inputs of phosphorus is required to alleviate phosphorus limitation (Tyrrell, 1999). Observations of the subtropical North Pacific Ocean suggest that nitrogen fixation has initiated a shift from nitrogen to phosphorus limitation (Karl et al., 1997). Arguably, iron limitation of nitrogen-fixers such as *Trichodesmium* spp. may have significant implications in open ocean subtropical gyre regions with

low aeolian inputs of the micronutrient (Kustka et al., 2003; Moore et al., 2009).

Tyrrell (1999) based his findings on reactive nitrogen (NO_3^-, NO_2^- and NH_4^+) and phosphate concentrations alone. However, organic and particulate contributions to both the nitrogen and phosphorus pools in the surface ocean are significant (Benner, 2003; Björkman et al., 2000). In a global analysis of N:P ratios from 16 studies of dissolved inorganic, organic and particulate nutrient concentrations, Downing (1997) found nitrogen to be the most likely limiting nutrient in estuarine and coastal environments where anthropogenic influences were significant. However, it was found that in the open ocean photic zone high non-Redfield ratios suggested phosphorus limitation (Downing, 1997). Indeed, diazotrophic nitrogen fixation and anthropogenic N inputs are set to increase the potential for P limitation in many regions of the world's oceans (Vidal et al, 2003; Xu et al., 2008; Krishnamurthy et al., 2010).

The rate at which phosphorus is turned over in a system, i.e. taken up and possibly released as organic matter before potential secondary utilisation, can give an indication of whether a system is phosphorus limited or not. If DIP concentrations are low then uptake rates are high and the turnover times are short. Turnover times of the order of 2-5 hours have been reported to indicate P deficiency in the Sargasso Sea (Suttle et al., 1990). Turnover rates are a function of *in situ* DIP and fluxes/uptake. Use of ^{33}P or ^{32}P uptake and turnover during incubation experiments can indicate P availability within natural aquatic systems (e.g. Xu et al., 2008). While these experiments are very useful, supplementary experiments are essential to give more conclusive evidence of P limitation.

A wide range of diagnostic criteria must be applied to allow definitive identification of nutrient deficiency. Microbial communities exhibit a variety of measurable responses to phosphorus limitation. These include: a) the induction of alkaline phosphatase activity (discussed below); b) enhanced uptake of DIP upon addition; c) utilisation and depletion of internal polyphosphate stores; d) net decrease in cell P quota; e) breakdown of the diel periodicity and light enhancement of DIP uptake rate; f) reduction in

ratios of intracellular metabolites to other metabolites; g) decrease in ratios of RNA to DNA and protein to carbohydrate; h) enhanced excretion and utilisation of DOP; i) reduced growth rate/cell yield; j) increased cell sinking rates (especially in diatoms); k) changes in cell surface morphology; and l) changes in species composition with time in phytoplankton communities. Cell functionality is also altered in measurable ways: RNA synthesis soon ceases during P limitation but upon nutrient enrichment P is transferred first to RNA and luxury carbon storage and cell cycles stop (Cembella et al., 1984). However, it is often hard to detect a number of these indicators accurately because natural assemblages are subject to multiple stresses and communities are a complex mix of autotrophs and heterotrophs.

Low ambient concentrations will have some control over phytoplankton yield, but if the nutrients are being rapidly recycled via microorganisms then growth rates may be sustained. Recent culture experiments with environmental isolates of bacteria, flagellates, dinoflagellates and diatoms show that when uptake is diffusion-limited there is a size-dependence to phosphate uptake affinity. Diatoms, which are a relatively large phytoplankton species, have the highest phosphate-uptake affinities after bacteria, and thus theoretically can outcompete similar sized flagellates in P-limiting conditions (Tambi et al., 2009). However, there are many reports of diatoms being less successful during P-limitation which reiterates the complexities involved in deciphering the complex nature of nutrient limitation from observing the net effect. This becomes even more complex with whole microbial communities. To illustrate this point, in the Gironde Plume region of the Bay of Biscay, bacteria dominated phosphate uptake leading the phytoplankton community to meet its P-requirements through accessing the DOP pool (Labry et al., 2002). Thus it is apparent that a measure of low ambient DIP concentrations is insufficient evidence that microalgae are P-limited given that many species can access DOP using phosphatases and also often have access to internal polyphosphates (Cembella et al., 1984).

1.3.3. Dissolved organic phosphorus (DOP)

Phytoplankton have a strong metabolic preference for the assimilation of inorganic phosphorus (DIP) over dissolved organic phosphorus (DOP)

compounds. For DIP, this is reflected by the nutrient's depth profile for which DIP concentrations are typically low in surface waters and increase with depth (e.g. Conan et al., 2007). Once assimilated P is incorporated into organic matter becoming part of more complex organic molecules. Dissolved organic matter (DOM), including DOP, is released back to the water column through a number of possible pathways (e.g. extracellular release by phytoplankton, grazer mediated release or excretion, and bacterial or viral cell lysis; Carlson, 2002)). Often, this DOM is recycled by microbial regeneration through enzyme-catalysed hydrolysis but during bloom events production and consumption may be decoupled and net DOM production may result. In this instance, DOM may be transported laterally, vertically or exported to the deep ocean (Karl & Björkman, 2002; Carlson et al., 1994; Abell et al., 2000; Mahaffey et al., 2004).

In the surface open ocean the dissolved phosphorus pool comprises ~15-35% inorganic phosphate and ~65-85% dissolved organic phosphate (DOP) and inorganic polyphosphate compounds (Karl and Yanagi, 1997). However the DOP pool is relatively unavailable to marine organisms as phosphorylated compounds cannot cross cytoplasmic membranes (Lugtenberg, 1987). Thus, organisms preferentially utilise inorganic phosphate. Before DOP can be assimilated it must first be converted to bioavailable orthophosphate through a largely extracellular hydrolytic process (e.g. Nicholson et al., 2006). This does not mean that DOP cannot be an important nutrient source for production. In open ocean regions such as the subtropical North Atlantic organic matter dominates the dissolved N and P pools. Lateral transport of organic nutrients from productive upwelling regions to oligotrophic gyres can sustain significant export production in the latter (Mahaffey et al., 2004; Roussenov et al., 2006; Torres-Valdes et al., 2009).

Composition of the DOP Pool

DOP is thought to be compositionally similar throughout the world ocean. The two major organic phosphorus groups in the ocean thought to occur in invariant proportion are phosphate esters and phosphonates; the difference being a C-P bond in the latter rather than a C-O-P ester link in the former (Clark et al., 1998; Kolowith et al., 2001; Karl et al., 2008). Within the

phosphate esters group are two significant subgroups: phosphomonoesters and phosphate diesters (Dyhrman et al., 2007). However, as DOP is typically determined as total dissolved phosphorus minus soluble reactive phosphorus, it can also include non-reactive inorganic compounds such as polyphosphates (Benitez-Nelson, 2000; Diaz et al., 2008). Studies of DOP composition indicate a dominance of monophosphate esters (Strickland and Solorzano, 1966; Karl and Yanagi, 1997), followed by nucleotides and nucleic acids (Chrost et al., 1986; Strickland and Solorzano, 1966), and then up to 25% of DOP in the form of phosphonates (Clark et al., 1998; Kolowith et al., 2001; Paytan et al., 2003) and approximately 10% as dissolved phospholipids (Suzumura et al., 1998). In a study of a temperate estuary in southwest England, phosphomonoesters dominated the DOP pool and the enzymatically hydrolysable fraction consistently represented 70% of the total DOP pool. Although DOP concentrations behaved non-conservatively within the estuary, the relative proportions remained similar with an apparently strong source of DOP coinciding with the turbidity maximum (Monbet et al., 2009). Thus, in coastal and shelf sea environments the terrestrial contribution to the bioavailable fraction of DOP may not be insignificant as has been suggested (e.g. Moran et al., 1991). However, it is not yet apparent to what extent this contribution may propagate into the shelf sea once is has escaped the estuarine environment.

On addition of upwelled 'new' DIP to the surface waters followed by a period of relaxation there is generally an observed increase in phytoplankton biomass and DOP production (Ruttenberg and Dyhrman, 2005). The DOP pool is important during periods of stratification in sustaining production. Intense regeneration of DOP is necessary to keep the supplied phosphorus in the photic surface waters. The length of stratified periods strongly influences the relative dominance of DOP and also its lability, as the more it is recycled the greater the refractory component becomes relative to the total DOP available (Ruttenberg and Dyhrman, 2005). As a result of intense surface recycling, DOP concentrations in the deep water of major ocean basins appear to be of similar concentration with an average DOM age of 6000 years and being dominated by the most refractory DOP compounds (Paytan and McLaughlin, 2007). Similarly, the dissolved phosphonate signal in the surface ocean is amplified relative to the 3% of organic phosphorus

found in living organisms and reflected in particulate organic phosphorus that primarily consists of P esters, being chemically distinct from DOP. This is because P esters are more labile and so are utilised by microorganisms more readily than phosphonates (Kolowith et al., 2001). While phosphonates are commonly assumed to be a significant component of DOP in the surface ocean and a potentially important P source to certain phytoplankton species (Nowack, 2003; Benitez-Nelson et al., 2004; Dyhrman et al., 2006; Gilbert et al., 2009), there is evidence that in some shelf sea environments phosphonates are less significant than in the open ocean (Monaghan and Ruttenberg, 1999). However, once below the surface layer, P esters and phosphonates in the DOP pool are remineralised at the same rate (Kolowith et al., 2001). Experimenting with cultured strains of *Trichodesmium spp.*, Dyhrman et al. (2009) found that this cyanobacterial species had a much higher phosphonate content (10 % of cellular particulate phosphorus) and thus are potentially a significant source of phosphonates in oligotrophic regions where they thrive (Dyhrman et al., 2009).

An important feature of DOM dynamics is that organic phosphorus is preferentially remineralised and generally more available than organic nitrogen or carbon (Kolowith et al., 2001; Hopkinson et al., 1997; Yoshimura et al., 2007). This is also true of particulate organic matter and particulate organic phosphorus, so that much phosphorus from the surface is retained in the euphotic and epipelagic zones through microbial degradation processes (Smith et al., 1985; Taylor et al., 2009). Thus, DOP concentrations are depleted before DON either with increasing depth in the water column or with lateral transport from the DOM source region (Torres-Valdes et al., 2009). The hydrolytic enzymes responsible for hydrolysis of the main components of the DOP and DON pools do not appear to operate wholly independently of one another. Leucine aminopeptidase activity, which hydrolyses DON, was shown in mesocosm experiments on Baltic Sea water to increase in parallel to an increase in alkaline phosphatase activity (Nausch, 2000).

1.3.4. Enzymatic hydrolysis of DOP: alkaline phosphatase activity (APA)

Functional Role

Microorganisms have a strong metabolic preference for the uptake of phosphate via a low affinity pathway. There is also a high affinity transport pathway that is repressible at high phosphate concentrations; this involves the catalysed hydrolysis of DOP to phosphate by the hydrolytic enzymes, phosphatases, at particle surfaces. Alkaline phosphatases, which hydrolyse phosphomonoesters, are widespread and found associated with bacteria, phytoplankton, zooplankton and freely dissolved (e.g. Cembella et al., 1984; Gambin et al., 1999; Vidal et al., 2003). Alkaline phosphatases hydrolyse the C-O-P bond irrelevant of organic moiety (Jansson et al., 1988). Herein, alkaline phosphatases will be referred to as phosphatases (although the term phosphatase refers to a large group of enzymes including intracellular acid phosphatases). A large part (approximately one third) of HMW DOP is not hydrolysable by the enzymes alkaline phosphatase and phosphodiesterase. This may be due to the blocking of labile ester bonds that these enzymes target from decomposition through the formation of macromolecular complexes (Suzumura et al., 1998).

Induction and Repression

Phosphatases are repressible and are synthesised during phosphate deficiency, usually accepted to be in response to depleted internal cellular phosphate as polyphosphate (Jansson et al., 1988; Dyhrman and Ruttenberg, 2006). Repression of the enzyme occurs when phosphate is above a critical concentration as DIP competes for the active sites on the enzyme surfaces, thus suppressing APA (alkaline phosphatase activity; Vidal et al., 2003; Dyhrman and Ruttenberg, 2006). When present, phosphatases are either constitutive or have been induced in response to substrate, and it is the induced enzymes only that can be repressed in response to the product, DIP (Cembella et al., 1984). In the Oregon coastal upwelling region, diatom APA was more repressible through the addition of DIP than that of dinoflagellates, suggesting inducible APA activity in the former and constitutive APA in the latter (Dyhrman and Ruttenberg, 2006). This may in part be due to the higher DNA content of dinoflagellates giving

them a higher P demand than diatoms (Huang et al., 2007). Thus, changes in the phosphomonoester availability may disproportionately affect different taxa (Dyhrman and Ruttenberg, 2006).

The activity of alkaline phosphatases varies with a number of environmental parameters, such as temperature, pH and limitation of metal ions integral to enzyme structure (Cembella et al., 1984). Divalent metal ions, such as zinc, at the enzyme active site are crucial to its functionality and thus phosphatase activity can also be inhibited by chelators such as EDTA which sequester the metal ions (Cembella et al., 1984). A recent study by Shaked et al. (2006) showed that batch cultures of *Emiliana huxleyi* were co-limited by Zn and phosphorus when concentrations of both DIP and Zn were sufficiently low (Shaked et al., 2006), while copper ions in solution inhibit alkaline phosphatase activity (Rueter, 1986). Ambient summer levels of UV-B radiation were found to suppress APA, particularly in the freely dissolved fraction, of Norwegian fjord samples (Garde and Gustavson, 1999). A study of dinoflagellates in the Caribbean and Sargasso Seas showed a diel pattern of APA with the highest activity during the day and the lowest activity preceding dawn. Vertical distribution of APA showed maximal activity in the surface mixed layer, and lowest at the thermocline. This study indicated that light levels at the time of sampling govern APA more greatly than light levels during the incubation period (Rivkin and Swift, 1979). Generally speaking, it is phytoplankton cell surface phosphatases that have been reportedly most susceptible to repression by the product, DIP (Jansson et al., 1988).

Alkaline Phosphatase Activity (APA) Environmental Assays

Enzyme activity can be measured in the environment through rate assays and enzyme labelled fluorescence techniques. The general protocol involves the addition of an artificial organic phosphorus substrate which is hydrolysed by the phosphatases present in the water sample. After a recorded length of time the organic product is detected either fluorescently, as in the case of e.g. MUF-P, or colorimetrically, as with e.g. p-nitrophenyl-phosphate. Alternatively the concentration of the product, orthophosphate, can be measured. The substrate is commonly added in excess to allow the reaction to proceed at maximum rate thus giving the maximum potential of

the system (Jansson et al., 1988). However, it is important to incubate over a range of concentrations as APA in the subtropical North Atlantic was found to reach saturation in the range as low as 0.25 μM up to 5 μM, and APA was sometimes inhibited by excess substrate, or the fluorescence of the product, MUF was quenched when at very high concentrations (Sebastian and Neill, 2004).

Substrate addition rate assays

Phosphatase activity can be measured through bulk community assays, differential filtration, particle size classes, in freely dissolved fractions or species specific e.g. *Trichodesmium*. In terms of carbon drawdown and ecosystem organic phosphorus cycling, whole community assays are a useful tool. To allow a tentative assessment of the nutrient status of various populations within a community size class specific APA is much more useful than whole activity. For instance, high APA in the phytoplankton particle-associated fraction combined with low APA in the freely dissolved fraction is indicative of a recent onset of P-stress (e.g. Labry et al., 2005). On the other hand high dissolved APA is indicative of persistent P-stress or limitation as freely dissolved APA is relatively stable and can survive over a period exceeding the generation time of many phytoplankton species, as found in the central Atlantic (Vidal et al., 2003) and in the Taiwan Strait (Ou et al., 2006). In the Gulf of Aqaba dissolved APA was found to have a lifetime of 2-40 days (Li et al., 1998). It has been suggested that colloidal associations are a key dynamic maintaining the stability of dissolved APA over long periods (Vidal et al., 2003). Conversely, high APA in the largest fraction is not necessarily indicative of P-stress within the autotrophic population as zooplankton can contribute significantly to APA. Approaching 80% of the total APA measured in a polluted Mediterranean bay was found to be associated with zooplankton, and the largest size fraction APA greatly exceeded that of the nano- and picoplankton size classes (Gambin et al., 1999). In the North Pacific Subtropical Gyre, cell-free APA contributed most to total activity during N limitation, switching to picoplankton cell bound APA after incubation under N-enriched conditions (Duhamel et al., 2010).

Size fractionated APA assays

Bacterial communities can often contribute significantly to bulk APA in various environments (e.g. Huang and Hong, 1999). Bacterially associated alkaline phosphatase differs from that of phytoplankton and zooplankton in that the high molecular weight moiety must first be cleaved by proteases before bacteria can utilise the enzyme (Nausch, 2000). While bacteria have a higher affinity for phosphate than phytoplankton (Tambi et al., 2009) and are often found to dominate phosphate uptake in low phosphorus environments (e.g. Labry et al., 2002) they are still often found to access the DOP pool as well even in high nutrient environments. For example, at a northwest African upwelling region high APA was coincident with high DIP concentrations. The measured APA was not DIP-repressible and thus was considered to be constitutive APA associated with DOC-limited bacteria (Sebastian et al., 2004). Previously, in the mesopelagic Indian Ocean, APA tracked DIP concentrations in an assumed link between bacterial growth and its dependence on DOM to alleviate C-limitation (Hoppe and Ullrich, 1999). Similarly, in the Northern Adriatic Sea bacterial production and APA were highest within marine snow associated communities (Karner and Herndl, 1992). In a mesocosm experiment Smith et al. (1992) found bacteria associated with aggregates expressed high levels of ectoenzymes releasing preferentially releasing DOP and DON from POM (Smith et al., 1992). From these selected examples it is apparent within the literature that bacteria commonly use alkaline phosphatase to access the organic moiety part of DOP as an 'easy' source of DOC (Kolowith et al., 2001). However, bacteria can also experience P-limitation in regions of extreme phosphate limitation such as the northwest Mediterranean (Thingstad et al., 1998).

Individual cell APA: Enzyme labelled fluorescence

Gonzalez-Gill et al. (1998) developed enzyme labelled fluorescence (ELF) for phytoplankton on laboratory cultures of various species. The principle behind the method is that the insoluble yellow-green product called CHPQ (2-(5'-chloro-2'hydroxyphenyl)-6-chloro-4-(^{3}H)-quinzolinone) precipitates at the site of hydrolysis activity. Their study was groundbreaking in that it proved the potential for assessing the P-status of individual phytoplankton cells (Gonzalez-Gill et al., 1998). Dyhrman and Palenik (1999) published the first application of ELF in field studies on the dinoflagellate *Prorocentrum*

minimum. Crucially during both of these studies ELF labelling was shown to be DIP-repressible. The latter study found that while APA induction was rapid at certain life stages of cells, the repression was always slow with 50% reduction in labelling after 3 days. There was a noted possible loss of surface associated enzymes as all labelled points were intracellular, but the repressible nature of the ELF labelling contradicts the suggestion that constitutive APA alone was being labelled (Dyhrman and Palenik, 1999). During a study in the Sargasso Sea, Lomas et al. (2004) found ELF staining of diatoms, dinoflatgellates, and autotrophic flagellates but only rarely in the case of coccoid cyanobacteria such as *Synechococcus*. The autotroph ELF-APA was dominated by diatoms, highlighting the importance of using ELF to identify specific responses to phosphorus stress within the bulk response (Lomas et al., 2004). In the Oregon coastal upwelling region ELF staining amongst diatoms tracked bulk APA and was DIP-repressible, while dinoflagellates expressed consistent staining suggesting constitutive APA (Dyhrman and Ruttenberg, 2006). While being a very useful tool, ELF cannot be used to accurately assess limitation without additional rate assay data although the degree of ELF labelling in *Trichodesmium spp.* populations in the tropical and subtropical western North Atlantic was recently found to correlate to DIP concentrations (range 5-520 nM; Hynes et al., 2009).

Interpreting APA and Limitations

Michaelis-Menten model can be applied to enzyme activity data. The model refers to a predator-prey, or enzyme-substrate, relationship where mortality (or hydrolysis) increases linearly with increasing prey/substrate concentration until it reaches a saturation point and plateaus, known as V_m (Michaelis and Menten, 1913; Li, 1983; Li and Kuang, 2007). Expressed mathematically:

$$V = \frac{V_m S}{K_m + S}$$

where V is the rate of uptake of the substrate at concentration S, V_m is the asymptote that V tends towards at high S values, K_m is the half saturation constant (i.e. S when V is half V_m) (Li, 1983). Thus, under Michaelis-Menten kinetics, DOP hydrolysis is limited by the affinity or coincidence of enzyme-

substrate complexation, which is limited by both enzyme abundance and substrate concentration and the time of hydrolysis itself.

Michaelis-Menten kinetics can be used to ascertain the tendency for phosphatases to combine with and hydrolyse substrate through determination of K_m. K_m represents the substrate concentration where the reaction proceeds at half its maximum rate. A low K_m value implies the enzyme has high affinity for the substrate. However, the use of Michaelis-Menten kinetics on a community scale, where species are all capable of synthesising a mixture of enzymes, is theoretically incorrect and also rather inaccurate as K_m is influenced by substrate, pH and temperature (Jansson et al., 1988). However, there are many instances where environmental data have conformed to Michaelis-Menten kinetics (Hoppe, 2003). The modern trend in alkaline phosphatase studies appears to be deviating from the traditional V_m and K_m values to simple rate measurements that are arguably more easily compared across natural systems (e.g. Sebastian et al., 2004; Taylor et al., 2009; Dyhrman and Ruttenberg, 2006; Vidal et al., 2003; Lomas et al., 2010; Mather et al., 2008; Duhamel et al., 2010).

As with all biological rate assays, there are limitations that mean any results cannot conclusively be assumed to reflect the *in situ* activity or phosphorus dynamics. 1) The substrates used in these rate assays are not natural and they are often not added at natural DOP concentrations. 2) Size fractionation of samples can lead to dissociation of surface-bound APA and cell lysis (Sebastian et al., 2004) while bulk APA does not resolve variations in size class nutrient status embedded within the net effect measured. 3) Bottle effects over the time period of the incubation. 4) Temperature and light both affect enzyme activity and will differ from that of *in situ* conditions. It is possible to minimise these limitations through employing short incubation times to avoid contamination, bacterial growth, a change in community and too great a deviation from the initial conditions at sampling. Bottle effects are also reduced this way, however in some instances the measured change is minimal and therefore to maximise the accuracy of analysis longer incubation times are necessary. In natural environments substrate availability, rather than enzyme activity alone, may limit organic nutrient hydrolysis. Hence, if this is the case then measured

APA alone cannot indicate accurate turnover rates without supplementary organic nutrient concentration data (Jansson et al., 1988).

In using APA as a proxy for nutrient limitation, community net activity and enzyme labelled fluorescence (ELF) are not necessarily accurate indicators. While both methods have shown APA to correlate to phosphate concentrations (e.g. Lomas et al., 2004; Hynes et al., 2009; Mather et al., 2008; Orchard 2010) there are other instances where this is not the case (e.g. Sebastian et al., 2004; Hoppe and Ullrich, 1999). Different taxa have different nutritional requirements, nutritional strategies with respect to internal phosphorus stores and regulation of alkaline phosphatase; indeed even within the same genus these differences have been observed (Ruttenberg and Dyhrman, 2005). Thus, attempting to assess phosphate limitation based on community APA alone is potentially highly misleading. For example, dinoflagellates have often been observed to have relatively high constitutive APA, whereas diatom APA is rather more inducible. If bulk community APA were measured to be high in a population dominated by dinoflagellates the implications in terms of nutrient limitation would be very different from that if the population were dominated by diatoms (Dyhrman and Ruttenberg, 2006). Ruttenberg and Dyhrman (2005) also suggest that microscale variability in phosphate availability may influence APA at a single cell level. Thus, if the phosphate status can vary greatly between different taxa within a community there will be inherent implications in terms of export production through sinking rates via cell size, density, and aggregation potential (Mackey et al., 2007).

Measuring APA and phosphate concentrations simultaneously does not necessarily reflect the nutrient conditions under which APA synthesis was initiated. There is a distinct lag between the external low DIP concentration and alkaline phosphatase expression and the corresponding increase in APA due to the time taken to synthesise the enzyme and the time taken for internal polyphosphate stores to become depleted (Mackey et al., 2007). Similarly, there is a lag in the repression of APA due to the time involved in breaking down the enzyme and particulate alkaline phosphatase may be released to the water column where it can remain active for periods of days to weeks (Jansson et al., 1988; Li et al., 1998).

Enzyme activity can be normalised to biomass (e.g. Cotner et al., 1997). This is commonly achieved using chlorophyll data (e.g. Guildford and Hecky, 2000), particulate organic carbon data (e.g. Rose and Axler, 1998) or particulate phosphorus (e.g. Cotner et al., 1997). However, normalising APA to a parameter such as organic carbon or phosphorus may not be a sensitive method as several fractions of the community being sampled may share that attribute. In some instances it is perhaps more useful to normalise APA to particulate phospholipids and their fatty acid derivatives, which can be used to more accurately distinguish between phytoplankton and bacterioplankton (e.g. Boschker and Middelburg, 2002; Suzumura 2005; Boschker et al., 2005; Espinosa et al., 2008; Rontani et al., 2009). This method of biomass normalisation can help indicate whether measured APA is occurring as a nutritional strategy associated with phytoplankton or as bacterial remineralisation activity. For example, the abundance of lipid biomarkers representative of bacterial biomass may correlate more strongly to measured APA than phytoplankton biomarkers, while a common property such as particulate phosphorus may or may not show any correlation to APA.

1.3.5. Determining the enzyme hydrolysable DOP fraction

Dissolved organic phosphorus is determined indirectly by measuring DIP before and after oxidation of DOP to DIP by using high temperature and/or pressure in the presence of an oxidising reagent, e.g. persulfate oxidation or UV oxidation. DIP is then determined again using the standard molylbdate blue method as total dissolved phosphorus (TDP), with DOP = TDP – $DIP_{pre\text{-}UV}$ (Strickland and Parsons, 1972). However, this method does not give any indication of the lability of the DOP as it is assumed that all of the organic phosphorus matter is oxidised. Karl and Yanagi (1997) developed a method that allowed partial characterisation of the dissolved phosphorus pool. Samples were oxidised over a range of incubation times (0 minutes, 20 minutes, 120 minutes) to determine soluble reactive phosphorus, phosphomonoesters (UV-labile), and nucleotides (UV-stable), respectively (Karl and Yanagi, 1997). While giving useful insight into the chemical stability of the DOP pool, such partial characterisation does not necessarily infer biological lability.

The phosphomonoester (PME) pool is commonly thought to be the largest, most reactive DOP pool in the surface ocean (Strickland and Solorzano, 1966; Karl and Yanagi, 1997). Strickland and Parsons (1972) detail a protocol for the determination of monophosphate esters through incubating samples with alkaline phosphatase cultured with the bacterium *Escherichia coli*. The theory behind this method is that over a sufficient incubation time the added alkaline phosphatase in a filtered seawater sample will convert the phosphomonoester component of DOP to DIP that remains in solution. In brief, this approach is not that dissimilar from total DOP determination except that DIP alone is measured before and after incubation with the enzyme, and the difference gives the phosphomonoester concentration (i.e. PME = DIP_{post} – DIP_{pre}). Variations of this method have been used in many studies to indicate the relative bioavailability of DOP in the surface waters of the open ocean regions (Moutin et al., 2008; Duhamel et al., 2010), enclosed seas (Misic and Harriague, 2008), and coastal regions (Taft et al., 1977; Huang and Hong, 1999), as well as in culture experiments (Rivkin and Swift, 1980).

Alkaline phosphatases facilitate the hydrolysis of phosphomonoesters to bioavailable phosphorus compounds. Therefore, when investigating APA an important consideration is natural substrate availability, i.e. PME concentration in the water column. It is important to bear in mind that the presence of DOP does not guarantee a source of phosphorus to microbial populations, as many of the more refractory DOP compounds (e.g. phosphonates) are not accessible to many species (Clark et al., 1998; Benitez-Nelson, 2000). The DOP pool is not simply comprised of phosphomonoesters and refractory DOP compounds, there is a sliding scale of bioavailability. On this scale there are also phosphodiesters, polyphosphates and phosphonates all of which are bioavailable in the presence of the appropriate enzymes, e.g. phosphodiesterases and phytases and represent the enzyme hydrolysable phosphorus (EHP) fraction (e.g. Monbet et al., 2009). Monbet et al., (2007) developed a protocol to assess the release of dissolved organic phosphorus species in natural water samples which they later successfully applied in the marine waters of the Tamar Estuary (Monbet et al., 2009). In these studies, the

phosphomonoester fraction hydrolysed by alkaline phosphatase (APase), the phosphodiesters fraction hydrolysed by phosphodiesterase (PDEase), and phytic acid by phytase were determined. The DOP fractions were determined through cumulative addition of enzymes, i.e. APase, APase + PDEase, and APase + PDEase + phytase (Monbet et al., 2007). Alkaline phosphatase releases DIP more easily from low molecular weight DOP than high molecular fractions, and the same is true of incubations with phosphodiesterases alone. However, incubation with APase and PDEase together facilitates 30 % more DOP hydrolysis than when incubated separately (Hino, 1989). Thus, a combination of enzymes reveals a truer representation of natural levels of bioavailable DOP than incubation with APase alone.

1.3.6. Summary of DOP and APA

In summary, using APA as an indicator of P limitation is not straight forward. Bacterial phosphatases expressed in response to organic carbon limitation and freely dissolved phosphatases may have been synthesised up to weeks previous to sampling, and zooplankton (Cembella et al., 1984; Kirchman et al., 1990; Gambin et al., 1999) can potentially significantly influence measured bulk APA (e.g. Sebastian et al., 2004). Constitutive activity can also be highly variable between different species (e.g. Dyhrman and Ruttenberg, 2006; Mackey et al., 2007). Thus determining the origin of measured APA (at very least particulate versus freely dissolved, preferably at individual cell level) and whether it is repressible or not is essential before accurate interpretation of nutrient limitation is possible.

Characterisation of the DOP pool by determining alkaline phosphatase substrate availability is also important when interpreting observed APA during incubation experiments. During incubations, substrate is supplied in excess and the community potential to hydrolyse PME is measured. *In situ* PME concentrations are probably far lower and APA may be substrate limited rather than enzyme limited (e.g. Kolowith et al., 2001).

However, the presence and degree of APA can provide important insight into organic matter remineralisation using APA facilitated DOP hydrolysis as a proxy for remineralisation of labile DOM. Dissolved organic matter

comprises one of the largest exchangeable carbon reservoirs in the global ocean (Carlson, 2002). Combined with PME data knowledge of enzyme activity can give meaningful insight into DOM lability and dynamics in aquatic environments, thus having implications for our understanding of carbon storage, transfers and export in such environments.

1.4. Research aims of the present study

Physical mixing processes play an influential role in shelf sea biogeochemical dynamics. The relatively shallow water column is susceptible to mixing on a range of temporal and spatial scales. For example, turbulence and shear at the thermocline vary through the spring-neap tidal cycle; sporadic wind events drive surface boundary mixing and can trigger inertial oscillations enhancing shear at the thermocline; and the interaction of the irregular shelf bathymetry with tidal currents will vary spatially across the shelf.

The Celtic Sea is thought to be nitrogen limited due to a number of indicators including low winter Redfield ratios (Hydes et al., 2004), thus studying phosphorus dynamics, and in particular DOP, offers a good proxy for general nutrient and dissolved organic matter interactions on the shelf. The DOP pool may not be utilised locally as a nutrient source, thus it potentially facilitates biogeochemically important carbon storage. However, to assess the relative importance of this requires determination of the magnitude of the DOP pool and its characterization, and the timescale of its turnover. In addition, a greater understanding of the internal cycling of phosphorus within the shelf sea environment is important in assessing the transfer potential to the ocean, and determining whether the Celtic Sea acts as a sink or source of phosphorus to the North Atlantic.

In the following chapters, techniques used to study phosphorus and data on phosphorus dynamics in the Celtic Sea are analysed and discussed. Chapter 2 gives details of the Methods used during the present study. Chapter 3, the first results chapter, discusses the temporally important influence of enhanced mixing due to wind and storm events on phosphorus dynamics. Chapter 4 discusses the spatial variability in phosphorus partitioning, predominantly focussing on the dissolved phase, across the

Celtic Sea shelf to the shelf break. In the final results chapter (Chapter 5), discussion is focused on the spatial variability of phosphorus pool dynamics at the continental slope region.

Bringing together these results I will address the following research questions:

- Is there a net accumulation of phosphorus in the dissolved organic phase, and therefore a net gain of DOM in the euphotic layer of the Celtic Sea during summer stratification?
- Does the Celtic Sea act as a sink or source of phosphorus to the phosphorus-limited North Atlantic?
- How might climate change and the associated increase in nitrogen in the ocean and meteorological changes, i.e. increased storm frequency, affect phosphorus and DOM dynamics in the Celtic Sea?

2. METHODS

2. Methods

Samples were collected during three separate research cruises. The first cruise was conducted in July 2008 in the Jones Bank region of the Celtic Sea (*RRS James Cook*, JC25). The aim of this cruise was to investigate the spring-neap tidal modulation of nutrient fluxes across the base of the seasonal thermocline with sampling beginning during a strong storm. The second cruise was conducted in June 2009 (*RV Celtic Explorer*, CE911) and consisted of several transects across the continental shelf slope west of Ireland in the Porcupine Bank region. The aim of this cruise was to investigate the influence of topographical features on the depth of certain pycnoclines and more importantly the nutricline. The third research cruise was conducted in June 2010 (*RRS Discovery*, D352) in the Celtic Sea. This cruise included time series sampling at a fixed location before, during and after a wind mixing event and a cross-shelf transect (on-shelf to shelf slope).

2.1. Sample collection

Seawater was sampled through the water column at 6-8 discrete depths in Niskin bottles attached to a rosette fitted with a Seabird Electronics 911 CTD instrument. Hydrographical CTD data included calibrated salinity and temperature (JC25, D352 and CE911), chlorophyll fluorescence and PAR (JC25 and D352). Full pre-dawn biogeochemical sampling depths were selected based on the down-cast temperature and fluorescence profiles as near surface, mid-surface mixed layer, thermocline or subsurface chlorophyll maximum, base of chlorophyll maximum, deep-mixed layer and bottom water. Once the sampling rosette was on deck, seawater samples were transferred from Niskin bottles to 10 L plastic carboys (acid washed and Milli-Q rinsed; 18.2 MΩ cm^{-1}; x3), using a short measure of silicon tubing after rinsing 3 times with sample. Subsamples were taken from the carboys in the wet laboratory on board.

All materials were acid washed (10 % HCl) and rinsed with Milli-Q water (18.2 Ωcm^{-1}; x3). Glassware and GFF filters were also combusted for 4 h at 450 °C prior to acid washing.

2.2. Dissolved phosphate determination

Water samples were filtered (47 mm Whatman GF/F, combusted for 4 h at 450 °C) under low vacuum pump pressure (<15 kPa). The limitation of using GF/F filters was that the 0.7 μm poresize allowed bacteria, colloids and particles smaller than 0.7 μm (including picoplankton) to pass through the filter. At the time, polycarbonate filters were used but found to interfere with dissolved organic phosphorus in an unexpected manner, with inconsistent removal of DOP occurring when particulates and phytoplankton biomass concentrations were higher. Meanwhile, polyethene filters were not viable due to the number of samples and the cost of the filters. Comparison of filtered and unfiltered samples from Liverpool Bay using the QuAAtro autoanalyser (as described below) indicated that particles did not contribute to the phosphomolybdate blue reaction during analysis. Therefore, the main interference with dissolved phosphorus concentrations resulting from filtering with GF/Fs was thought to relate to phase transformations that may have occurred during sample storage. However, as it was necessary to conduct some form of filtration on samples before storage, filtration with GF/F was considered the most appropriate technique.

In cases where samples were not analysed on board (JC25 and CE911), the 0.7 μm filtrates were stored in 250 mL HDPE bottles (acid washed and Milli-Q rinsed; 18.2 $M\Omega cm^{-1}$; x3) at -18 °C until analysis.

Soluble reactive phosphorus (SRP, herein considered synonymous with dissolved inorganic phosphorus, DIP) was determined by the standard phosphomolybdate blue method (Murphy and Riley, 1962) using a Bran and Leubbe QuAAtro 5-channel autoanalyser (detection limit, 0.05 μM PO_4^{3-}).

Method validation:

Internal laboratory standards (OSIL) made to final concentrations of either 0.5 μM or 1 μM in artificial seawater were analysed alongside samples to compare inter-analysis reproducibility and accuracy (within ± 2 %).

During analysis of surface samples, DIP was often found to be very low (0.1-0.2 μM). The reagent blank was determined through calculating the difference between the baseline when all reagents were running through the system and the baseline when molybdate was replaced by Milli-Q water (18.2 $M\Omega cm^{-1}$). The limit of detection was calculated as the baseline blank plus three standard deviations of the baseline signal (Miller and Miller, 2005). The highest limit of detection for phosphate was calculated as 0.05 μM (for other nutrients the limits of detection were calculated to be 0.1 μM N+N, 0.5 μM Si, and 0.05 μM NO_2).

To confirm the accuracy of the low phosphate concentrations and rule out instrument error in blank determination at low concentration, a selection of samples were pre-concentrated using the MAGIC protocol (Karl and Tien, 1992) before reanalysis. In brief, 50 mL triplicates of samples were treated with 1.25 mL NaOH (1 M) to induce the co-precipitation of DIP and magnesium when incubated for 5 min, followed by short mixing and another 5 min incubation (20°C). The cloudy precipitate formed (brucite) was separated from solution by centrifugation (1000 x g for 60 min, 20 °C) and the supernatant discarded. The precipitate was then redissolved in 8.5 mL of 0.1 M HCl and sonicated for 15 min. Samples were made to 10 mL volume with 0.1 M HCl, giving 5-fold concentration of DIP.

Table 2.1. Values labelled 'QuAAtro' refer to those obtained from direct analysis of seawater samples whereas values labelled 'MAGIC' refer to values obtained for samples that were first pre-concentrated using the protocol of Karl and Tien (1992). Values are given in μM.

	Quaatro μM	MAGIC μM	% Error
Sample A	0.12	0.09	26.7
Sample B	0.15	0.16	4.0

2.3. Dissolved organic phosphorus (DOP) determination

Total dissolved phosphorus (TDP) was determined by UV-oxidation (Armstrong et al., 1996). UV oxidation has previously been reported to give lower recoveries than persulfate oxidation and high temperature oxidation methods due to poorer recovery of ATP, guanosine-5 diphosphate and

polyphosphate during UV oxidation (Ridal and Moore, 1992; Ormaza-Gonzalez and Statham, 1996). Therefore, using the UV oxidation method may result in underestimation of the DOP pool but the degree of this underestimation will depend on the composition of the DOP pool. As some samples were oxidised during ship-board experiments, UV oxidation was chosen as it is a cleaner and safer method of oxidation and the same methods were used throughout to give results the project internal consistency assuming similar composition of the DOP pool.

Samples were photo-oxidised at ~82°C for 2 h in 10 mL aliquots using a Metrohm 705 UV Digester fitted with a high pressure mercury lamp. The method is based on the photolytic generation of OH radicals that subsequently react with organic compounds and decompose them. With each oxidation experiment, at least one sample was oxidised in triplicate to indicate reproducibility.

DOP was calculated from the difference between total dissolved phosphorus (TDP) and soluble reactive phosphorus (SRP), i.e. DOP = TDP - SRP. The standard deviation, or 'error', of this analysis was calculated using the following equation:

$$Error = \sqrt{(sd_{SRP}^2 + sd_{TDP}^2)/(n-1)}$$

where sd_{SRP} is the standard deviation of the soluble reactive phosphorus measurement and sd_{TDP} is the standard deviation associated with UV-oxidation and subsequent total dissolved phosphorus measurements (Miller and Miller, 2005).

Method validation:

In a Metrohm UV-oxidiser, samples are placed in one of 11 positions (with position 12 housing a thermometer in a test tube of water to monitor the temperature of the reaction) encircling a high pressure mercury bulb that emits UV radiation. Faulty UV-bulbs can irradiate samples unevenly, oxidising samples at certain positions more strongly than those at others, such regions are referred to as 'hotspots'. The UV-bulb was tested for

hotspots by oxidising replicate samples in all vial positions for 2 h, giving a standard deviation of 0.02 – 0.09 μM, which corresponded to a covariance of 2.29 – 5.03 % (samples 1 and 3, respectively; Fig. 2.1).

Oxidation efficiency was tested by incubating replicate aliquots of 5 samples over a time course to discern when TDP reached a plateau thus suggesting complete oxidation of dissolved organic phosphorus (DOP). A plateau was consistently reached after 2 h of incubation (Fig. 2.2).

Precision and recovery efficiency of various organic phosphorus constituents was confirmed through oxidation and analysis of model compounds (adenosine-mono-phosphate (AMP); adenosine-di-phosphate (ADP); adenosine-tri-phosphate (ATP); 2'-deoxyguanosine 5'-monophosphate disodium salt hydrate (dGMP), and phospho(enol)pyruvic acid monopotassium salt (PEP)). Consistently low recoveries of ADP and ATP were found (Table 2.2), as has been previously reported for ADP, ATP (Thomson-Bulldis, 1997; Benitez-Nelson, 2000) and for polyphosphates (Armstrong et al., 1960). Nucleotides can contribute up to 50 % of the total DOP pool (Karl and Yanagi, 1997), thus potentially inefficient recovery of this group may limit the accuracy of DOP measurements made during this study. As the composition of the DOP pool can vary greatly, it is not possible to apply a standardised correction factor for poor recovery of ADP and ATP.

During the course of my work a replacement bulb was installed in the UV-oxidiser. The original bulb had blown during an experiment where the water-flow which cooled the system failed causing the bulb to rapidly overheat. The replacement bulb was tested as described above. The 'hotspot' test yielded a covariance of 1.91 % for all sample positions, the time course also showed 2 hours to be an adequate incubation period, and model compound recoveries are displayed in Table 2.3.

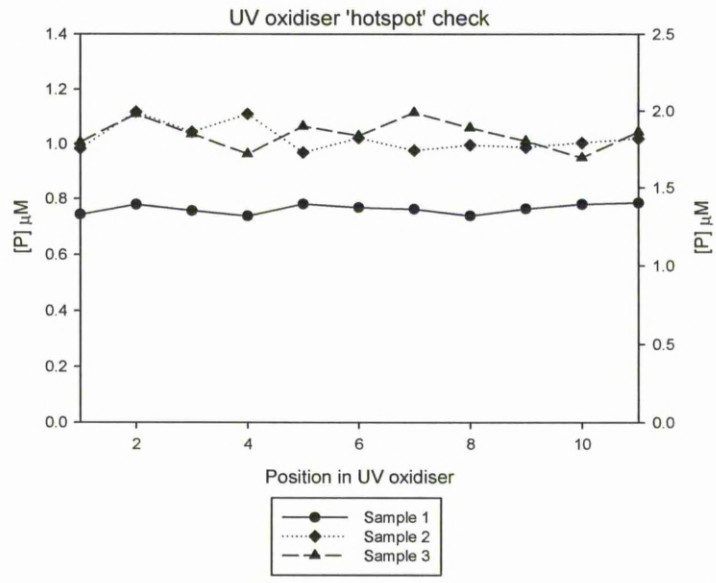

Figure 2.1. Variation in UV-oxidation efficiency relative to the position of replicate aliquots of 3 different samples. These experiments did not indicate any 'hotspots' on the UV bulb, thus suggesting even oxidation efficiency in all positions. Concentrations are shown in µM.

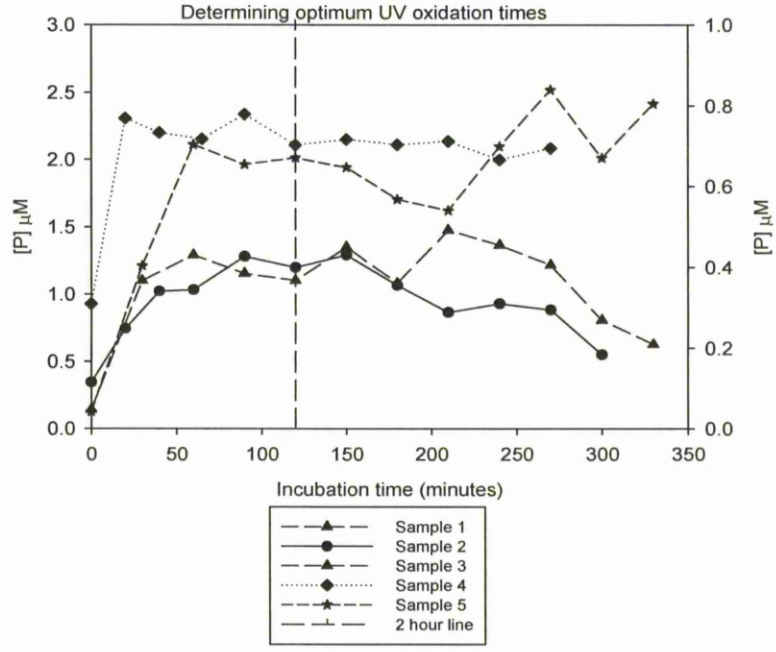

Figure 2.2. Variation in total dissolved phosphorus (µM) of replicate aliquots of 4 different samples over a UV-oxidation time course.

Table 2.2. UV-oxidation recovery results for model organic phosphorus compounds. The oxidation classification relates to whether the concentration refers to before ('raw') or after 2 h UV-oxidation. The concentration added refers to the concentration expected assuming 100% oxidation and recovery.

Oxidation	Raw	Raw	2hr UV	2hr UV
Conc. Added	1μM	2μM	1μM	2μM
ATP	0.03	0.05	**1.52**	**0.33**
ADP	0.07	0.10	**0.29**	**0.44**
AMP	0.00	0.01	**0.92**	**1.97**
dGMP	0.01	0.05	**0.81**	**1.59**
PEP	0.02	0.01	**1.04**	**2.04**
OSIL	0.96	0.97		
DIW	0.01			

Table 2.3. UV-oxidation results for model organic phosphorus compounds, second bulb. Values are blank corrected.

	Compound	% Recovered	% Stdev	
	AMP	113.34	1.05	
	ADP	11.54	2.31	
	ATP	9.49	10.02	
	dGMP	79.24	1.21	
	PEP	116.18	1.28	

2.4. Determination of the phosphomonoester fraction of the DOP pool

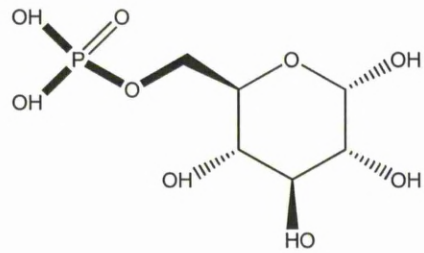

Figure 2.3. Glucose-6-phosphate; an example of a phosphomonoester.

While UV-hydrolysis of seawater samples can be used to assay total UV-reactive DOP, only a fraction of this pool may be susceptible to enzymatic hydrolysis and therefore available to phytoplankton and microbial communities. Phosphomonoesters can dominate the DOP pool in surface waters (Strickland and Solorzano, 1966; Karl and Yanagi, 1997) and with simple monoester bonds (either P-O-P or C-O-P bonds; Fig. 2.3) they are also the most bioavailable as they are susceptible to hydrolysis (Clark et al., 1998; Kolowith et al., 2001; Karl et al., 2008). Alkaline phosphatase specifically hydrolyses monoester bonds and is commercially available. In a similar way to the DOP protocol, the phosphomonoester fraction is determined as the difference in phosphate concentration before and after incubation of samples with commercially bought alkaline phosphatase as described in the protocol of Monbet et al. (2007).

Phosphomonoester concentrations were determined at the same depths as alkaline phosphatase activity assays on D352 and at all sampling depths on JC25, but not CE911. The method used in this study was based on the

published protocol of Monbet et al. (2007), which had also been successfully applied to estuarine water samples (Monbet et al., 2009).

Seawater samples were filtered through Millipore polyethene membrane filters (nominal pore size 0.2 μm, diameter 47 mm) under vacuum pressure (<15 kPa) to remove all phytoplankton and bacteria that might assimilate the enzymatically liberated phosphate. Five 25 mL subsamples were collected in separate Sterilin vials (Fisherbrand) per sampling depth. This allowed for two controls (T_{zero} and T_{final}) and triplicate enzyme incubations. Alkaline phosphatase was prepared in 0.1 M Tris buffer (pH 9) solution to a final concentration of 1 unit mL^{-1} buffer. Magnesium chloride was added to the buffer solution (final concentration 2 μM $MgCl_2$) as an enzyme activator. The enzyme solution was then added at 5.5 % v/v as in the original Monbet et al. (2007) protocol, which in this case was 1.5 mL. Once treated with enzyme solution, samples were incubated at ambient room temperature (~18 °C) for 24 hours. Samples were then frozen and later analysed on the QuAAtro 5-channel autoanalyser (Seal Analytical) as described in section 2.2.

Method validation:

Enzyme induced hydrolytic breakdown of organic phosphorus compounds was tested on the representative model compound D-glucose 6-phosphate dipotassium salt hydrate ($C_6H_{11}K_2O_9P.xH_2O$); 2; Fig.2.3). Although this is likely a very simple molecule relative to real samples, it nonetheless allowed determination of recovery through enzyme-hydrolysis and reproducibility. Once corrected for alkaline phosphatase mixture and abiotic compound breakdown contributions to measured phosphate concentrations, incubations were found to give 92.2 % recovery (± 8%, n=9).

2.5. Particulate phosphorus (PPhos) determination

Particulate phosphorus was determined after filtration of 1 L of seawater sample collected onto 0.7 μm GF/F (25 mm; Whatman; combusted at 450 °C for 4 h and acid cleaned). Sample filters were stored in glass test tubes (combusted and acid cleaned) at -18 °C until analysis. Particulate phosphorus was determined according to the Hawaii Ocean Time series protocol (Karl et al., 1991). Samples were combusted at 450 °C for 4.5 h in

a muffle furnace. After cooling, 5 mL of 0.5 M HCl (VWR Analytical Grade) was added and samples were incubated for 60 minutes at room temperature before centrifugation at 3000 x g for 30 minutes. The supernatant was diluted (1:4 sample to DIW) and analysed using the standard phosphomolybdate blue method (Murphy and Riley, 1962) using a Bran and Leubbe QuAAtro 5-channel autoanalyser. Precision and accuracy of analysis were determined through conducting the method with Apple Leaves (NIST); an international reference material. Measurements were blank corrected (acid-cleaned GFF, combusted at 450 °C for 4 h). The limit of detection for PPhos determination was 0.001 μM.

Method validation:

Particulate phosphorus recovery was assessed through analysis of 10 freeze-dried apple leaf samples ranging from 0.4-0.9 mg. The mean percentage recovery was 83.2 ± 8.69 % (covariance 10.44%). It is thought that part of the variability may have resulted from the tin vials that were used to weigh out the apple leaves collapsing upon combustion and not dissolving in the latter stages of the method, potentially hindering phosphorus dissolution. After communication with Karin Bjorkman of the Hawaii Ocean Times series team, a new approach to certified reference material (CRM) recovery checks was employed. Pre-weighed apple leaves were mixed with distilled water to form a dilute slurry (20 mg apple leaf powder in 10 mL distilled water of Milli-Q standard). The slurry was vortexed constantly to maintain an even suspension, briefly stopping to remove 250 μL aliquots that were transferred to test tubes. The test tubes were loosely capped with combusted foil, dried overnight at 50°C before being foiled tightly and combusted at 450 °C for 4.5 hours. The method was then as recorded above. Phosphorus recovery determined through this new method was 100.5 ± 3.9 % (n=20). Another set of CRMs were run with GFF filters. These gave a mean recovery of 96.3 ± 4.4 % (n=7), once blank corrected.

2.6. Alkaline phosphatase activity – rate assays

Alkaline phosphatase activity (APA) rate assays were conducted on unfiltered seawater samples collected from discrete depths, typically from either near-surface and SCM depths during JC25 and CE911, with

additional sampling at the base of the thermocline and bottom mixed layer depths during D352. The rationale for not filtering samples was that this would provide total community APA, rather than individual size classes, and would avoid cell lysis caused by filtering which may increase enzyme activity. While detail on size-class distribution of APA would have been interesting, in terms of DOM dynamics total community APA was thought to be sufficient, particularly in instances where accompanying cell-specific APA data was available.

APA was measured fluorometrically (Ammerman, 1993). In brief, samples were incubated on-deck at ambient surface seawater temperature (maintained by the ship's underway flow system) at adjusted light intensity for respective water column depths in 250 mL acid-cleaned clear polycarbonate bottles. The fluorogenic artificial enzyme substrate, methylumbelliferyll phosphate (MUFP; Sigma Aldrich), was added to replicate samples at various final concentrations (200 nM, 400 nM, 800 nM, 1200 nM, and 1600 nM). Controls (DIW, 400 nM MUFP; boiled sample, 400 nM) and sample blanks (seawater, no MUFP) were incubated and measured simultaneously with the samples. Hydrolysis of MUFP to the fluorescent product methylumbelliferyll (MUF) was measured at 2 h intervals over a 12 h incubation period. Change in fluorescence was measured, after pipetting 3 mL sample, with 1 mL 50 mM sodium tetraborate buffer (pH 10.5) into an acid-cleaned glass test tube, using a Turner 10AU fluorometer (excitation 365 nm, emission 455 nm). MUF standards (Sigma Aldrich) were shown to give a linear change in fluorescence over the anticipated concentration range.

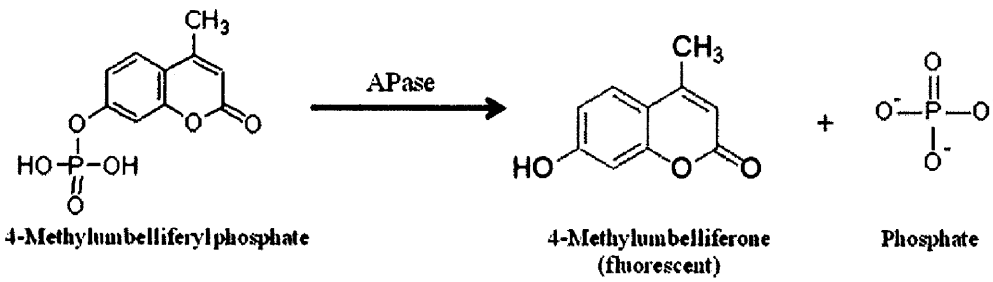

Figure 2.4. A simplified diagram of the hydrolysis of the artificial enzyme substrate 4-methylumbelliferyl phosphate by alkaline phosphatase to produce the fluorogenic product 4-methylumbelliferone and a phosphate molecule.

2.7. Cell specific alkaline phosphatase activity – enzyme labelled fluorescence (ELF)

Cell-specific APA was measured during D352 using the procedure for ELF-97 labelling as described in Dyhrman and Palenik (1999). The method used here was adapted as the method described by Dyhrman and Palenik (1999) involves cell concentration by centrifugation, which was not appropriate for this research. Instead, a method whereby cells were concentrated by filtration on a polycarbonate filter (0.8 μm pore size) was adopted after communication with Sonya Dyhrman of Woods Hole and as described in Rees et al. (2009). In brief, 1 L of seawater was collected on 25 mm polycarbonate filter (0.8 μm nominal pore size) under low vacuum pressure (<15 kPa), without drying. The filter was immediately placed on a 25 mm GF/F in a petri dish and 1 mL of 70% ethanol (Fisher Scientific) added before incubating for 30 min in the dark at 4 °C. The polycarbonate filter was then transferred to a new petri dish and GF/F before 400 μL of 1:20 ELF-97 reagent (Molecular Probes) was added. The filters were then incubated for 45 min in the dark at 4 °C. Once the incubation was completed the filter was transferred back to the filter rig and rinsed with approximately 10 mL of sterile, low phosphorus seawater. The polycarbonate filter was mounted onto a microscope slide using the mounting medium provided in the ELF Phosphatase Detection kit (Molecular Probes) and stored in the dark at 4 °C until examination. Samples were examined with a Zeiss epifluorescence microscope (courtesy of Paul Loughnane, University of Liverpool Biological Sciences Department) using a DAPI long pass filter set (emission 520 nm, excitation 350 nm set at 100 x magnification).

2.8. Nutrient addition experiments

Alkaline phosphatase activity may be constitutive or induced. When activity is constitutive it is not repressible through the addition of phosphate, unlike induced activity which occurs as a result of phosphorus stress. Whether alkaline phosphatase activity is inducible or repressible in a community can give a good indication of the dynamics of DOP turnover in a system.

In polycarbonate bottles, unfiltered seawater samples were incubated for 48 hours with either 4 μM phosphate (as $KHPO_4$) or 10 μM glycine. A control was incubated alongside the treatments in light adjusted on-deck incubators, kept at sea surface water temperature. After 48 hours, sub-samples were taken and incubated with methylumbelliferyl phosphate (MUFP) as described in section 2.6.

2.9. Phosphate fluxes

During JC25 turbulent kinetic energy dissipation profiles (ε) were obtained during periods of near continuous water column sampling using a free falling vertical microstructure profiler (VMP; Rockland Scientific International VMP750; data courtesy of Dr Matthew Palmer, NOCL) with accompanying temperature measurements. Profiling was terminated intermittently to allow for reference CTD profiles. VMP temperature was calibrated with CTD-temperature. Eddy diffusivity (Kz) was calculated from TKE dissipation (e.g. Sharples et al., 2007):

$$Kz = \Gamma \frac{\varepsilon}{N^2} \ (m^2 s^{-1})$$

Where, Γ is the mixing efficiency considered to be constant at 0.2, N is the buoyancy frequency (s) calculated using the VMP density profile (ρ, kg m^{-3}):

$$N^2 = -\frac{g}{\rho}\left(\frac{\delta\rho}{\delta z}\right) \text{ in } s^{-2}$$

With g = 9.81 m s^{-2} and z is depth in metres (positive upward).

Phosphate concentrations were correlated to temperature across the lower thermocline layer ($p < 0.001$; Fig 2.5). VMP data were used to determine the change in stratification and thus the depth of the base of the thermocline based on Buoyancy frequency (N^2). Buoyancy frequency values of ~$5x10^{-5}$ (corresponding to a temperature change of >0.01 °C) were taken to depict the base of the thermocline, although a little variation was required to account for changing structure between series. Corresponding phosphate concentrations were calculated from temperature at 1 m above and below the base of the thermocline using the equation derived from the

temperature-phosphate relationship observed in the lower thermocline during JC25 (Fig 2.5).

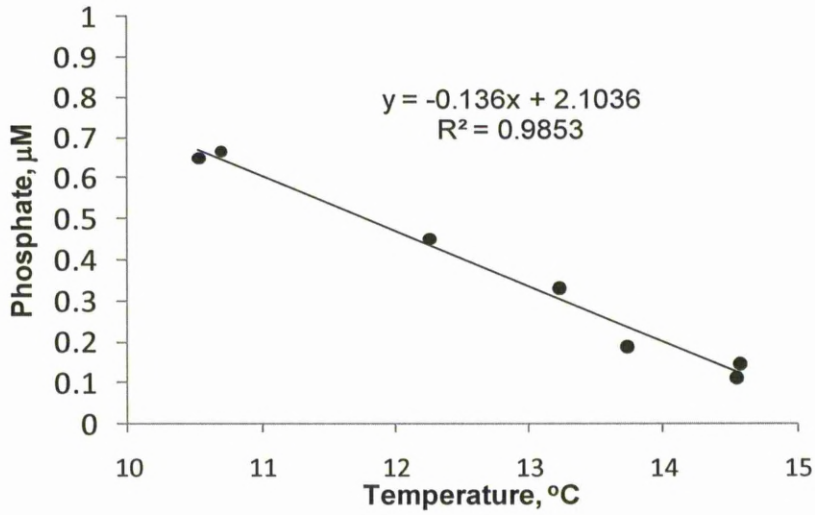

Figure 2.5) Thermocline layer phosphate concentrations against accompanying CTD- derived temperature.

The phosphate flux for each profile was calculated as in Sharples (2007):

$$PO_4^{3-}\ flux = -Kz\left(\frac{\delta PO_4^{3-}}{\delta z}\right)\ mmol\ m^{-2}\ s^{-1}$$

The phosphate flux was calculated over a time series of profiles (approximately covering a tidal period of ~ 12.4 hours), and from this the daily flux of phosphate across the base of the thermocline was estimated.

3. TEMPORAL VARIABILITY OF PHOSPHORUS DYNAMICS IN THE CELTIC SEA:

WIND MIXING EVENTS

3. Temporal variability of phosphorus dynamics in the Celtic Sea: wind mixing events

Summary

At the shelf edge, internal tides play an important role in mixing the water column. On-shelf waters can be isolated from these processes and in such regions wind mixing becomes an important process causing mixing across the thermocline during summer stratification. In this chapter, data are presented from two cruises. The majority of data was collected in June 2008 during a research cruise on the *RRS James Cook* in the Jones Bank region of the Celtic Sea after a strong wind mixing event. The second research cruise was in July 2010 and data were collected aboard the *RRS Discovery* before and after a wind-mixing event. During the latter cruise, mixing experiments were conducted whereby deep water was artificially mixed with thermocline waters and incubated on deck whilst tracking biogeochemical rates and parameters.

As the initial objective of the 2008 Jones Bank cruise was to observe the influence of tidal currents interacting with a submerged shallow bank, the data are initially presented in relation to the initial objective before analysing the much stronger temporal trends relating to the wind-mixing event signal. The 2010 Celtic Sea cruise data are then drawn upon and discussed together in relation to whether such events act to drive a net gain or loss of dissolved organic phosphorus.

3.1. Introduction

The Celtic Sea forms part of the temperate northwest European shelf sea system, bordered by an irregular shelf edge with the North Atlantic to the west, St Georges Channel and the Irish Sea to the north, and the English Channel to the east (Fig 3.1). The water column is relatively shallow, ranging from ~70 m over tidal sand banks to <200 m across the shelf. Tidal streams range from ~0.38 to 0.75 ms^{-1} (Pingree and Mardell, 1985; Pingree et al., 1976; Williams and Conway, 1984) with typical M_2 tidal amplitudes ranging from 0.2-0.5 ms^{-1} (Sharples, 2008).

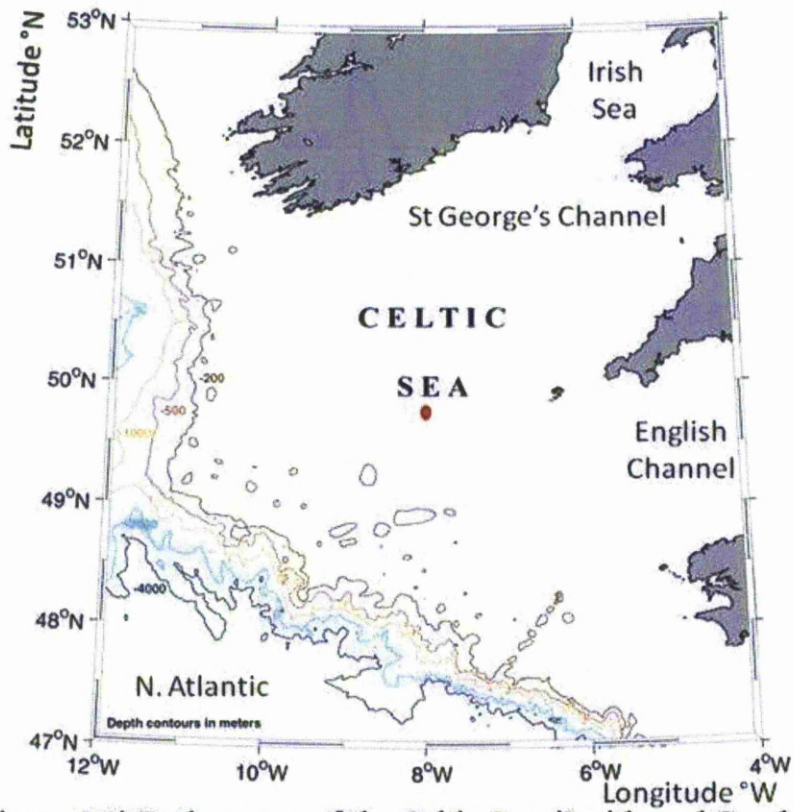

Figure 3.1) Bathymetry of the Celtic Sea (Smith and Sandwell, 1997); the red dot indicates Jones Bank.

Competing vertical mixing and stabilising effects, namely tidal mixing and solar heating, respectively, dictate water column structure in the Celtic Sea. During the winter months the water column is strongly mixed as tidal and wind mixing, and convection from surface heat loss overcome surface heating (Pingree et al., 1976). At this time, surface nutrient concentrations are high, but phytoplankton biomass remains low as production is limited by light (Hydes et al., 2004; Hickman et al., 2009).

Water column stability becomes enhanced as solar heating increases in spring. In deeper regions where tidal streams are weaker, thermal buoyancy forces overcome mixing and a seasonal thermocline becomes established, typically sometime in April (Pingree et al., 1976). The development of the thermocline is key to subsequent biogeochemical processes in the water column. Biological production varies seasonally with water column stability. At the onset of summertime stratification, light limitation of phytoplankton

production is alleviated for those phytoplankton trapped above the thermocline. A spring bloom develops in the surface mixed layer (SML) until growth is limited by nutrient availability and grazing pressure (Kiorboe, 1993).

Summertime stratification remains until its breakdown in the autumn as solar heating decreases. Until then exchanges between the buoyant surface mixed layer (SML) and bottom mixed layer (BML) are suppressed by the thermocline barrier. As such, surface concentrations of inorganic nutrients and chlorophyll are relatively low (Pemberton et al., 2004). However, summertime shelf sea productivity remains relatively high due to the development of a subsurface chlorophyll maximum (SCM; Rippeth, 2005).

In the Celtic Sea, the SCM is laterally patchy. It occurs in the euphotic zone at ~5 % surface PAR (photosynthetically available radiation), towards the base of the thermocline, and is associated with the nitracline (Sharples et al., 2001; Hickman et al., 2009). Previous studies report that the SCM develops within the thermocline as phytoplankton survival is favoured by the relatively low turbulence, and sufficient light and nutrient levels to support growth (Sharples and Tett, 1994; Ross and Sharples, 2007). Nutrients sustaining the SCM are supplied through diapycnal fluxes from below the thermocline which are driven by turbulent dissipation of internal waves and inertial oscillation-induced shear stresses (Sharples et al., 2001; Sharples, 2008). These diapycnal fluxes provide nitrate to the SCM at a typical rate of ~2 mmol m^{-2} d^{-1} (Sharples et al., 2001), allowing SCM-production to have a high f-ratio and fuelling an important source of organic carbon within the system (Probyn et al., 1995). When tides and internal waves cause mixing at the nutricline and drive upward fluxes of nutrients, they also drive concomitant downward mixing of phytoplankton and have an assumed export potential (Sharples et al., 2001; Sharples, 2008). For SCM patches to exist a balance must be met between nutrient supply and phytoplankton dispersal (Pingree et al., 1976).

Boundary mixing resulting from the 'drag' of tidal currents across the shelf seabed can potentially result in spring-neap variability of turbulent mixing at the base of the thermocline. During stratification, wind-events are also

important in determining the physical structure of the water column; most notably the SML and thermocline. Wind-driven boundary mixing can deepen the thermocline entraining nutrients from deeper in the water column and potentially enhancing production in the SCM (Sharples and Tett, 1994) or the SML (Yin et al., 1995).

Previously, studies on nutrient fluxes in shelf seas have focussed on nitrate fluxes (Tweddle, 2007; Rippeth et al., 2007, 2009; Sharples et al., 2007) rather than phosphate. In the surface layer, ammonium can offer a crucial nitrogen source that can sustain phytoplankton production. However, there is no equivalent regenerated nutrient source of phosphorus. Thus, investigating the magnitude of phosphate fluxes across the base of the thermocline and the resultant transfers and assimilation rates of phosphorus through the water column is important to our understanding of nutrient dynamics in shelf seas. The following chapter aims to address the questions:

- How do tidal and wind mixing affect phosphate fluxes across the base of the thermocline?
- Is there a net gain of DOP after such events, how labile is it and what is its fate?
- What are the implications for shelf sea productivity?

In July 2008, as part of the Oceans 2025 programme Theme 3 "Shelf and Coastal Processes", a NERC-funded research cruise was conducted in the Celtic Sea on the *RRS James Cook*. The overall cruise objective was to investigate the impacts of Jones Bank, a large submerged bank, on the physical, chemical, biological and ecological characteristics of a stratified shelf sea. Jones Bank is one of the shallowest, innermost banks of the large northeast trending tidal sand bank system in the outer Celtic Sea. Jones Bank is situated 200 km from the shelf break; the bank itself is in ~70 m water while the surrounding water column is typically ~120 m deep (Fig 3.2). The principle hypothesis was that Jones Bank significantly perturbs the thermocline generating very strong local interior mixing, enhancing nutrient fluxes and primary production.

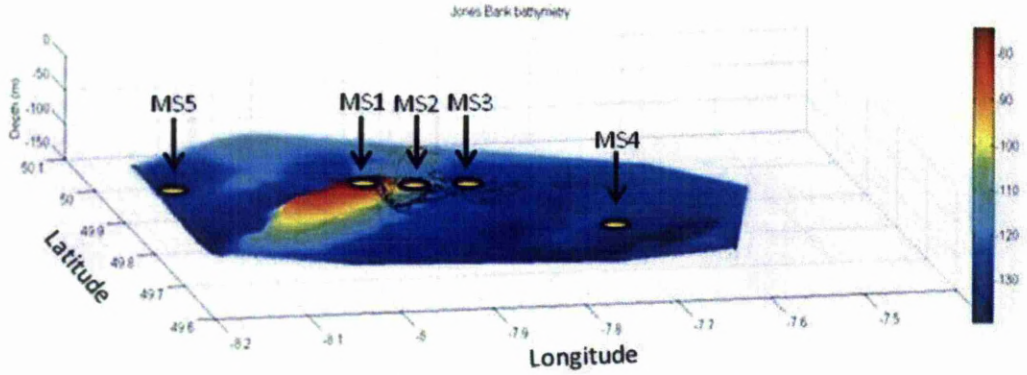

Figure 3.2) Bathymetry of Jones Bank; black line indicates the cruise track.

Sampling was conducted in the Jones Bank region over a 15-day period in July 2008 (decimal day 187 to 202). Sampling commenced during spring tides and continued across neap tides to the subsequent spring cycle. The depth of the water column ranged from 70-130 m depending on the location over Jones Bank and the surrounding shelf at the time of sampling (Table 3.1). A storm event with wind speeds up to 20 ms^{-1} coincided with the first spring tidal sampling, after which wind speeds fell to 8 ms^{-1} by the neap cycle and 12 ms^{-1} during the latter spring cycle.

During the 2010 Celtic Sea cruise on board the *RRS Discovery* (cruise details described fully in Chapter 4) data were collected to investigate the effects of wind induced mixing and pulses of mixing across the thermocline of the seasonally stratified Celtic shelf sea. During the cruise at an on-shelf station, 2 biogeochemical sampling CTD casts were conducted before and after a wind mixing event. Following on from this, mixing experiments were conducted on board, whereby varying ratios of bottom mixed layer (BML) water was mixed with thermocline waters and incubated over fixed lengths of time in on-deck incubators simulating thermocline temperature and light field. During these incubations, nutrients were sampled at regular intervals and DOP and APA were measured at the beginning and end of the incubation.

Table 3.1. Summary of station positions and their respective relationship to bank/current interactions (mean nominal depths are quoted).

Station	Depth (m)	Latitude (°N)	Longitude (°W)	Relationship with topographical mixing
MS1	70	49 51.21	07 56.80	Bank summit
MS2	110	49 56.30	07 52.58	Leeward of bank, strong mixing
MS3	125	49 56.30	07 48.83	Northeast of bank, isolated from effects
MS4	130	49 45.00	07 40.00	Southeast of bank, downstream
MS5	125	50 00.00	08 09.00	Northwest of bank, isolated

The majority of results and discussion in the following chapter relate to the 2008 Jones Bank cruise. The original hypothesis of tidal currents causing enhanced mixing over the bank is addressed first, before analysing the temporal trends in data caused by the extreme wind mixing event that occurred prior to sampling.

3.2. Results

3.2.1. Hydrography

During sampling on the earlier spring tide, bursts of turbulent dissipation were observed to propagate from the bed to the base of the thermocline (day 187.8 at ~ 40 m depth) over Jones Bank (Fig. 3.3, a). At the same time, wind driven boundary mixing was observed to penetrate the surface 20 m. Although the corresponding temperature profiles showed evidence of erosion of the base of the thermocline (e.g. at decimal day 187.8; Fig. 3.3, b), mixing was never sufficient to overcome stratification (Fig. 3.3, b).

a)

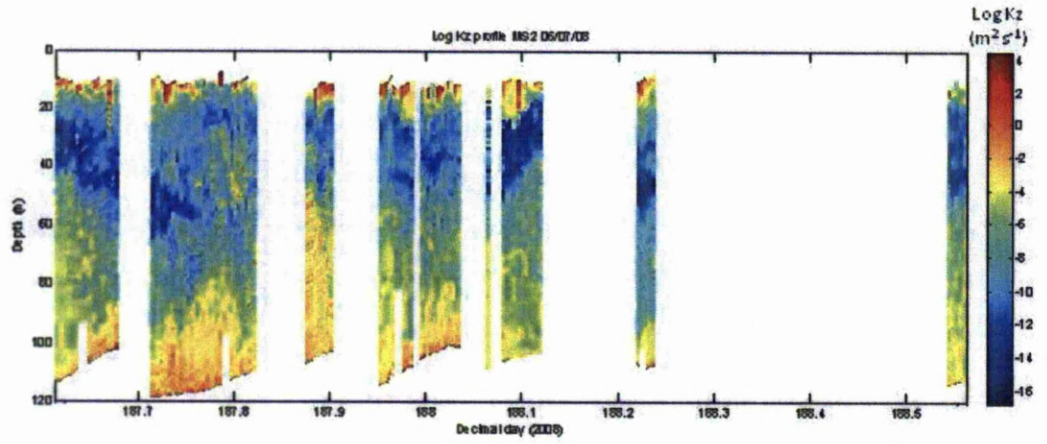

b)

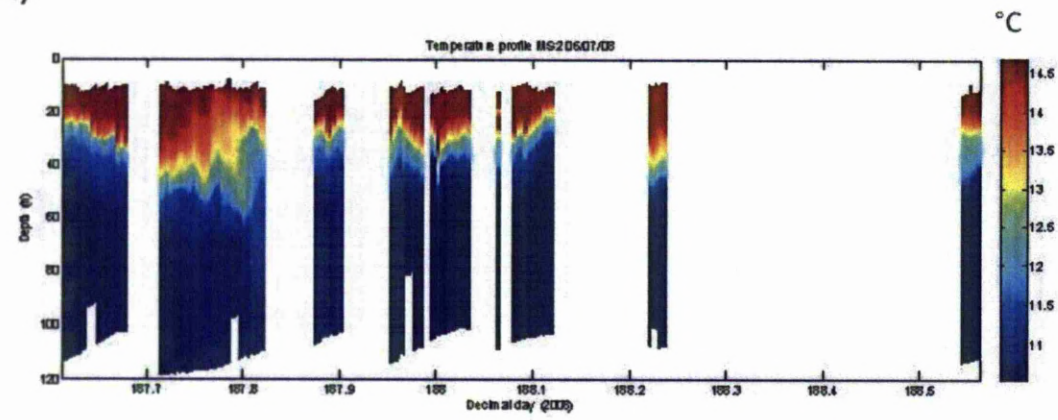

Figure 3.3| a) Depth profiles of eddy diffusivity (log Kz) over time at Jones Bank during the earlier, stormy spring tide; and b) corresponding temperature profiles. Gaps in the data resulted from breaks in sampling to allow for CTD sampling and instrument failure. Data courtesy of Dr Matthew Palmer, NOCL.

Thermal stratification of the water column was a persistent feature (Fig. 3.4, a). As such, the water column maintained a three layer structure consisting of a surface mixed layer (SML, T ~ 14 – 16 °C), a thermocline of varying thickness, and a bottom mixed layer (BML, T 10.6 ± 0.06 °C).

a)

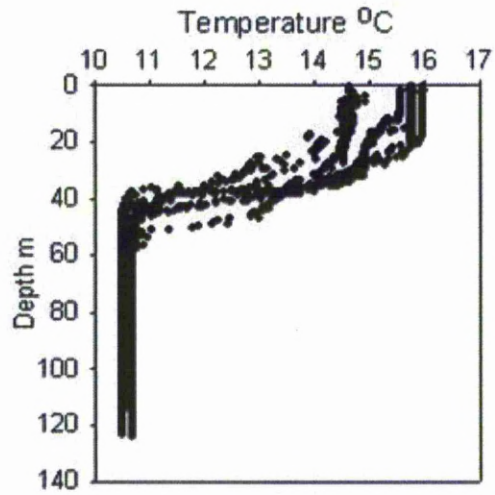

b)

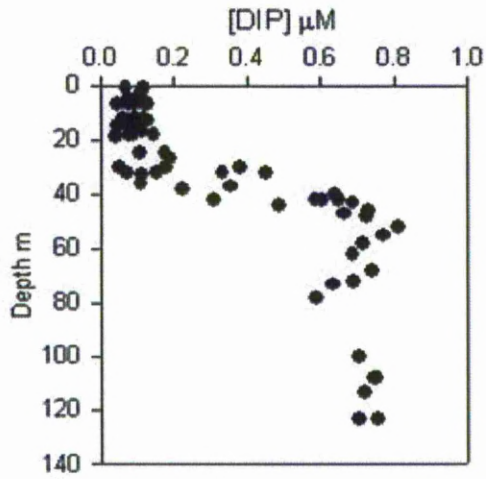

Figure 3.4) a) Temperature (°C) profiles for each biogeochemical CTD cast during the cruise; and b) corresponding phosphate (µM) profiles.

BML phosphate concentrations in this study were similar to winter concentrations for the Celtic Sea of ~ 0.53 – 0.68 μM reported in Hydes et al. (2004) and were consistently higher than SML concentrations. These high phosphate concentrations (~0.6-0.8 μM) in the BML reflect remineralisation of organic and detrital matter, probably originating in the euphotic layer, and winter recharge of the shelf with oceanic water. Conversely, biological uptake and assimilation of phosphate in the euphotic zone meant that SML concentrations were low (~0.1 μM; Fig 3.4, b). The thermocline acted as a boundary between these two layers – hosting the phosphocline, and facilitating some transfer while restricting general exchanges between the two layers. Thus, thermocline layer thickness was a significant controlling factor on phosphocline characteristics.

Calibrated CTD-fluorescence data indicated low chlorophyll *a* concentrations in the BML (~0.1 μg L^{-1}) and concentrations ranging from ~0.1-1.3 μg L^{-1} in the thermocline and SML (Fig. 3.5, a). Particulate phosphorus (PPhos) concentrations also suggested higher biomass in the euphotic zone than in the BML (<0.2 μM compared to 0.03 ± 0.02 μM, respectively; Fig. 3.5, b). Such a distribution can be attributed to the attenuation of light through the water column favouring phytoplankton survival in the euphotic SML and thermocline layers (surface 40 m; Sharples and Tett, 1994; Hickman et al., 2009), but not the BML. Supporting carbon fixation data (provided by L. Gilpin, Napier University) suggest that for the majority of sampling primary production rates were highest in the surface 15 m (Fig. 3.6) as has been found previously in the Celtic Sea (Joint et al., 1986).

a)

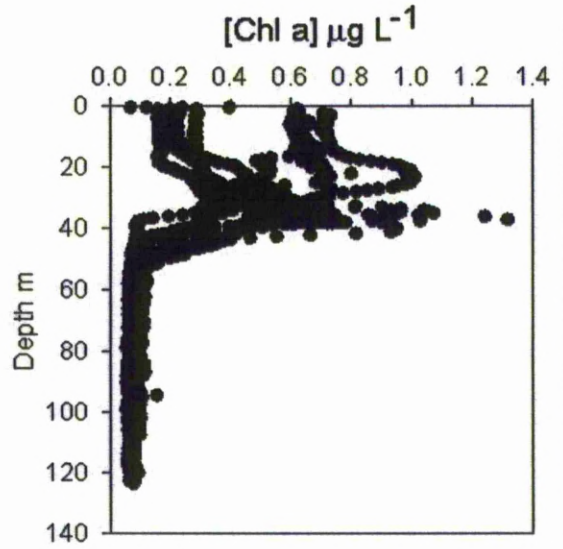

b)

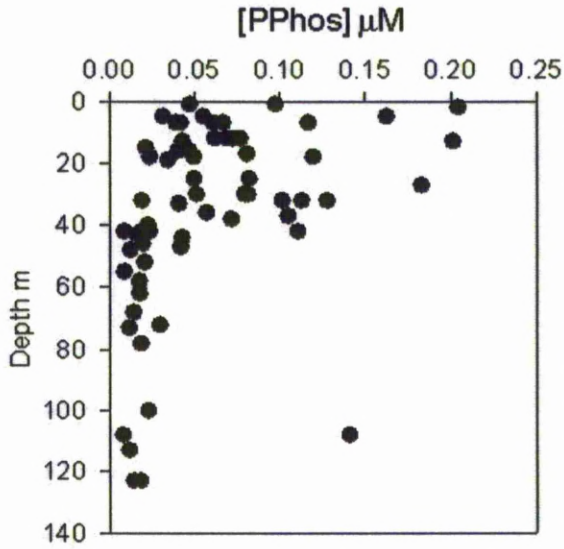

Figure 3.5) a) Chlorophyll (calibrated CTD fluorescence; µg L^{-1}) profiles for each biogeochemical CTD cast during the cruise; and b) corresponding particulate phosphorus (µM) profiles.

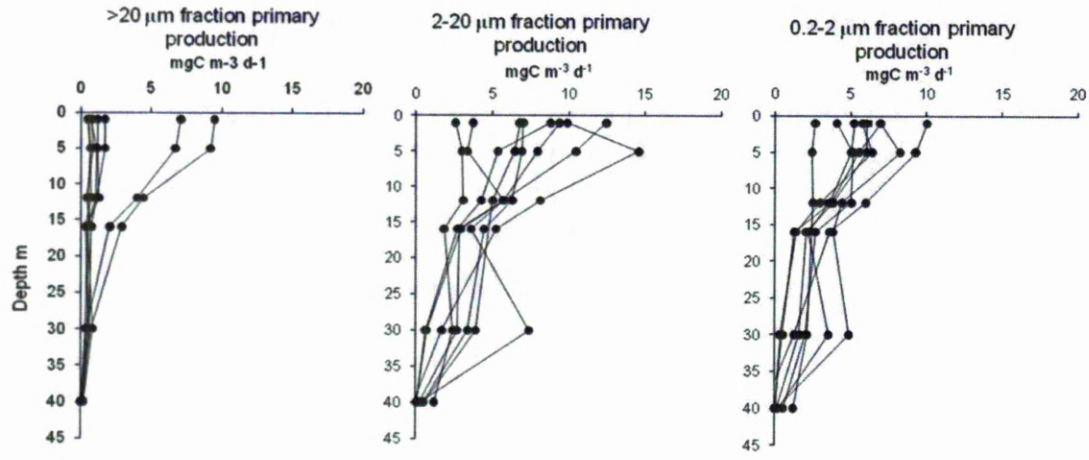

Figure 3.6) Primary production profiles for all pre-dawn biogeochemical CTD casts; left to right: >20 µm, 2-20 µm and 0.2-2 µm size classes. Data courtesy of Dr Linda Gilpin, Napier University.

Dissolved organic phosphorus (DOP) was observed at all depths, but concentrations were slightly higher in the SML and thermocline (~0.1-0.3 µM) relative to the BML (~0.1 µM; Fig 3.7, a). In the SML, 65 ± 14 % of TDP was DOP, with a range of 16 – 85 %. The proportion of DOP in the SML-TDP pool increased with time after the storm. After day 196, the percentage DOP was comparable to the range quoted for open ocean surface waters of 65 - 85 % (Karl and Yanagi, 1997). Partial characterisation of the DOP pool indicated that the highest phosphomonoester (PME) concentrations were in the euphotic zone (≤0.15 µM; Fig 3.7, b). Monoesters are considered to be the most labile fraction of the DOP pool (followed sequentially by diesters and phosphonates; e.g. Kolowith et al., 2001) and their presence suggests a relatively fresh component to the bulk DOP pool. The association between vertical profiles for DOP, chlorophyll *a*, carbon fixation rates, and PPhos combined with PME data suggested *in situ* production of DOP in the euphotic zone linked to primary production (e.g. Hopkinson et al., 1997).

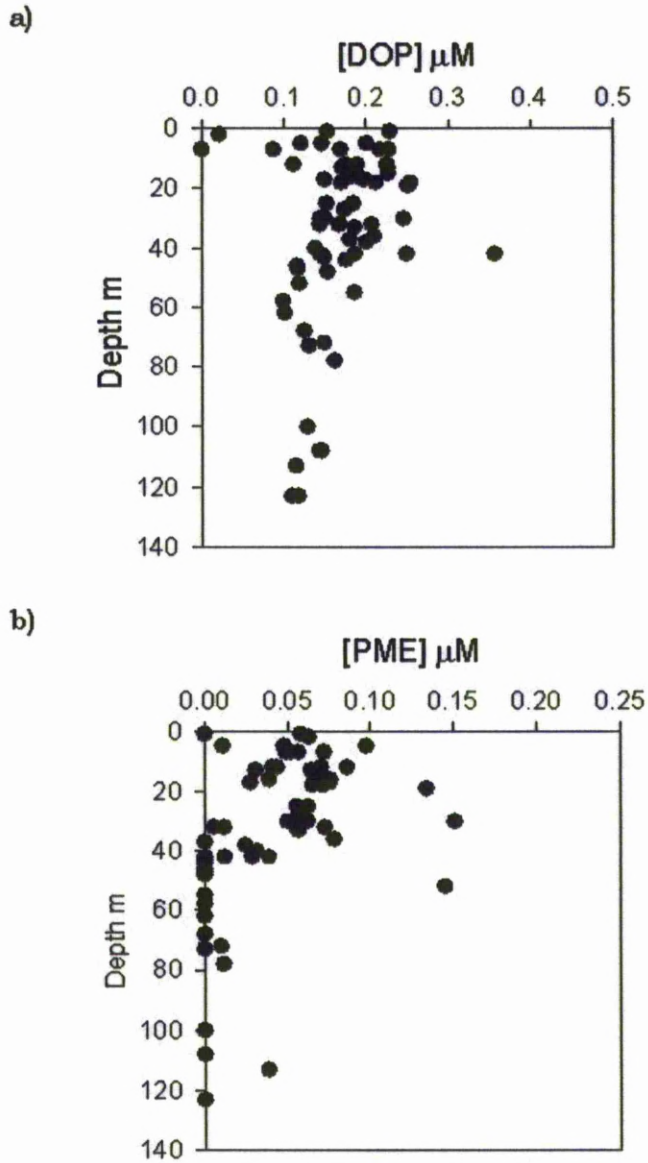

Figure 3.7) a) Bulk dissolved organic phosphorus (DOP; µM) profiles for each biogeochemical CTD cast; and b) corresponding phosphomonoester (PME; µM) profiles.

3.2.2. The interaction of tidal currents with Jones Bank – spatial trends

Stations were categorised into one of three groups depending on whether they were upstream- (Group I; MS3 and MS5), on/above- (Group II; stations MS1 and MS2), or downstream (Group III; station MS4; Table 3.1) of Jones Bank according to the mean residual flow. Data are presented in Tables 3.2 and 3.3.

Table 3.2) Physical and chlorophyll data for groups I, II and III; columns indicate sea surface temperature (SST, °C), buoyancy frequency (N^2), surface mixed layer depth (SML depth, m), depth of the base of the thermocline (base thermo, m), depth of the subsurface chlorophyll maxima (SCM depth, m), and chlorophyll concentration of the SCM (SCM peak, $\mu g\ L^{-1}$).

Group	CTD #	Demical day	Station	SST	$N^2 \times 10^{-4}$	SML depth	Base thermo	SCM depth	SCM peak
				°C	s	m	m	m	$\mu g\ L^{-1}$
I	1	186	3	14.89	4.23	28	51	32	3.42
	22	197	3	15.97	2.77	7	42	32	0.60
	23	198	3	15.77	2.95	13	48	30	0.93
	24	198	3	16.05	2.87	11	46	32	1.09
	25	198	3	16.10	3.02	9	46	33	0.88
	26	199	5	15.76	3.06	14	46	33	2.08
	27	200	5	15.76	3.41	19	52	34	1.63
	28	200	5	15.67	3.94	21	50	32	1.75
	29	200	5	15.90	2.95	18	42	30	0.78
Average				**15.76**	**3.24**	**15.56**	**47.00**	**32.00**	**1.46**
Stdev				0.36	0.513	6.60	3.61	1.32	0.89
II	10	190	1	14.65	2.38	17	43	18	0.68
	11	190	1	14.67	2.18	24	54	26	0.64
	31	200	1	15.93	3.10	24	55	34	0.66
	33	202	1	15.96	4.75	22	46	38	1.00
	34	202	1	15.98	3.61	22	46	33	0.93
	2	187	2	14.58	2.72	22	48	25	0.72
	3	187	2	14.63	2.20	15	46	17	0.69
	5	187	2	14.65	3.60	20	64	12	0.71
	6	188	2	14.55	1.62	24	44	18	0.75
	7	188	2	14.49	1.60	23	67	22	0.68
	8	188	2	14.58	1.92	14	56	15	0.87
	9	188	2	14.60	2.92	11	51	9	0.90
	19	195	2	15.37	3.98	24	47	32	0.94
	20	195	2	15.62	4.33	27	46	28	0.64
	21	196	2	15.58	2.97	31	47	38	0.75
	30	200	2	16.01	3.39	23	56	45	1.25
Average				**15.12**	**2.95**	**21.44**	**51.00**	**25.63**	**0.80**
Stdev				0.63	0.947	5.05	7.09	10.43	0.17
III	12	192	4	14.78	2.20	21	54	27	0.94
	13	192	4	15.01	2.37	12	49	17	0.94
	14	193	4	15.07	2.29	17	53	27	0.97
	15	193	4	15.00	2.91	18	49	25	1.13
	16	193	4	15.19	2.04	17	47	24	1.13
	17	193	4	15.05	3.44	17	53	17	1.22
	32	200	4	15.94	4.42	18	50	30	1.52
Average				**15.15**	**2.81**	**17.14**	**50.71**	**23.86**	**1.12**
Stdev				0.37	0.858	2.67	2.63	5.05	0.21

All significant values (p) were determined using one-way ANOVA tests as specified. There were no significant differences between groups for sea surface temperature (Tukey test, $p>0.05$), buoyancy frequency (Tukey test, $p>0.05$), and the depth of the base of the thermocline (Kruskal Wallis test, $p>0.05$). Physical parameters showed no significant differences between

groups I and II, however there were significant differences between groups I and III for SML depth (Tukey test, $p>0.05$), SCM depth (Dunn's test, $p>0.05$), and SCM peak intensity (Dunn's test, $p>0.05$).

Table 3.3| Phosphate (DIP), dissolved organic phosphorus (DOP), particulate phosphorus (PPhos) and phosphomonoester (PME) data for groups I, II and III; a) surface concentrations (μM); b) mean layer concentrations (μM); and c) integrated values (mmol m^{-2}).

a)

Group	CTD #	Demical day	Station	Surface [P]			
				DIP	DOP	PPhos	PME
				μM			
I	23	198	3	0.07	0.20	0.06	0.10
	27	200	5	0.07	0.23	0.05	0.06
II	2	187	2	0.11	0.02	0.20	0.06
	6	188	2	0.12	0.15	0.10	0.00
	10	190	1	0.10	0.15	0.03	0.01
	21	196	2	0.09	0.17	0.07	0.05
	33	202	1	0.05	0.23	0.04	0.06
III	12	192	4	0.13	0.09	0.06	0.07

b)

Group	CTD #	Demical day	Station	Surface layer mean				Thermocline layer mean			
				DIP	DOP	PPhos	PME	DIP	DOP	PPhos	PME
				μM				μM			
I	23	198	3	0.07	0.21	0.06	0.09	0.32	0.19	0.05	0.04
	27	200	5	0.07	0.23	0.04	0.05	0.22	0.21	0.04	0.04
II	2	187	2	0.13	0.12	0.14	0.06	0.42	0.18	0.13	0.05
	6	188	2	0.14	0.15	0.10	0.06	0.41	0.15	0.10	0.06
	10	190	1	0.10	0.17	0.05	0.03	0.32	0.16	0.05	0.05
	21	196	2	0.09	0.18	0.07	0.06	0.33	0.19	0.04	0.03
	33	202	1	0.05	0.23	0.03	0.09	0.29	0.27	0.04	0.07
III	12	192	4	0.10	0.11	0.08	0.07	0.21	0.14	0.07	0.04

c)

Group	CTD #	Demical day	Station	Surface layer integrated				Thermocline layer integrated			
				DIP	DOP	PPhos	PME	DIP	DOP	PPhos	PME
				mmol m^{-2}				mmol m^{-3}			
I	23	198	3	1.27	4.07	1.12	1.73	13.03	8.77	2.47	2.16
	27	200	5	2.11	6.34	1.16	1.23	6.55	8.40	1.61	2.16
II	2	187	2	3.45	2.58	3.64	1.68	11.00	5.90	5.06	1.93
	6	188	2	3.83	4.33	3.06	1.58	13.86	5.66	3.98	0.89
	10	190	1	2.04	3.45	1.14	0.63	15.09	8.41	3.11	2.67
	21	196	2	1.55	3.02	0.80	1.00	8.65	9.42	2.18	1.70
	33	202	1	1.20	5.83	0.76	1.69	5.19	10.41	1.87	4.88
III	12	192	4	2.34	2.26	1.57	1.55	10.44	7.11	3.53	1.81

There were no significant differences (one way ANOVA) in phosphorus data between groups, except for thermocline mean DOP concentration (Tukey test, $p<0.05$) although the significance of a mean concentration of a gradient is perhaps weak, particularly when $n = 1$ for group III (Table 3.3).

The lack of significant differences between groups suggests that spatial trends in water column characteristics arising due to topographical effects were complicated by the initial storm event. So rather than resolving spatial differences induced by Jones Bank topography interacting with tidal currents, the data were assessed in terms of temporal post-storm trends.

3.2.3. The influence of an extreme wind mixing event - temporal trends

3.2.3.1. Physical parameters

Sea surface temperature (SST) increased linearly ($p<0.001$; Fig 3.8, a) over the 15-day sampling period from 14.5 °C to 16 °C suggesting reduced deepwater inputs to the SML and increased surface warming. As BML temperatures remained consistent at ~10.5 °C, the increase in SML temperatures enhanced the thermocline gradient, strengthening stratification and water column stability. This is also reflected by the increase in buoyancy frequency (N^2; $p<0.001$; Fig 3.8, b) across the thermocline. However, the lack of trends in the depths of both the SML (Fig 3.8, c) and the depth of the base of the thermocline (Fig 3.8, d) suggest that internal tidal wave activity may have continued to perturb the thermocline after the storm subsided.

3.2.3.2. Chlorophyll and primary production

During the study the depth ($p<0.001$; Fig 3.9, a) and intensity of the SCM increased (chlorophyll *a* concentration, $p<0.05$; Fig. 3.9, b). The change in the vertical distribution of chlorophyll *a* (Fig. 3.10) during the study suggests that initially the enhanced wind-driven boundary mixing caused entrainment of thermocline waters and phytoplankton biomass from the subsurface chlorophyll maxima (SCM) into the SML (Yin et al., 1995). This resulted in a broad dispersal of phytoplankton biomass through the SML which was subsequently driven deeper during the progression to neap tides.

By day 194, the SCM had become closely associated with the base of the thermocline. Here, sufficient light and a diapycnal nutrient supply from

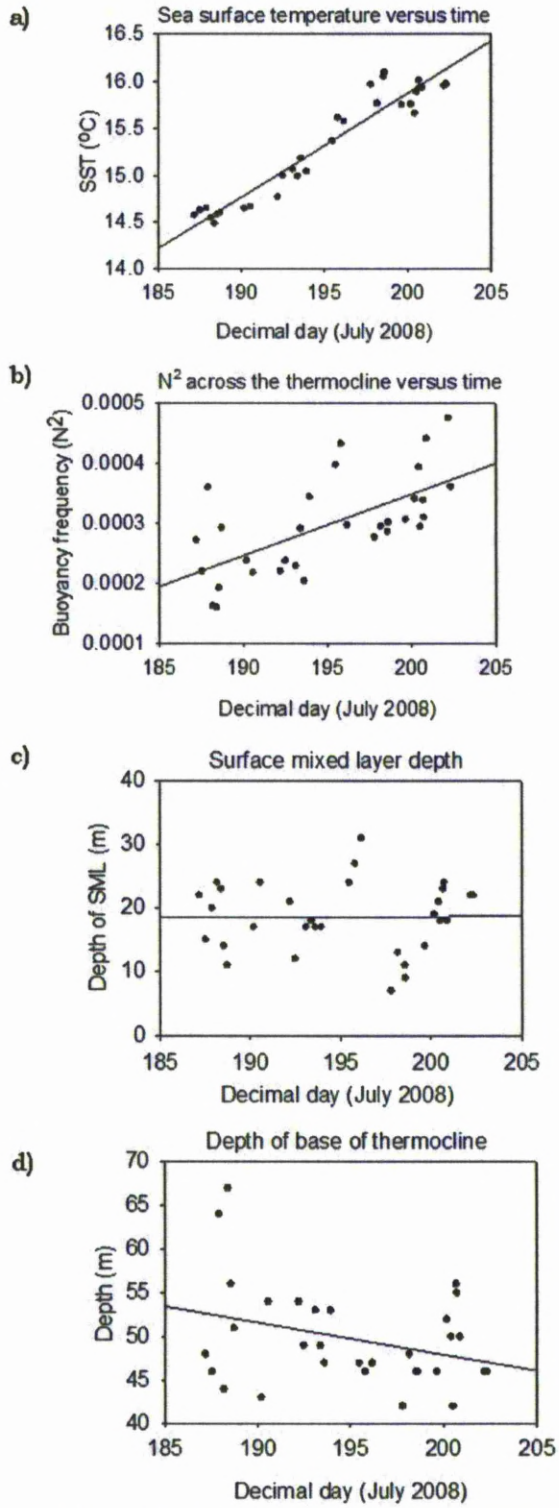

Figure 3.8) temporal trends in a) sea surface temperatue ($p<0.01$); b) buoyancy frequency ($p<0.001$); c) surface mixed layer depth ($p>0.05$); and d) depth of the base of the thermocline ($p>0.05$).

below the thermocline favoured survival, allowing phytoplankton to accumulate in a region of the water column with relatively low turbulence (Ross and Sharples, 2007).

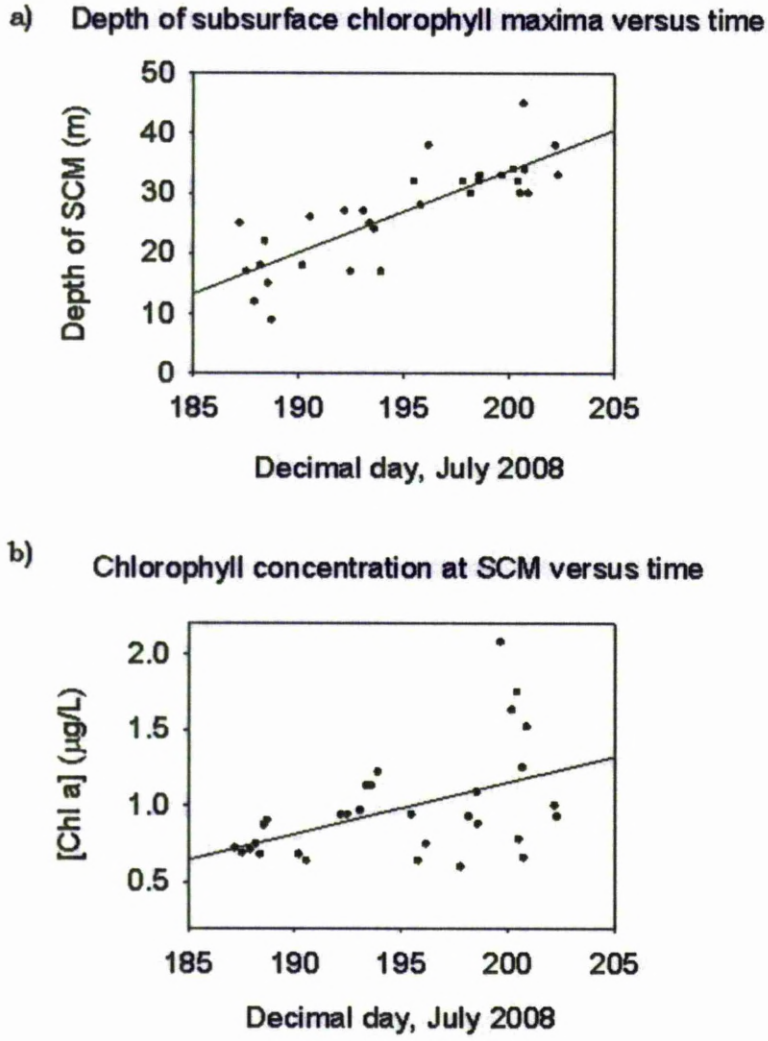

Figure 3.9) Temporal trends in a) depth of the subsurface chlorophyll maxima ($p<0.001$); and b) chlorophyll concentration at the subsurface chlorophyll maxima ($p<0.05$).

Changes in water column structure and mixing appeared to strongly influence primary production (production data courtesy of Linda Gilpin, Napier University). Larger phytoplankton species were most responsive to variations in mixing, being at their most productive when both tidal and wind mixing were strongest. Nanoplankton generally dominated production with larger phytoplankton contributing significantly during the initial bloom event when surface boundary mixing was stronger, consistent with Joint et al., (1986). Euphotic layer-integrated total primary production decreased

during sampling ($p<0.05$; Fig. 3.11, a) from ~350 mg C m^{-2} d^{-1} to ~250 mg C m^{-2} d^{-1}. The larger size class (>20 μm) of phytoplankton showed the greatest decrease in production rates (from ~140 mg C m^{-2} d^{-1} on day 186 to ~20 mg C m^{-2} d^{-1} on day 202; Fig. 3.11, b), while smaller size classes showed no distinct trends (Fig. 3.11, c and d).

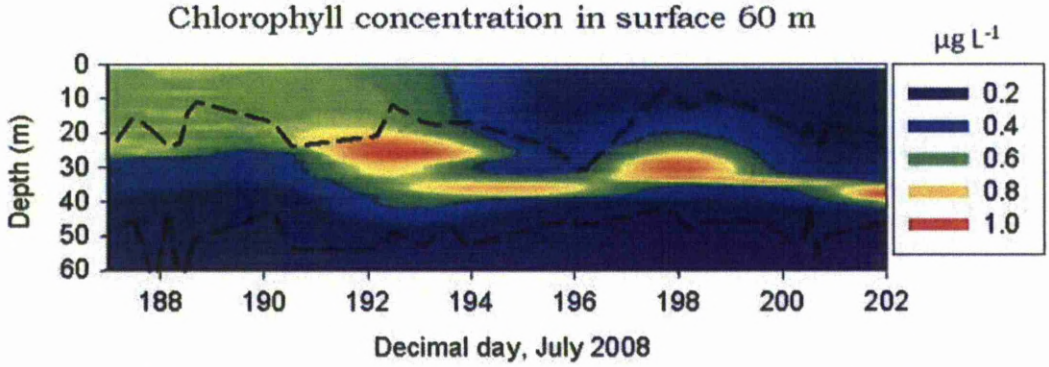

Figure 3.10| Depth profile of chlorophyll concentration over time during the study; black lines indicate the upper and lower bounds of the thermocline layer.

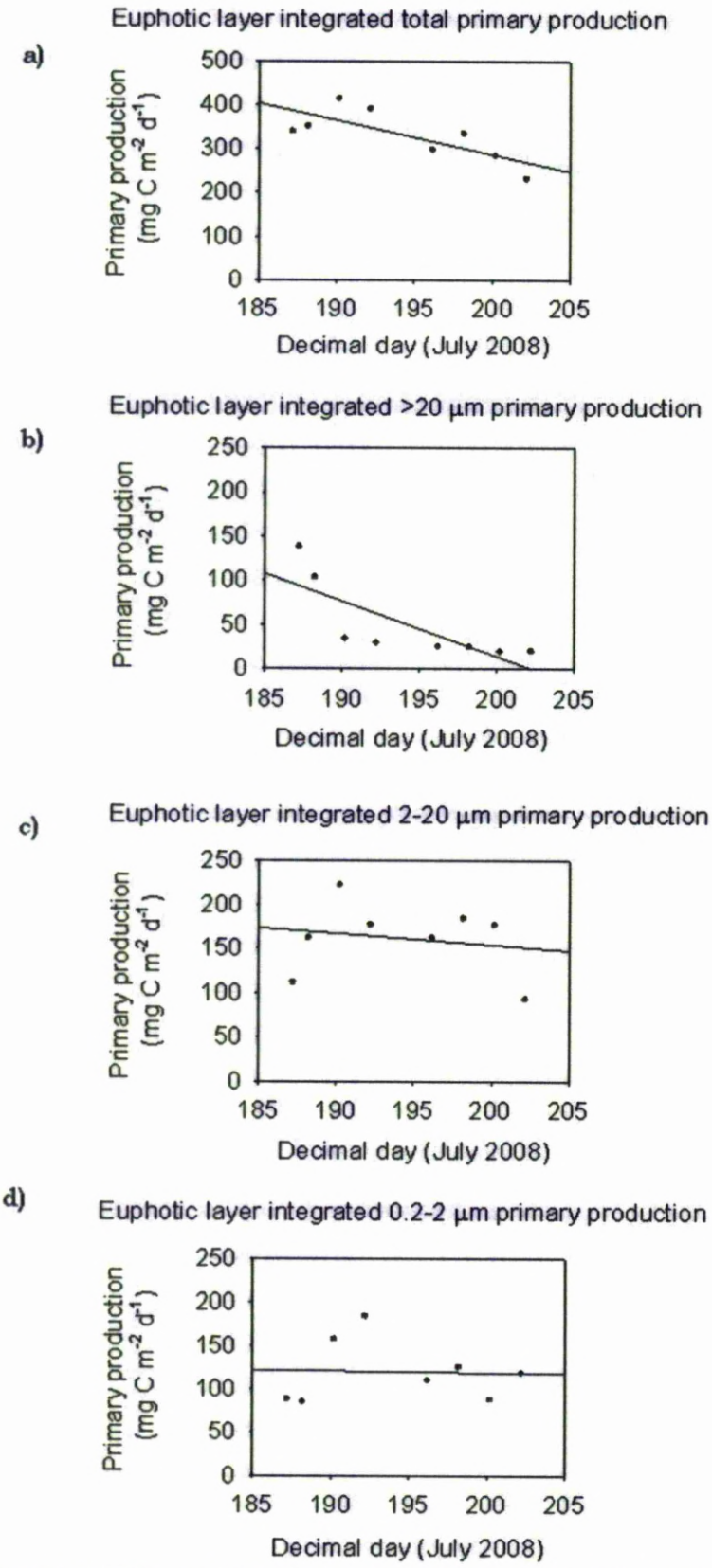

Figure 3.11) Temporal trends in euphotic layer-integrated primary production for a) total ($p<0.05$); b) >20 µm ($p<0.05$); c) 2-20 µm ($p>0.05$); and d) 0.2-2 µm ($p>0.05$).

3.2.3.3. Turbulent dissipation and phosphate fluxes

Observed turbulent dissipation (Fig. 3.12) and phosphate flux (Table 3.4) at the base of the thermocline support the suggestion of enhanced mixing during the stormy spring tide as observed from chlorophyll and production data. Turbulent dissipation profiles show that the displacement of tidal currents by Jones Bank topography initiated internal wave activity within the water column displacing the thermocline (Dr Matthew Palmer, pers. comm.). The log K_z time series (provided by Dr Matthew Palmer; Fig. 3.12) indicate that much stronger turbulent energy dissipation occurred through the water column originating from the bed-boundary during the spring tide cycles than during the neap tide cycle. In some instances, these strong bursts penetrated the base of the thermocline and drove enhanced diapycnal nutrient fluxes into the thermocline layer (Sharples et al., 2001; Tweddle et al., in prog.). This is reflected in the phosphate flux estimates which were higher during spring tides than on neap tides (~1.2 mmol m^{-2} d^{-1} and 0.03 mmol m^{-2} d^{-1}, respectively; Table 3.4). These highly dynamic fluxes varied by up to 5 orders of magnitude within single tidal cycles due to the sporadic nature of turbulent dissipation at the base of the thermocline.

Table 3.4. A summary of estimated daily phosphate fluxes (mmol m^{-2} d^{-1}) across the base of the thermocline during the stormy spring (day 188), the neap cycle (day 196) and the latter spring cycle (day 203). Given the sporadic nature of turbulent mixing at the base of the thermocline, minimum and maximum calculated fluxes are presented in addition to the calculated daily flux estimates.

Decimal day	Surface [DIP] μM	Mean Kz m^2 s^{-1}	Mean flux mmol m^2 s^{-1}	Flux range mmol m^2 s^{-1}	Daily flux mmol m^2 d^{-1}
188	0.12	0.0043	1.39×10^{-5}	9.4×10^{-9} to 3.2×10^{-4}	1.2
196	0.09	0.0001	4.03×10^{-7}	1.5×10^{-9} to 4.2×10^{-5}	0.03
203	0.05	0.0046	1.37×10^{-5}	1.9×10^{-9} to 6.3×10^{-4}	1.18

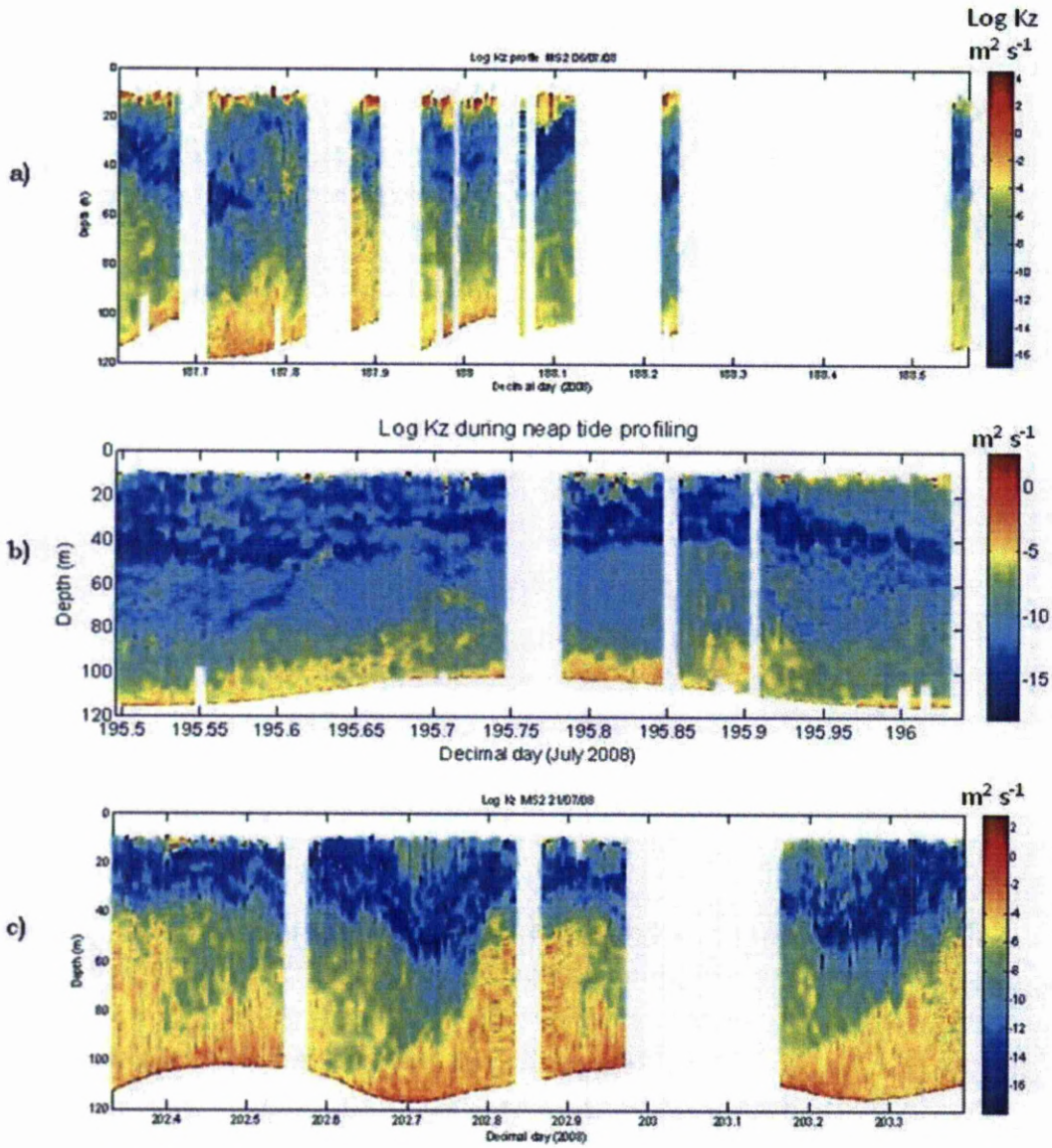

Figure 3.12) Eddy diffusivity (log Kz) depth profiles at Jones Bank plotted against time during a) the early, stormy spring; b) the neap tidal cycle; and c) the latter spring cycle. Data courtesy of Dr Matthew Palmer, NOCL.

3.2.3.4. Phosphate assimilation versus supply

Phosphate flux estimates were of similar magnitude during the stormy spring tide and the latter calm spring tide (1.20 and 1.18 mmol P m^{-2} d^{-1}, respectively). However, after the storm mean phosphate concentrations significantly decreased in the SML and thermocline ($p<0.001$ and $p<0.05$, respectively; Fig. 3.13, a and b) as did integrated values ($p<0.05$ and $p>0.05$, respectively; Fig. 3.13, c and d). This suggests that the storm did influence water column phosphate dynamics despite suggestions to the contrary from the flux data. It is likely that wind-induced entrainment of thermocline waters into the SML increased SML phosphate concentrations

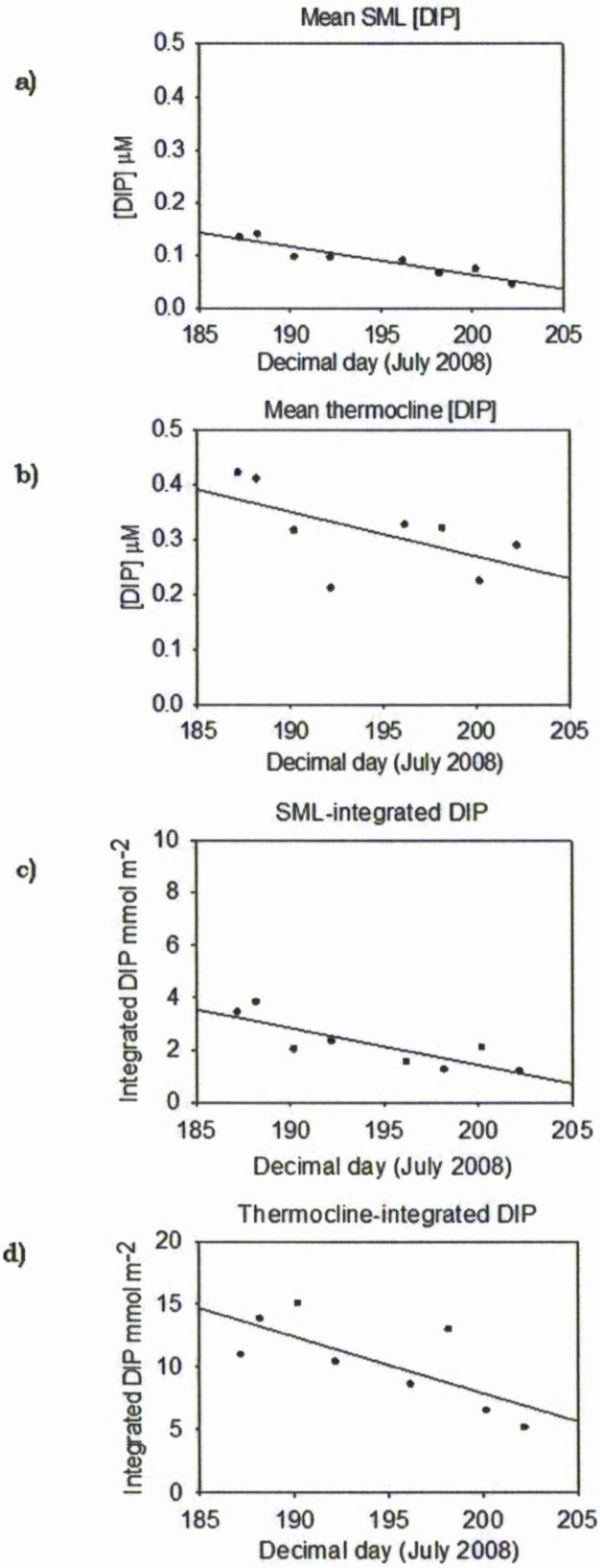

Figure 3.13) Temporal trends in mean phosphate (DIP, µM) concentrations in a) the surface mixed layer ($p<0.001$); and b) the thermocline layer ($p<0.05$); and integrated phosphate values in c) the surface mixed layer ($p<0.05$); and d) the thermocline layer ($p>0.05$).

(Yin et al, 1995); while dilution of the SCM reduced the efficiency with which the new nutrient flux was assimilated within the thermocline layer (Hickman et al., 2009). Therefore, higher phosphate concentrations were observed at this time. The subsequent decrease likely resulted from biological assimilation of phosphate coupled with reduced inputs of BML water to the euphotic zone (as suggested from SST and N^2 data).

Phosphate assimilation rates were estimated from carbon fixation rate data in two ways. In the first, phosphate assimilation estimation was calculated based on previously published data (Rees et al., 1999; Table 3.5) on phosphate uptake rates during a Celtic Sea shelf edge bloom event. Calculating nutrient uptake ratios and assimilation rates based on data presented in later chapters was considered but rejected. While dissolved and particulate nutrient ratios are presented in chapter 5, there is no accompanying community composition data or rate data, such as carbon fixation rates. Given the inclusion of bacterial and zooplankton biomass in the measured ratios of the particulate nutrient pool, nutrient assimilation rates calculated based on bulk nutrient pool ratios would not be comparable those derived from to carbon fixation rates, which would only represent phytoplankton nutrient assimilation. Also, nutrient ratios reported in chapter 5 varied greatly along the shelf edge, possibly reflecting spatial variations in physical mixing and community composition across the shelf edge region. The phytoplankton community composition data available in this chapter suggests a degree of bloom-growth with diatoms being present earlier in sampling. Therefore, it is I believe it is not unreasonable to compare uptake rates form this post-storm bloom event with that of the spring bloom reported by Rees et al. (1999).

Rees et al. (1999) reported the C:P uptake ratio for the >2 μm size fraction which was applied to corresponding C fixation data obtained during the current study, with the addition of an assumed constant P uptake rate of 0.25 mmol P m^{-2} d^{-1} for the <2 μm size class (Rees et al., 1999). This method gave total phosphate assimilation rates during the first spring, neap and latter spring cycles of 0.31 mmol P m^{-2} d^{-1}, 0.26 mmol P m^{-2} d^{-1} and 0.20 mmol P m^{-2} d^{-1}, respectively.

Table 3.5. A summary of estimated phosphate assimilation based on the values reported by Rees et al. (1999).

Day	DIP	DOP	PPhos	PME	C fixation total	C fixation >2 µm	DIP flux	APA	P assimilation >2 µm	P assimilation total	C:P
	mmol m^{-2}				mmol C m^{-2} d^{-1}		mmol P m^{-2} d^{-1}		mmol P m^{-2} d^{-1}		
187	9.57	5.57	5.48	2.53	28.31	20.86 75%	1.20	0.006	0.06	0.31	91
195	4.28	7.66	1.94	2.24	24.89	15.64 63%	0.03	0.005	0.01	0.26	96
202	2.99	9.51	1.60	3.70	19.41	9.47 49%	1.18	0.009	-0.05	0.20	97

The second estimate of phosphate assimilation was through application of the Redfield ratio (106 C: P; table 3.6) to carbon fixation data. This gave total phosphate assimilation rates during the first spring, neap and latter spring cycles of 0.27 mmol P m^{-2} d^{-1}, 0.23 mmol P m^{-2} d^{-1} and 0.18 mmol P m^{-2} d^{-1}, respectively. The notable difference in phosphorus assimilation estimates for the >2 µm fraction may be due to differences in nutrient assimilation ratios between the different growth strategies of the bloom community sampled by Rees et al. (1999) and the generalist community assumed by the Redfield ratio (e.g. Arrigo, 2005).

Table 3.6) Summary of euphotic layer (surface 40 m) integrated phosphate (DIP), dissolved organic phosphorus (DOP), particulate phosphorus (PPhos) , phosphomonoester (PME) values (mmol m^{-2}); carbon fixation rates; phosphate fluxes at the base of the thermocline; alkaline phosphatase hydrolysis rates; and phosphate assimilation estimated from the Redfield ratio during the early, stormy spring cycle (day 187), the neap tidal cycle(day 195) and the latter spring cycle(day 202).

Day	DIP	DOP	PPhos	PME	C fixation total	C fixation >2 µm	DIP flux	APA	P assimilation >2 µm	P assimilation total	C:P
	mmol m^{-2}				mmol C m^{-2} d^{-1}		mmol P m^{-2} d^{-1}		mmol P m^{-2} d^{-1}		
187	9.57	5.57	5.48	2.53	28.31	20.86 75%	1.20	0.006	0.20	0.27	106
195	4.28	7.66	1.94	2.24	24.89	15.64 63%	0.03	0.005	0.15	0.23	106
202	2.99	9.51	1.60	3.70	19.41	9.47 49%	1.18	0.009	0.09	0.18	106

Both methods have significant caveats in their estimations (e.g. assumed similarity and consistency of phytoplankton assemblages, omission of the bacterial contribution to uptake, and assumed C:P assimilation ratios) but

cautious interpretation suggests that diapycnal fluxes of phosphate are supplied in excess of assimilation during spring tides, while there is a deficit supply during the neap cycle.

3.2.3.5. Lability and turnover of the dissolved organic phosphorus pool

Following assimilation, organisms incorporate phosphate into complex cellular organic molecules, such as phospholipids, ATP and DNA. Through a number of possible pathways (e.g. extracellular release by phytoplankton, grazer mediated release or excretion, and bacterial or viral cell lysis) organic phosphorus is released to the water column in the dissolved phase. Once in the water column, DOP is regenerated through enzyme-catalysed hydrolysis in the microbial loop (Carlson, 2002).

In phosphate-deplete conditions, some organisms express genes that code for the synthesis of DOP-hydrolysing enzymes, such as the enzyme alkaline phosphatase which hydrolyses the labile phosphomonoester bond. Alkaline phosphatase is a ubiquitous enzyme associated with phytoplankton, zooplankton, and bacteria but may also occur freely dissolved in the water column. As many DOP-hydrolysing enzymes are inducible during times of phosphorus-stress, their presence is sometimes used to assess the phosphorus-status of communities. However, they also have constitutive roles within some phytoplankton species and bacteria (Cembella et al., 1984; Vidal et al., 2003).

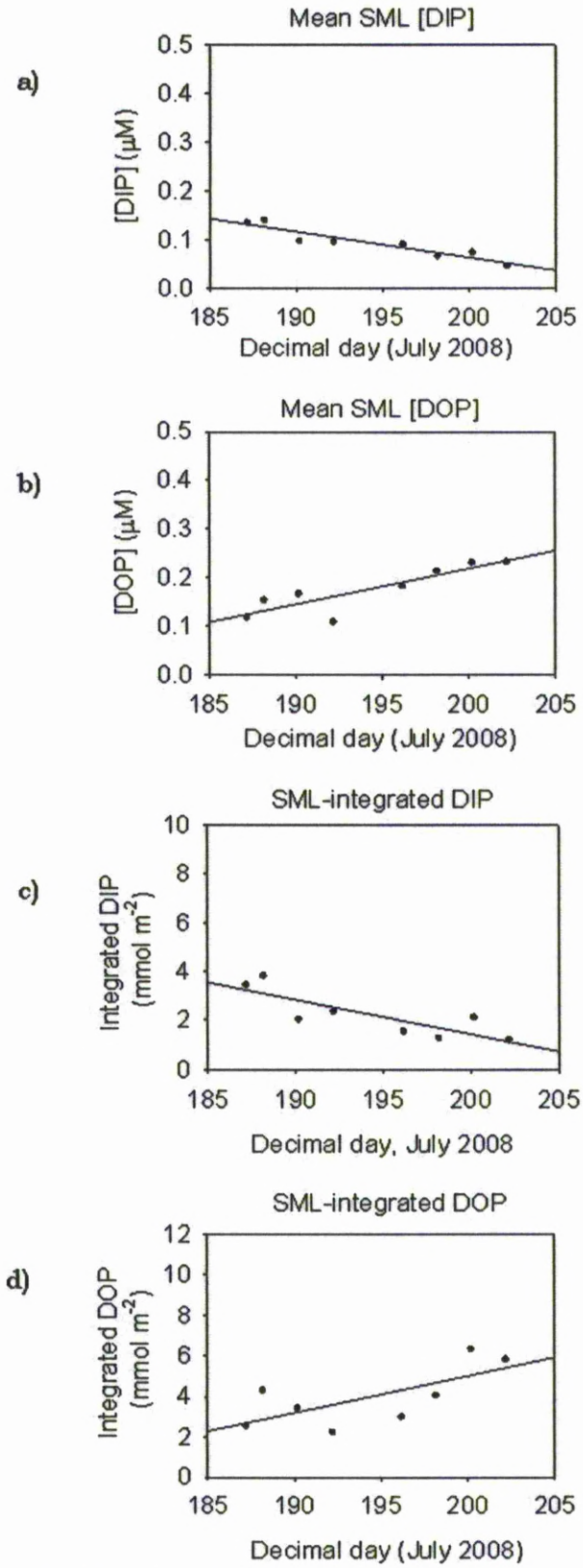

Figure 3.14) Temporal trends in mean dissolved organic phosphorus (DOP, µM) concentrations in a) the surface mixed layer ($p<0.05$); and b) the thermocline layer ($p<0.05$); and integrated phosphate values in c) the surface mixed layer ($p>0.05$); and d) the thermocline layer ($p<0.05$).

During periods of enhanced production, such as bloom events, DOP production and consumption processes may become decoupled leading to an accumulation of DOP in the water column (Karl and Björkman, 2002). In this study, mean DOP concentrations in the SML and thermocline increased ($p<0.05$; Fig. 3.14, a and b) as did integrated DOP ($p>0.05$ and $p<0.05$, respectively; Fig. 3.14, c and d) suggesting that DOP was being produced in excess of consumption and export processes.

No significant temporal trends were observed in phosphomonoester concentration or integrated values ($p>0.05$; Fig. 3.15), but the presence of this labile fraction of the DOP pool suggests *in situ* production and fresh DOP in the euphotic layer (Clark et al., 1998). Phosphomonoesters are much more labile than the other constituents of the bulk DOP pool (namely diesters and phosphonates); therefore they are typically the first fraction of the DOP pool to be accessed in times of phosphate-stress (Kolowith et al., 2001). However, measured alkaline phosphatase activity (APA) hydrolysis rates were low throughout the study and turnover of the PME pool was relatively slow, so DOP was able to accumulate.

Measured APA hydrolysis rates increased during the study (Fig. 3.16) but showed no significant correlation with time, substrate availability (PME; Fig 3.16, c and d) or chlorophyll *a* (in this instance a proxy for phytoplankton biomass; data not shown). The lack of any significant relationship may result from lag times in induction and repression of the enzyme. In addition, each species has a different P-requirement and nutritional status (Cembella et al., 1984). Therefore, inconsistent community sampling arising from temporal changes in community structure and sampling resolution of populations may mask any trend in APA (Jansson et al., 1988; Martiny et al., 2009). Phytoplankton populations are known to stratify within the SCM at times of relative stability within the water column (Hickman et al., 2009). The significance of this is that replicate Niskin bottle samples of the SCM across a 1-metre section of the water column most likely subject to internal wave activity may not provide consistent representation of community assemblages. This might explain why mean SCM-APA was more variable than SML-APA (0.09-0.23 nM P h^{-1} and 0.11-0.19 nM P h^{-1}, respectively).

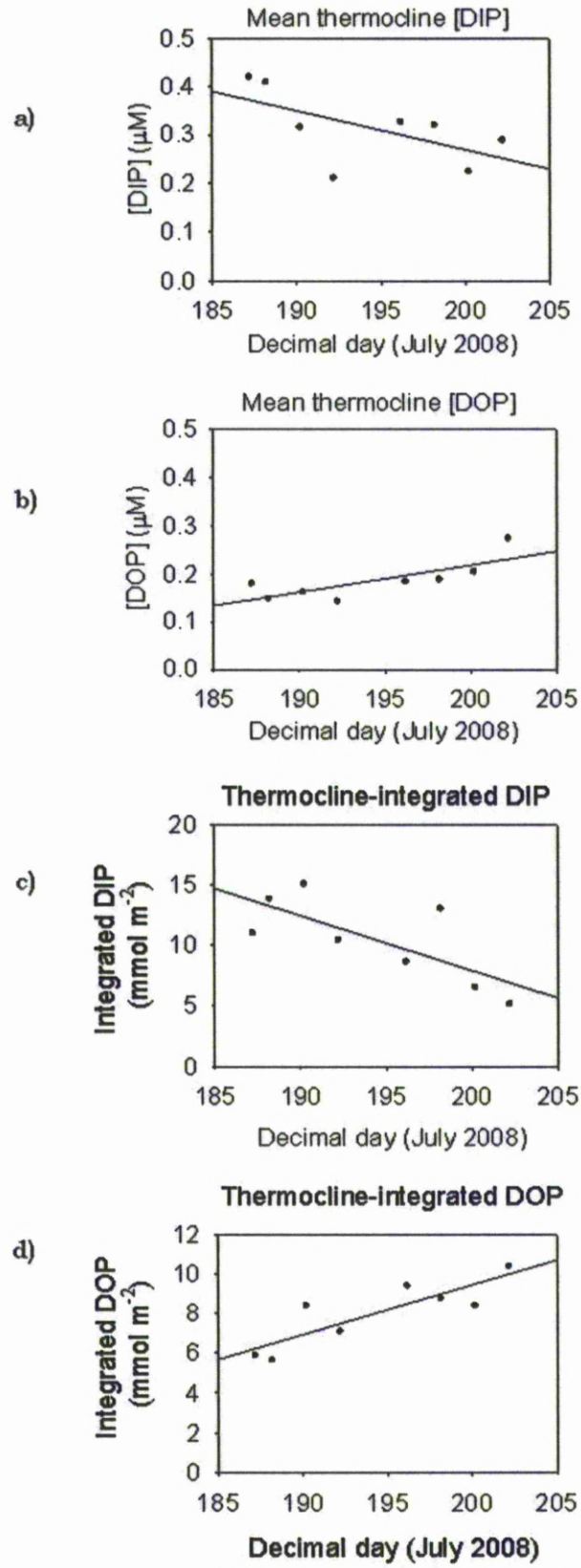

Figure 3.15) Temporal trends in mean phosphomonoester (PME, µM) concentrations in a) the surface mixed layer ($p>0.05$); and b) the thermocline layer ($p>0.05$); and integrated PME values in c) the surface mixed layer ($p>0.05$); and d) the thermocline layer ($p>0.05$).

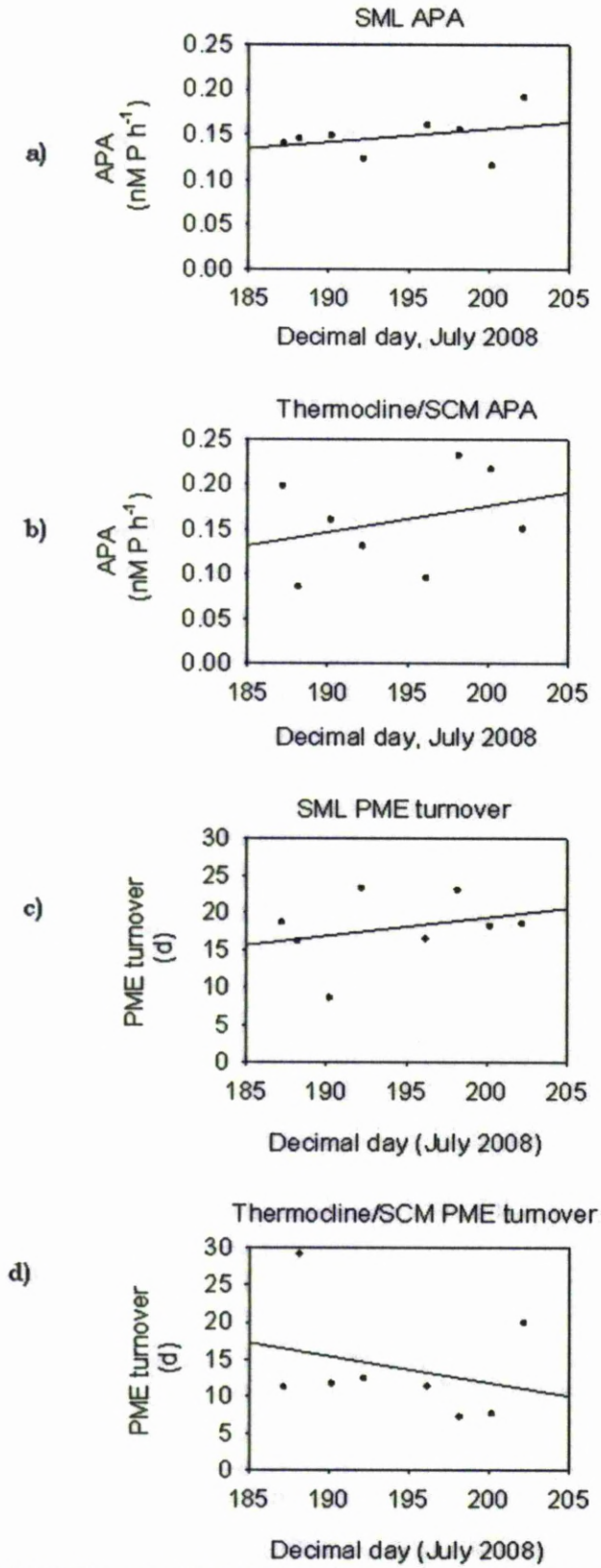

Figure 3.16) Temporal trends in a) the surface mixed layer alkaline phosphatase activity ($p>0.05$); and b) the thermocline layer/subsurface chlorophyll maxima alkaline phosphatase activity ($p>0.05$); and c) surface mixed layer phosphomonoester turnover rates ($p>0.05$); and d) the thermocline layer/subsurface chlorophyll maxima phosphomonoester turnover rates ($p>0.05$).

3.2.3.6. Particulate nutrient changes

Integrated particulate phosphorus concentrations decreased in both the SML and thermocline during the study ($p<0.05$); potentially resulting from decreased phytoplankton biomass and carbon fixation (reflected by chlorophyll and primary production data), export of particulates or enhanced remineralisation.

Integrated particulate nutrient data indicate that at the beginning of the study ratios of C:N:P in the SML were relatively close to Redfield at ~100:15:1 (Fig 3.17). In the thermocline, the integrated particulate ratios were closer to 50:10:1. The particulate nitrogen to PPhos and particulate organic carbon to PPhos ratios increased over the same period in the SML and thermocline ($p<0.05$; Fig 3.17) suggesting preferential remineralisation of phosphorus relative to nitrogen and organic carbon. This could either be a reflection of higher bacterial activity facilitating more rapid remineralisation rates, or a progressive change in the bioavailability of particulate organic matter after the storm (Benitez-Nelson et al., 2007).

3.2.3.7. Phosphorus budget

A crude phosphorus budget was formulated (using data from Table 3.6 and employing P assimilation estimates based on the Redfield ratio) to estimate changes in euphotic layer phosphorus dynamics between the storm and neap cycle, and the neap and latter spring tidal cycle.

During the 8-day period between the stormy spring on decimal day 187 and the neap cycle on day 195, euphotic layer integrated total phosphorus (DIP, DOP plus PPhos) decreased by 6.74 mmol m^{-2} (from 20.62 mmol m^{-2} to 13.88 mmol m^{-2}). Based on estimated phosphate flux versus P assimilation, assuming APA-facilitated hydrolysis contributed to P assimilation (all rates calculated as the mean of the measured rates applied over the 8 day period) a potential net gain of dissolved phosphate in the euphotic layer of 1.56 mmol m^{-2} was calculated.

Euphotic layer integrated total phosphorus decreased by 3.23 mmol m^{-2} (from 17.42 mmol m^{-2} to 14.10 mmol m^{-2}) during the following neap to spring cycle (between decimal days 195 and 202). Phosphate flux and

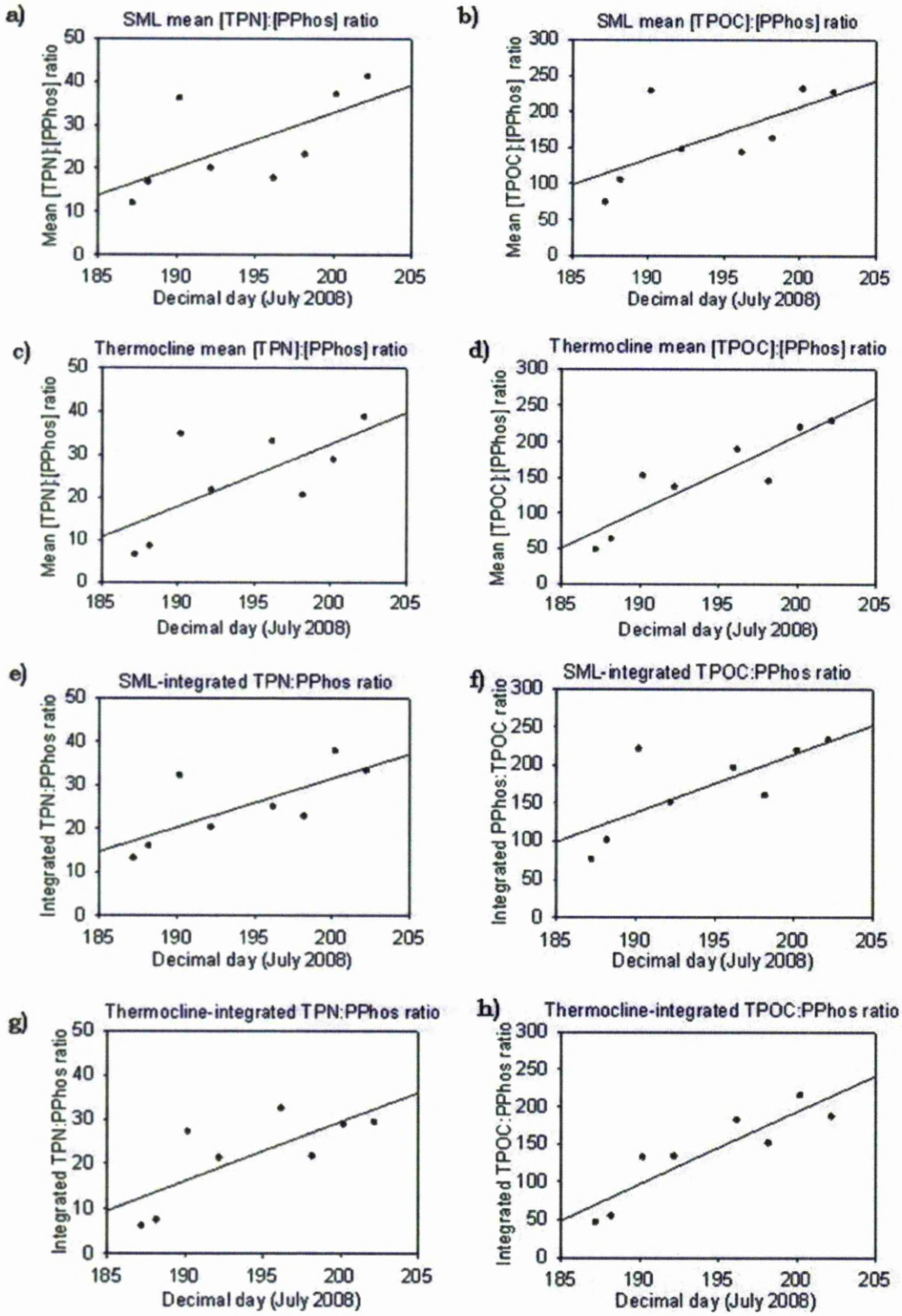

Figure 3.17) Temporal trends in: a) the ratio of mean total particulate nitrogen to particulate phosphorus concentration in the SML ($p<0.05$); b) the ratio of mean particulate organic carbon to particulate phosphorus concentration in the SML ($p<0.05$); c) the ratio of mean total particulate nitrogen to particulate phosphorus concentration in the thermocline ($p<0.05$); d) the ratio of mean particulate organic

carbon to particulate phosphorus concentration in the thermocline ($p<0.05$); e) the ratio of SML-integrated total particulate nitrogen to particulate phosphorus ($p<0.05$); f) the ratio of SML-integrated particulate organic carbon to particulate phosphorus ($p<0.05$); g) the ratio of thermocline-integrated total particulate nitrogen to particulate phosphorus ($p<0.05$); h) the ratio of thermocline-integrated particulate organic carbon to particulate phosphorus ($p<0.05$).

assimilation rate estimates suggest a gain of 2.3 mmol m^{-2} dissolved phosphate should be expected.

The loss of phosphorus from the euphotic layer was greater during the stormy spring–neap tidal cycle than the neap–spring cycle, suggesting that the system was reaching a more balanced state in the latter part of the study. The inference being that the excess phosphate supplied to the euphotic layer during the storm is lost from the surface layer relatively quickly (Table 3.6).

3.2.4. Celtic Sea 2010: Wind mixing event

During a research cruise in the Celtic Sea in June 2010, the water column at 49°25.11 N 008°59.47W was sampled before and after a wind mixing event that occurred on decimal day 158. Full biogeochemical sampling was conducted at days 156.1 (before the wind event) and 160.1 (after the wind event), with 7 intervening physical data CTDs.

Temperature data show thermal stratification persisted throughout the wind mixing event (Fig. 3.18) although there was significant turbulent dissipation at the base of the thermocline (Charlotte Williams, pers. comm.). The effect of this mixing is perhaps more apparent in the reduced chlorophyll concentration in the SCM at the base of the thermocline (~ 40 m; Fig. 3.19).

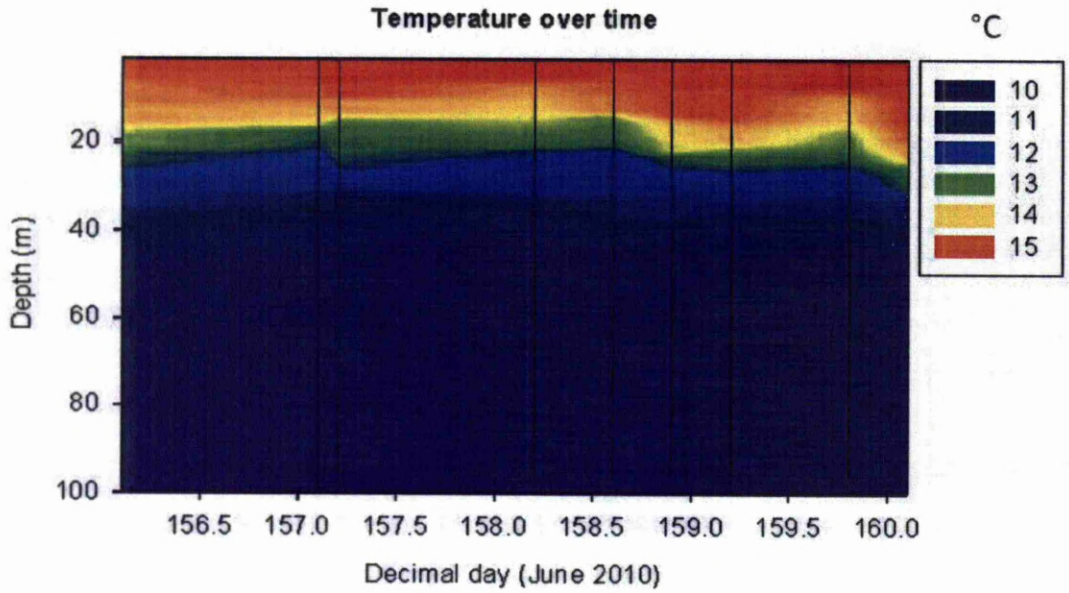

Figure 3.18) Time series contour of temperature (°C, warmer colours indicating higher temperatures) with the times of sampling marked by vertical black lines.

Euphotic layer integrated data (i.e. integrated between the surface and the base of the thermocline; Table 3.7) showed significant increases in both phosphate and DOP after the wind event, with the percentage DOP of the total dissolved phosphorus pool increasing from 18 % to 32 %, i.e. there was a greater increase in DOP. This suggests a net gain in phosphorus in the euphotic zone during the wind event, and significant transfer of that phosphorus to the organic pool although the proportion of DOP in the TDP pool was much lower than the 65-85 % observed in open ocean surface waters (Karl and Yanagi, 1997).

Table 3.7) Euphotic layer (surface to base of thermocline) integrated values before and after the wind event for phosphate (DIP, mmol m^2 ± 95 % confidence interval), dissolved organic phosphorus (DOP, mmol m^2 ± 95 % confidence interval), percentage DOP of total dissolved phosphorus pool (TDP), and chlorophyll (mg m^2).

Euphotic layer integrated values	Before wind event Decimal day 156	After wind event Decimal day 160
DIP (mmol m^{-2} ± 95 % CI)	7.73 ± 0.14	8.42 ± 0.10
DOP (mmol m^{-2} ± 95 % CI)	1.65 ± 0.62	3.91 ± 0.36
PPhos (mmol m^{-2} ± 95 % CI)	3.73 ± 0.05	3.13 ± 0.07
DOP (% of TDP)	18	32
Chlorophyll (mg m^{-2})	35.4	31.8

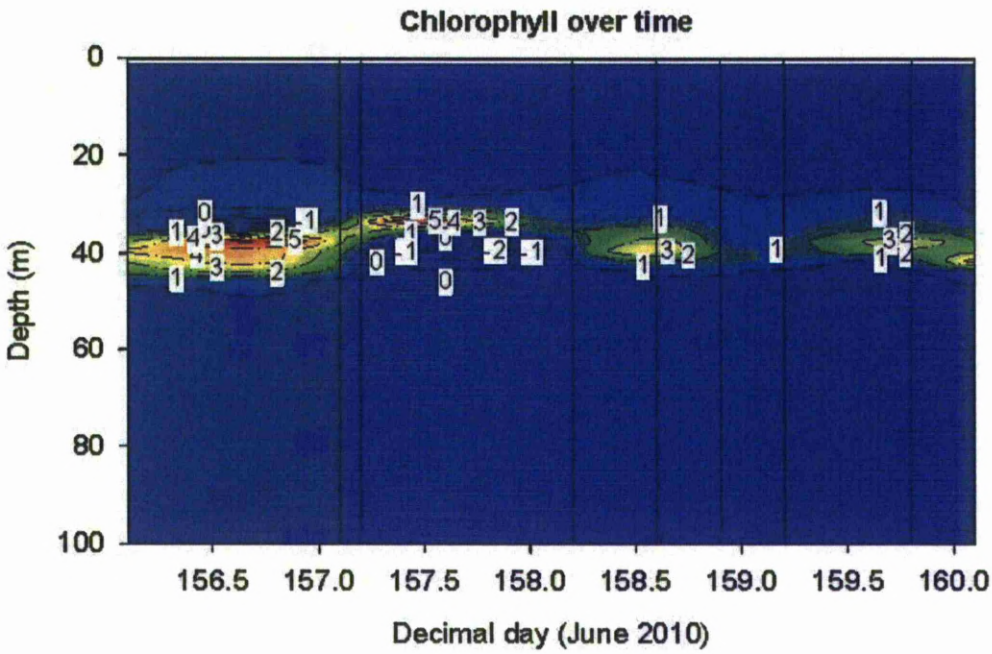

Figure 3.19) Time series contour of chlorophyll concentration (µg L^{-1}, warmer colours indicating higher concentrations) with the times of sampling marked by vertical black lines.

Meanwhile, PPhos decreased from 3.73 ± 0.05 mmol m^{-2} to 3.13 ± 0.07 mmol m^{-2} and there was no clear difference in integrated chlorophyll values over the same period. The lack of any increase in chlorophyll over the same

period as significant increases in nutrient values suggests that a phytoplankton biomass response to nutrient availability was not observed in over the sampling time frame. This may have been due to a number of possible factors, including a lag time in phytoplankton growth response, growth limitation by another nutrient or efficient phytoplankton biomass removal via processes such as zooplankton grazing or mixing below the thermocline. In the BML, DOP concentrations significantly increased from 0 ± 0.06 μM before the wind event to 0.08 ± 0.02 μM afterwards suggesting inputs of organic matter to the BML from either the euphotic layers above or the sediment interface below. Phosphate concentrations also increased, but were not significantly different (0.66 ± 0.02 μM and 0.69 ± 0.02 μM, respectively).

Table 3.8) Phosphomonoester concentration (PME, μM ± 95 % confidence interval) before and after the wind event measured at the surface (approximately 10 m depth), subsurface chlorophyll maximum (SCM), base of the thermocline and bottom mixed layer (BML).

PME concentration (μM ± 1 s.d.)	Before wind event Decimal day 156	After wind event Decimal day 160
Surface	0.096 ± 0.050	0.030 ± 0.007
SCM	0.184 ± 0.035	0.050 ± 0.005
Base of thermocline	0.151 ± 0.019	0.030 ± 0.007
BML	0.160 ± 0.021	0.110 ± 0.013

Phosphomonoester concentrations were significantly lower after the wind event at the SCM, base of the thermocline and in the BML (Table 3.8), while APA showed significant increases in hydrolysis rates at all depths, particularly at the base of the thermocline and in the BML (Table 3.9). The result of these changes was that PME turnover times were significantly faster after the wind event than they were beforehand (Table 3.10), suggesting than any fresh labile DOP was rapidly hydrolysed and that the observed increase in DOP comprised less labile components. Enzyme labelled fluorescence (ELF) staining leaves a green fluorescent residue at the site of enzyme hydrolysis of the substrate. ELF staining experiments

conducted during the current study indicated that a large portion of APA present was associated with very small particles (presumed to be bactiera given the lack of repression of APA below the thermocline) and larger particle surfaces (Fig. 3.21).

Table 3.9) Alkaline phosphatase activity (APA, nM P h^{-1} ± 95 % confidence interval) before and after the wind event measured at the surface (approximately 10 m depth), subsurface chlorophyll maximum (SCM), base of the thermocline and bottom mixed layer (BML).

APA (nM P h^{-1} ± 95 % C.I.)	Before wind event Decimal day 156	After wind event Decimal day 160
Surface	0.01 ± 0.005	0.04 ± 0.01
SCM	0.39 ± 0.02	1.05 ± 0.32
Base of thermocline	0.46 ± 0.01	1.26 ± 0.38
BML	0.32 ± 0.02	1.54 ± 0.47

Table 3.10) Phosphomonoester turnover (days) for before and after the wind event; calculated from PME concentration and alkaline phosphatase activity data.

PME turnover (days)	Before wind event Decimal day 156	After wind event Decimal day 160
Surface	400	31.3
SCM	19.7	2.0
Base of thermocline	13.7	1.0
BML	20.8	3.0

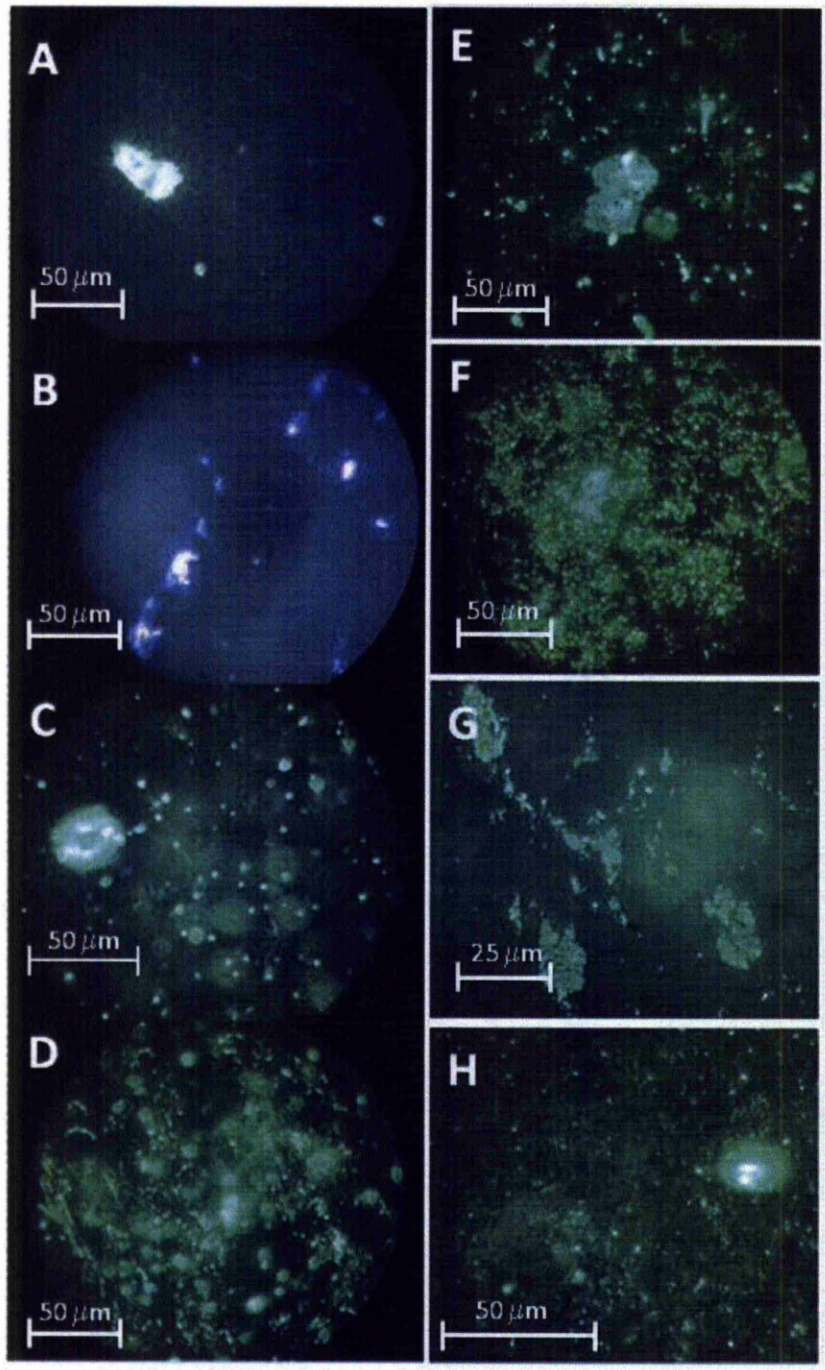

Figure 3.21) Enzyme labelled fluorescence microscope images indicating alkaline phosphatase activity sites in green. A-D show samples from CTD 6 at the SML, SCM, base of the thermocline and BML, respectively. E-H show samples from CTD 17 at the SML, SCM, base of the thermocline and BML, respectively.

3.2.5. Celtic Sea 2010: mixing experiments

During D352, a set of mixing experiments were conducted whereby 10 L carboys of water collected from varying regions of the thermocline and SCM had BML water added (10% addition v/v) to them to simulate mixing events. Replicate samples (at least triplicate) were incubated on-deck at adjusted light levels and sea surface temperature, and were sampled at regular intervals (see Fig. 3.22 – 3.27). Control incubations (at least duplicates) were run in parallel whereby thermocline/SCM water was incubated without the addition of BML water and sampled simultaneously.

A time series of phosphate and nitrate plus nitrite concentrations was measured during the mixing experiments (data courtesy of Charlotte Williams, University of Liverpool; Figs. 3.22 - 3.27). The temporal resolution of sampling during mixing experiment 1 (T_{final} = 92 h) was low in comparison to subsequent experiments. Over the full duration of this incubation, nutrient uptake rates were 0.048 μM N h^{-1} and 0.004 μM P h^{-1} (12 N:P uptake ratio) in the treatment and 0.063 μM N h^{-1} and 0.005 μM P h^{-1} (12.6 N:P uptake ratio) in the control (Figs. 3.22 and 3.23).

In mixing experiment 2 for treatments 2 and 3, nitrite plus nitrogen reach a minimum before phosphate (approximately hours 46 and 76, respectively). The mean nutrient uptake rates during experiment 2 were 0.46 μM N h^{-1} and 0.10 μM P h^{-1} (4.6 N:P uptake ratio) for the treatment; and 0.07 μM N h^{-1} and 0.04 μM P h^{-1} (1.6 N:P uptake ratio) for the control.

In mixing experiment 3 concentrations were generally much lower than previous experiments, and nitrite plus nitrate reached 0.03 ± 0.01 μM in both controls and treatments within 27 hours (Fig. 3.27) and phosphate decreased to 0.08 ± 0.01 μM (Fig. 3.26). The mean nutrient uptake rates during experiment 3 were 0.01 μM N h^{-1} and 0.002 μM P h^{-1} (5 N:P uptake ratio) for the treatment; and 0.00003 μM N h^{-1} and 0.0005 μM P h^{-1} (0.6 N:P uptake ratio) for the control.

At T_0, the Redfield ratios of dissolved nutrients ([N+N]: P) for each mixing experiment treatment were 10.0, 7.8, and 4.0, respectively. By the end of

the mixing experiments the Redfield ratios of dissolved nutrients were 3.81, 2.81 and 1.40, respectively. This suggests production was nitrogen limited in all three experiments, indicative of the nutrient status of system from which the samples originated.

During mixing experiment 1, APA was measured at 24-48 h intervals over the 96 h incubation period. Significant increases ($p<0.05$) were observed in both controls and treatments, with a larger increase in the control (from 0.78 nM P h^{-1} at T_0 to 7.28 nM P h^{-1} at T_{96}) despite the treatment having a higher initial hydrolysis rate (1.07 nM P h^{-1}; Table 3.11). The higher initial APA in the treatment than control suggests that alkaline phosphatase was added with the BML-water that was used to spike the treatment. While the higher APA at T_{final} in the control suggests potentially higher nutrient stress than in the treatment. In the latter mixing experiments APA was only measured at T_0 and $T_{final\ (76)}$. In mixing experiment 2, APA significantly increased in both the controls and treatments, however there was no significant difference between control and treatment (Table 3.11). In mixing experiment 3 there were no significant differences between T_0 or T_{76} in either the control or treatment (Table 3.11).

DOP was determined at T_0 and T_{76} during mixing experiment 2 (Table 3.12). There was a significant increase in DOP in the treatment (0.06 ± 0.15 μM at T_0 and 0.47 ± 0.03 μM at T_{76}). Meanwhile, DOP in the control increased from 0.06 ± 0.15 μM to 0.35 ± 0.14 μM. Despite the treatment showing a significant increase in DOP, at T_{76} the control and treatment were not significantly different from one another.

Table 3.11) Summary of alkaline phosphatase activity (nM P h^{-1}) measured during the Celtic Sea 2010 mixing experiments for the control thermocline/SCM waters, and the SCM+BML mixes (95 % confidence intervals shown).

Experiment	Time (h)	APA (nM P h^{-1})			
		Control	95 % C.I.	Treatment	95 % C.I.
1	0	0.78	-	1.07	0.23
	24	1.26	-	2.34	1.54
	48	3.24	-	2.59	0.14
	96	7.28	-	3.57	0.11
2	0	1.93	-	1.62	0.55
	76	2.42	0.05	2.94	0.66
3	0	1.76	-	1.12	0.76
	76	1.27	0.64	1.46	0.32

Table 3.12) Summary of dissolved organic phosphorus (DOP; µM) concentrations determined at T zero and T final during mixing experiment 2.

	[DOP] µM			
	CTRL	95 % CI	MIX	95 % CI
T zero	0.06	0.15		
T final	0.35	0.14	0.47	0.03

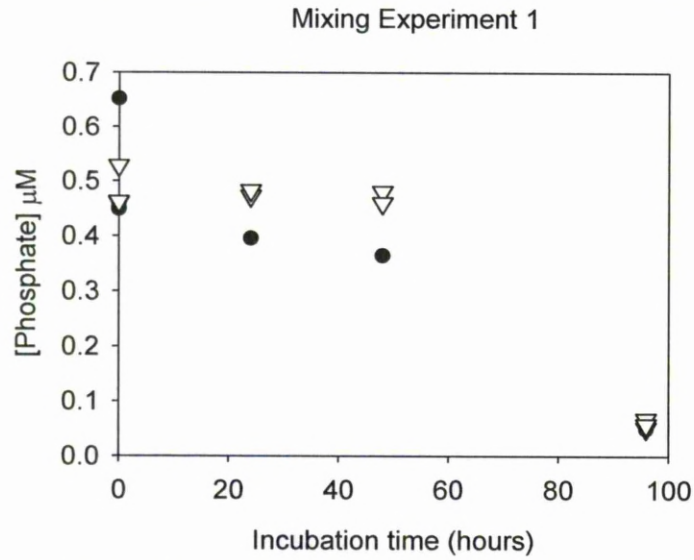

Figure 3.22) Phosphate (µM) plotted against incubation time (hours) during mixing experiment 1 for treatments (inverted triangle) and controls (solid circle).

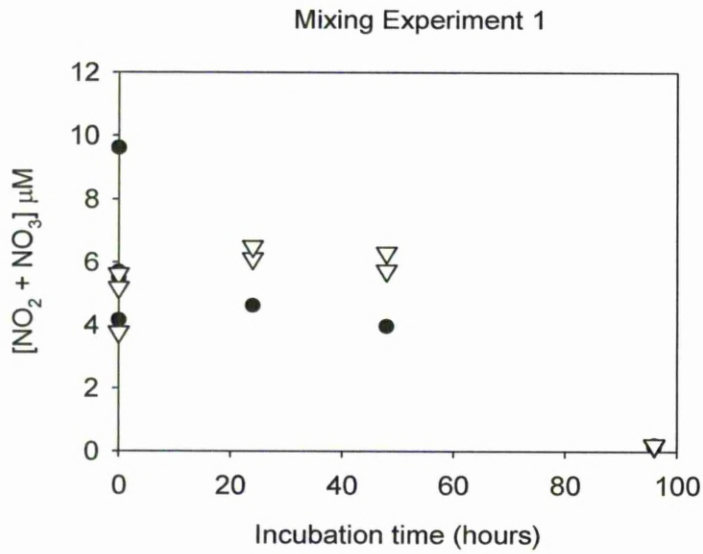

Figure 3.23) Nitrite plus nitrate (µM) plotted against incubation time (hours) during mixing experiment 1 for treatments (inverted triangle) and controls (solid circle).

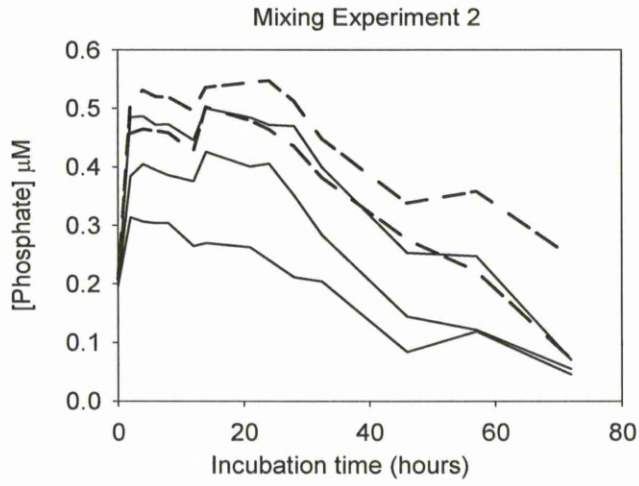

Figure 3.24) Phosphate (µM) plotted against incubation time (hours) during mixing experiment 2 for 3 mixed treatments (solid line) and 2 control incubations (dashed line).

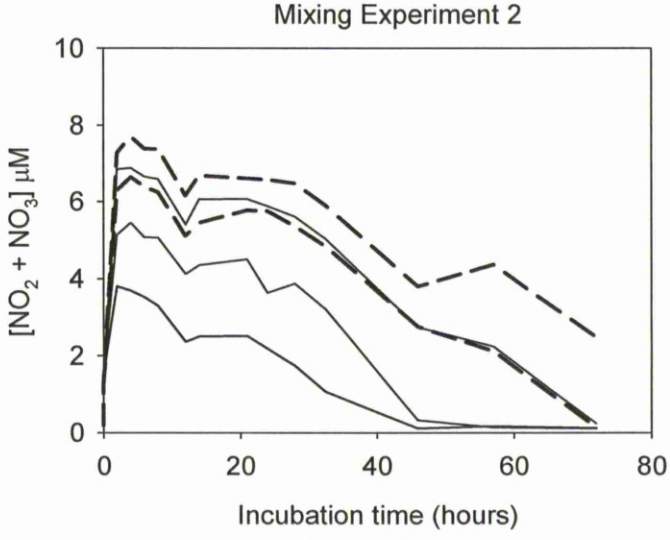

Figure 3.25) Nitrite plus nitrate (µM) plotted against incubation time (hours) during mixing experiment 2 for 3 mixed treatments (solid line) and 2 control incubations (dashed line).

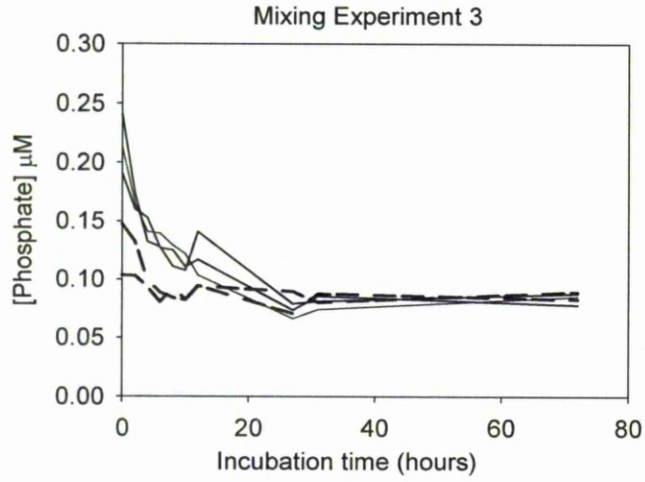

Figure 3.26) Phosphate (µM) plotted against incubation time (hours) during mixing experiment 3; for 3 mixed treatments (solid line) and 2 control incubations (dashed line).

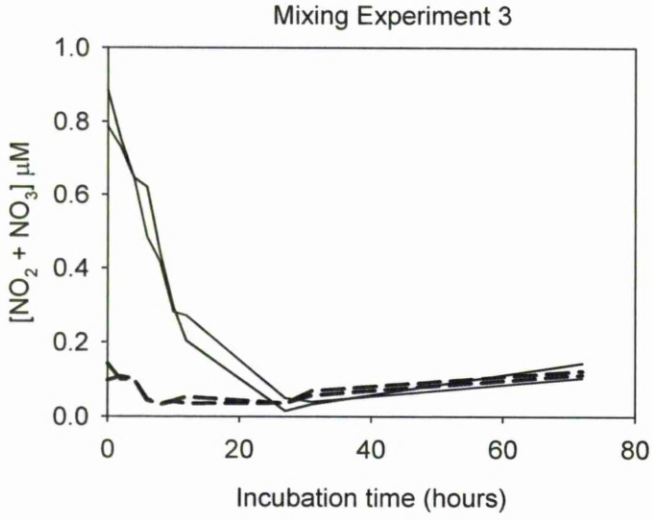

Figure 3.27) Nitrite plus nitrate (µM) plotted against incubation time (hours) during mixing experiment 3 for 3 mixed treatments (solid line) and 2 control incubations (dashed line).

3.3. Discussion

3.3.1. Comparison with previous studies

Surface phosphate concentrations observed during this study were consistent with previous summertime observations of Hydes et al. (2001; <0.1 μM), but are lower than those observed by Pemberton et al. (2004) and Rees et al. (1999), which are of the order of 0.2 – 0.3 μM, respectively. Differences with the latter studies probably relate to the sampling region, i.e. frontal and shelf edge versus mid-shelf, and the time of sampling. For example, Rees et al. (1999) sampled during the spring bloom event at the onset of stratification (April/May) whereas the current study sampled during summer stratification (June).

Dissolved organic phosphorus concentrations are also consistent with the 0.1 – 0.2 μM range observed by Hydes et al. (2001), as is also the case with particulate phosphorus concentrations (0.01 – 0.2 μM). Calibrated chlorophyll concentrations show marked similarities to the mean chlorophyll *a* concentrations of 0.4 μg L^{-1} quoted by Hydes et al. (2001), 1.6 – 2.5 μg L^{-1} quoted by Pemberton et al. (2004) at the SCM, and the 1.44 ± 1.35 μg L^{-1} of Hickman et al. (2009) for the same region.

3.3.2. Model open ocean scenario

Dissolved organic phosphorus is formed when microorganisms assimilate phosphate from the water column and incorporate the phosphorus into their cellular organic matter, such as phospholipids, RNA and DNA. These more complex (phosphorus) organic molecules are subsequently released back to the water column via a number of possible pathways, including extracellular release from phytoplankton, grazer mediated release or excretion, and bacterial or viral cell lysis as dissolved organic phosphorus (DOP; Carlson, 2002). Freshly produced DOP is generally speaking more labile and therefore biologically available than recalcitrant or refractory DOP. As DOP ages it undergoes remineralisation via the microbial loop and through abiotic processes such as photodegradation. As DOP is degraded each product is a smaller and less bioavailable DOP fraction. Therefore, DOP concentrations are generally higher in the euphotic layers as that is where primary production and DOP production is highest.

In deep water, there are fewer *in situ* sources of fresh DOP than in the euphotic zone and so DOP becomes diluted and the more labile fractions are remineralised. Thus, deep ocean DOP concentrations are typically low and represent the background refractory component of the DOP pool (Benitez-Nelson, 2000). Therefore, in a model open ocean environment one would expect net production and accumulation of DOP in the euphotic layer relative to the deep water, where net consumption of DOP generally results in refractory background levels (Karl and Bjorkman, 2002; Carlson et al., 2000).

3.3.3. Shelf sea scenarios – the current study

The shelf sea environment is somewhat different to that of the open ocean. The much shallower water column (<200 m cf. max ~ 3800 m) enhances the effects of wind and tidal mixing. As a result the water column is well mixed during the winter, only stratifying in deeper regions in the summertime when thermal buoyancy forcing overcomes stirring and mixing effects (Rippeth, 2005). At the onset and breakdown of stratification there are respective spring and autumnal bloom events. In the intervening stratified period, the highest primary production rates are associated with the subsurface chlorophyll maximum (SCM; Sharples et al., 2001; Rippeth et al., 2009).

SCM develop associated with the base of the thermocline. Here, phytoplankton survival is favoured by a nutrient supply from below the thermocline, sufficiently high irradiance for photosynthesis and sufficiently low turbulence that they remain in their advantageous position in the water column (Sharples and Tett, 1994). Nutrients are supplied by a diapycnal flux driven by tide and wind mixing (Sharples, 2008; Simpson et al., 1996). As the nutrients are supplied from the deep water they are often considered to be 'new' nutrients, thus fuelling 'new' production at the SCM and a net carbon drawdown. The presence of the SCM generally isolates this nutrient flux from directly propagating to the SML (e.g. Hickman et al., 2009). Thus during stratification, primary production in the SML is largely considered to rely on regenerated nutrients.

Variation in mixing and phosphate flux

The Jones Bank data suggest that the coincidence of the storm event with the earlier spring tide did not greatly enhance phosphate fluxes across the base of the thermocline relative to the subsequent, less windy spring tide. Phosphate fluxes are enhanced when turbulent kinetic energy dissipation is high and vertical nutrient gradients are strong. During the storm, wind-driven boundary mixing penetrated the surface 20 m of the water column, entraining thermocline waters into the SML, similar to the observations reported by Yin et al., 1995. In the same vein, wind-driven boundary mixing was not observed to penetrate to the base of the thermocline so the storm event would have only enhanced the phosphate flux if it triggered inertial oscillations in the SML thus enhancing shear at the thermocline (Rippeth, 2005). Therefore, internal tides appear to have had the greatest influence over turbulence and phosphate flux across the base of the thermocline at Jones Bank. Whereas during the 2010 Celtic Sea (D352) cruise, wind driven inertial shear was driving nutrient fluxes across the base of the thermocline and occurred at the inertial frequency (~15 hours) over the storm period (Charlotte Williams, pers. comm.). The wind-driven flux during the D352 cruise was sufficient to exceed biological assimilation rates as a net gain in euphotic layer phosphate was observed. This suggests that in deeper regions of shelf seas away from irregular topography and submerged banks where tidally driven mixing may dominate fluxes such as at Jones Bank, wind-driven fluxes may be important in supplying diapycnal nutrient fluxes to the euphotic zone.

Phosphate supply versus assimilation

Phosphate assimilation experiments were not conducted during this study. However, reported assimilation rate data (Rees et al., 1999) and assumed Redfield uptake ratios were applied to estimate P uptake rates from carbon fixation data. This was the considered best method available for estimating phosphorus assimilation rates (discussed above). However, Arrigo (2005) states that the uptake ratio of nutrients by microorganisms varies greatly depending on whether they are at survivalist, growth or generalist life stages, therefore the current method does carry significant limitations. Comparison of phosphate flux data across the base of the thermocline at

Jones Bank and estimated phosphate assimilation rates suggested an excess supply of phosphate during the spring tides, and a deficit supply during the intervening neap tide. This has previously been reported for nitrate in the Celtic Sea also (Sharples et al., 2007). However, phosphate assimilation rates here were most likely underestimated as bacterial uptake was not accounted for although potentially had a significant contribution (<50 %; Rees et al., 1999; Tambi et al., 2009).

This in part explains the observed decrease in phosphate in the SML and thermocline at Jones Bank, but does not explain why an increase in phosphate was not observed on the subsequent spring tidal cycle. It is possible that the intense SCM that were observed during sampling of the latter spring tide intercepted and assimilated the phosphate flux, transferring the new phosphorus to the organic phase (e.g. Karl and Bjorkman, 2002).

The results of the mixing experiments conducted during the 2010 Celtic Sea cruise suggest that phosphate supplied to the SCM during an isolated mixing event would have been assimilated within 27-76 hours. In the Jones Bank data set, the mean SML and thermocline phosphate concentrations continue to decrease throughout the 15-day sampling period. This may be that phosphate was supplied in excess of the simulated proportion during the mixing experiment, thus taking the nitrogen-limited microbial community longer to assimilate the phosphate. Alternatively, it may be that in the natural sampling environment enhanced phosphate fluxes are not isolated events in the same way that the simulated mixing experiments were, particularly in a region of active tidal mixing such as Jones Bank. Therefore, it is possible that during the stormy spring tide sampling period fluxes were at their maximum, but that rather than suddenly decreasing during the switch to calm neaps these fluxes decreased gradually, thus supplying a waning nutrient supply to the base of the euphotic zone.

Changes in primary production

At Jones Bank, euphotic layer primary production rates were highest during the stormy spring tide when primary production by larger phytoplankton was at its highest. The high productivity of the larger size

classes was likely a result of the advantageous conditions offered as a result of new nutrient fluxed to the SML, sufficient light availability and reduced grazing pressure.

Strong tidal currents enhanced diapycnal nutrient fluxes across the base of the thermocline and wind mixing caused the subsequent entrainment of nutrients and biomass into the SML. There, with sufficient light and nutrient availability, larger phytoplankton species were not out-competed by smaller cells and were able to grow at rates exceeding zooplankton grazing rates (Nielsen and Kiorboe, 1991).

Generally during summertime stratification in shelf seas, larger phytoplankton species are efficiently grazed by zooplankton which focus on the SCM where their prey are most abundant (Hobson and Lorenzen, 1972; Scrope-Howe and Jones, 1986). However, during the storm at Jones Bank the SCM was dispersed through the SML, decoupling the efficient predator-prey relationship through dilution effects and a lag time between the increase in phytoplankton biomass and that of zooplankton. This allowed the larger phytoplankton species to be their most productive during the storm and the vertical export potential of particulate organic matter was greater.

Smaller phytoplankton outcompete larger species in low nutrient environments and there is no reason why they would not do so in nutrient replete conditions either (Kiorboe, 1993). Unlike larger phytoplankton, smaller species are grazed by microzooplankton which can maintain a relatively consistent grazing pressure during variations in phytoplankton growth rate (Nielsen and Kiorboe, 1991). In addition, previous studies (e.g. Rees et al., 1999) have found that larger phytoplankton can outcompete picoplankton at times of enhanced mixing as they are better adapted to accommodate higher PAR. However, in this study it is thought that the lower production rates in the smaller size classes during the initial intense mixing period were the result of differential grazing pressures and dilution of biomass with BML water.

Primary production rates at Jones Bank decreased during the study, presumably as the nutrient fluxes to the SML became isolated by the enhanced stratification in the lee of the storm (Rippeth et al., 2009) and the larger phytoplankton populations declined during the switch to regenerated production in the SML (as in Pemberton et al., 2004) and the responsive increase in zooplankton grazing pressure (Nielsen and Kiorboe, 1991). The data support this suggestion, showing a relatively rapid decrease in production rates for the large phytoplankton size class after after the stormy spring tide (from ~ 130 mg C m^{-2} d^{-1} to ~ 35 mg C m^{-2} d^{-1} over 3 days).

After the stormy spring tide, the highest primary production rates remained in the surface water at Jones Bank despite the development of intense SCM associated with the thermocline. Phytoplankton photoacclimation can result in the chlorophyll maximum being distinct from the biomass maximum (Moore et al., 2006; Hickman et al., 2009). This may account for the offset between chlorophyll and carbon fixation in the current data. Whilst carbon fixation in the SML may exceed that at the thermocline, SML production was presumed regenerated due to the very low inorganic nutrient concentrations (particularly in the latter part of the study) and it is thermocline layer carbon fixation that is most likely driven by new nutrient fluxes and thus driving a net carbon drawdown (Pemberton et al., 2004; Rippeth, 2005). The accumulation of dissolved organic phosphorus (DOP) at the SCM suggests enhanced primary production in this region of the water column, so perhaps efficient grazing of larger size classes suppressed this signal in the measured carbon fixation rates (Hobson and Lorenzen, 1972). Grazing would also contribute to the DOP pool and in the relatively low turbulence of the thermocline (Sharples and Tett, 1994), DOP accumulation may be further facilitated by reduced physical mixing and removal processes.

During the 2010 Celtic Sea research cruise, however, primary production and bacterial production data show very different water column distributions and changes in rate relating to the wind-event (A. Panton, pers. comm.). At this deeper mid-shelf station primary production and bacterial production rates were highest at the SCM (38 – 40 m) rather than

at the surface. Despite driving nutrient fluxes across the base of the thermocline and into the euphotic zone, this storm did not appear to enhance production at the SCM, with primary production rates decreasing from 54.0 mg C m^{-3} d^{-1} to 28.2 mg C m^{-3} d^{-1}; and bacterial production decreasing slightly from 6.0 mg C m^{-3} d^{-1} to 5.84 mg C m^{-3} d^{-1} (data courtesy of A. Panton, University of Liverpool). This is also reflected in the euphotic zone integrated values (469 g C m^{-2} to 426 g C m^{-2} primary production, and 207 g C m^{-2} to 195 g C m^{-2} bacterial production). This data appears to suggest that neither bacterial production nor primary production rates were greatly impacted by the wind event (reductions of 9.2 % and 5.9%, respectively).

Dissolved organic phosphorus

Dissolved organic matter is biologically derived and produced in the euphotic zone (Hopkinson et al., 1997). A net gain in DOP after a mixing event was observed at Jones Bank, in the 2010 Celtic Sea dataset and in the mixing experiment data. At Jones Bank, DOP accumulated in the surface layers while there was a concomitant decrease in DIP values. It is thought that this DOP was produced *in situ* and was linked to primary production either by direct phytoplankton exudation, associated release during zooplankton grazing or release via bacterial/viral cell lysis (Carlson, 2002). Phosphomonoesters were present throughout the study in the presence of alkaline phosphatase capable of hydrolysing the pool in a matter of days (average 15 ± 5 days), suggesting that the pool was relatively labile and fresh but not subject to autotrophic biological consumption (e.g. Ducklow, 2000).

Increased DOP concentrations were observed at the thermocline at Jones Bank associated with the development of SCM. New production sustained by diapycnal nutrient fluxes across the base of the thermocline may have resulted in a decoupling of *in situ* DOM production (e.g. exudation by phytoplankton or release during zooplankton grazing) and consumption processes (Hopkinson et al., 1997). As zooplankton grazing is focussed on the SCM during summer stratification (Hobson and Lorenzen, 1972) in response to biological stimuli such as organic nutrients (Williams and Poulet, 1986), DOM release during sloppy grazing may be a significant

source of DOP at the SCM. The relatively low turbulence within the thermocline may also have favoured accumulation of this DOP, with export events to deep water at times when diapycnal nutrient fluxes were enhanced (Sharples and Tett, 1994; Sharples, 2008).

Generally, labile DOM is subject to biological removal processes and more refractory DOM is subject to abiotic processes such as photodegradation (Moran and Zepp, 1997). Alkaline phosphatase (APase) is a generally ubiquitous group of enzymes facilitating the hydrolysis of phosphomonoester bonds and can be associated with phytoplankton, zooplankton, bacteria or freely dissolved (Cembella et al., 1984). APase can be induced by organisms in response to phosphorus stress but can also be a constitutive element of physiological processes (e.g. Dyhrman and Ruttenberg, 2006). However, DOM removal by phytoplankton in response to nutrient stress is not the most significant biotic sink of DOP. Bacterial processes provide a significant sink for DOM via transformation from and to particulates and remineralisation to inorganic nutrients (Pomeroy, 1974). Bacteria preferentially access the DOP pool during luxury uptake of nutrients (Carlson and Ducklow, 1995) and consumption often correlates to substrate availability (Shiah et al., 2000; Hopkinson et al., 1997); often hydrolysing labile DOP as an easy source of carbon (e.g. Carlson and Ducklow, 1995; Sebastian et al., 2004; Luo et al., 2011). In the 2010 Celtic Sea study, ELF staining indicated that at all depths in the water column APA was largely attributable to bacteria and often associated with particle surfaces, suggesting that on-shelf bacterial remineralisation was the largest biotic sink of labile DOP.

At Jones Bank, APA rates were generally very low compared to other studies (see Table 3.7) and did not correlate to PPhos or chlorophyll concentrations suggesting that DOP was not a significant source of phosphorus for the phytoplankton community, as seen by Lomas et al., 2010. It is possible, but believed unlikely, that the lack of any clear correlation between APA and plankton may have arisen from lag times between induction and repression of the enzyme (Ruttenberg and Dyhrman, 2005). However, the highest APA rates were measured at the SCM when phosphate fluxes to the thermocline were enhanced. ELF staining indicated that this may have been associated

with bacteria and particle surfaces. Previous studies (e.g. Pemberton et al., 2004) and data from the mixing experiments conducted during the 2010 cruise indicate that the Celtic Sea is nitrogen limited. In which case, APA was highest in the presence of phosphate in a nitrogen-limited system, which is counterintuitive if APA was induced in response to phosphorus stress (e.g. Jansson et al., 1988).

There are thought to be two possible explanations: sampling resolution of the potentially stratified phytoplankton populations within the SCM (Hickman et al., 2009); or a common origin of APA and DIP from below the thermocline (Sebastian et al., 2004). Were the latter to be the case, then it would also explain why no correlation to chlorophyll or PPhos (>0.7 μm) was observed at Jones Bank. This also suggests that the primary DOP removal process in the region was bacterial remineralisation below the thermocline (Pomeroy, 1974), presumably as a labile source of DOC (e.g. Carlson and Ducklow, 1995; Huang and Hong, 1999; Labry et al., 2002; Sebastian et al., 2004; Hoppe and Ullrich, 1999; Luo et al., 2011). Therefore, APA may have correlated to bacterial production or biomass rather than chlorophyll or PPhos (>0.7 μm) which would typically indicate phytoplankton biomass. Joint and Pomeroy (1987) who found that bacterial production in the Celtic Sea is linked to temperature rather than primary production, which may also give some explanation to the lack of any significant correlations in APA and the measured rates and parameters.

However, bacterial-APA may not be directly correlated to bacterial production. In the 2010 Celtic Sea data, euphotic layer integrated DOP increased after the wind event (from 1.65 ± 0.62 mmol m^{-2} to 3.91 ± 0.36 mmol m^{-2}). Alkaline phosphatase activities also increased at all depths measured (see table 3.10) and ELF staining indicated a dominance of a bacterial contribution, yet bacterial production decreased after the storm. When bacteria are nutrient limited they favour nutrient acquisition over growth, and vice versa when they are in nutrient replete conditions (Church, 2000). Thus, in low nutrient conditions bacteria require a higher N:P nutrient source for synthesis of transport proteins whereas in nutrient replete conditions bacteria require a more phosphorus rich nutrient source for the synthesis of nucleic acids and so on (Church, 2000). Therefore, there

is large variability in the nutrient uptake stoichiometry of a heterotrophic bacterial community depending on their nutrient status. So perhaps the post-storm enhancement of labile DOP remineralisation, if bacteria-dominated, is not directly linked to bacterial production or perhaps other trophic interactions such as zooplankton grazing play an important role.

Actual APA hydrolysis rates are dependent on prevalence of the enzyme and abundance of substrate. Determination of APA via the addition of an artificial substrate at concentrations potentially much higher than background concentrations could be perceived to indicate potential hydrolysis rates rather than reflect *in situ* hydrolysis rates in the water column. Phosphomonoester concentrations decreased after the storm, while APA rates increased. If it is correct to assume that the observed APA was a bacterial response to DOC limitation, then after the storm once phosphomonoesters were becoming depleted bacterial communities may have become increasingly DOC-stressed, affecting their productivity. As alkaline phosphatase persists in the water column for extended periods (days to weeks; Jansson et al., 1988; Li et al., 1998) after its synthesis and can occur freely dissolved, it is possible that the high APA recorded after the storm is a relic of earlier bacterial productivity at a time when phosphomonoesters were more abundant.

3.3.4. Export potential

The Celtic Sea is nitrogen rather than phosphorus limited (Pemberton et al., 2004; this study's mixing experiments). Thus, assimilated phosphorus is converted to organic matter and released as DOP via biological processes. In a nitrogen limited system, DOP can form a potentially significant part of the DOM pool (Conan et al., 2007). Accumulation of DOP in the surface layers of the Celtic Sea was observed during this study after a strong mixing event. In light of the low APA rates throughout the study, it is thought that DOP was actually diluted initially by deep waters during the storm and the observed accumulation was in fact a 'stabilisation' of surface DOP concentrations. However, there was evidence of labile DOP below the thermocline during the stormy spring and DOP was present in the deep water throughout.

Generally, microzooplankton-respiration at the thermocline acts as a DOM sink and a barrier to the downward export of DOM from the euphotic zone (Vidal et al., 1999). Turbulent kinetic energy dissipation and mixing at the base of the thermocline induced by internal tides may act to disrupt this efficient DOM sink, facilitating bursts of enhanced export similar to the converse diapycnal nutrient flux into the SCM. Thus, it is not thought that the stormy spring cycle caused a net gain in surface DOP but acted to export a significant amount of DOP and PPhos below the thermocline.

The efficiency of shelf sea carbon export is reliant on a high C:N:P ratio. DOP was observed in the deep water throughout sampling despite undergoing preferential remineralisation. This suggests a relatively inefficient carbon export pathway (Hopkinson et al., 1997). Remineralisation by bacteria and zooplankton is a significant biological pathway for the production of refractory DOM (Amon and Benner, 1996; Sebastian et al., 2004; Tanaka et al., 2005) and can rapidly convert labile DOM to more refractory components (Ogawa et al., 2001). However, the measured remineralisation rates here were low suggesting that biotic conversion pathways were relatively inefficient. So depending on residence time below the thermocline, exported DOM may still be relatively labile when it is returned to the surface layers during periods of enhanced diapycnal mixing

and therefore the shelf sea region studied only offered temporary carbon storage rather than a permanent sink.

3.4. Conclusions

This study has shown that storm events in shelf seas drive significant exchanges between surface, thermocline and bottom waters. Inorganic nutrient fluxes across the base of the thermocline fuel new production at the SCM; a process that is enhanced during storm and strong tidal events. This enhanced primary production drives net accumulation of DOP in the surface layers, with evidence of export to the bottom water during times of enhanced turbulence at the thermocline. Given the slow biological turnover rates of DOP measured in this study, this could potentially be a significant export pathway within the shelf sea pump. However, a number of questions remain: what is the residence time of organic matter below the thermocline and is this sufficient to be considered as "export"? What fraction of organic matter is remineralised, and what proportion is converted to refractory carbon-rich organic matter, i.e. how efficient is shelf sea export? Is there water mass exchange of shelf sea bottom water with the deep open ocean, thus facilitating true export? The latter question is discussed further in the following chapter.

4. CROSS-SHELF SPATIAL VARIABILITY OF PHOSPHORUS DYNAMICS IN THE CELTIC SEA

4. Cross shelf spatial variability of phosphorus dynamics in the Celtic Sea

Summary

Shelf seas are highly productive and physically dynamic environments. Spatial and temporal variability of physical mixing processes can be significant, and in turn this can impact biogeochemical processes that support high productivity. In this chapter, data from a research cruise (*RRS Discovery;* D352) that sampled a cross-shelf transect in the Celtic Sea is presented to reveal the spatial variability in phosphorus partitioning. The potential for DOP accumulation, its lability and turnover, and potential export to the North Atlantic are discussed.

4.1. Introduction

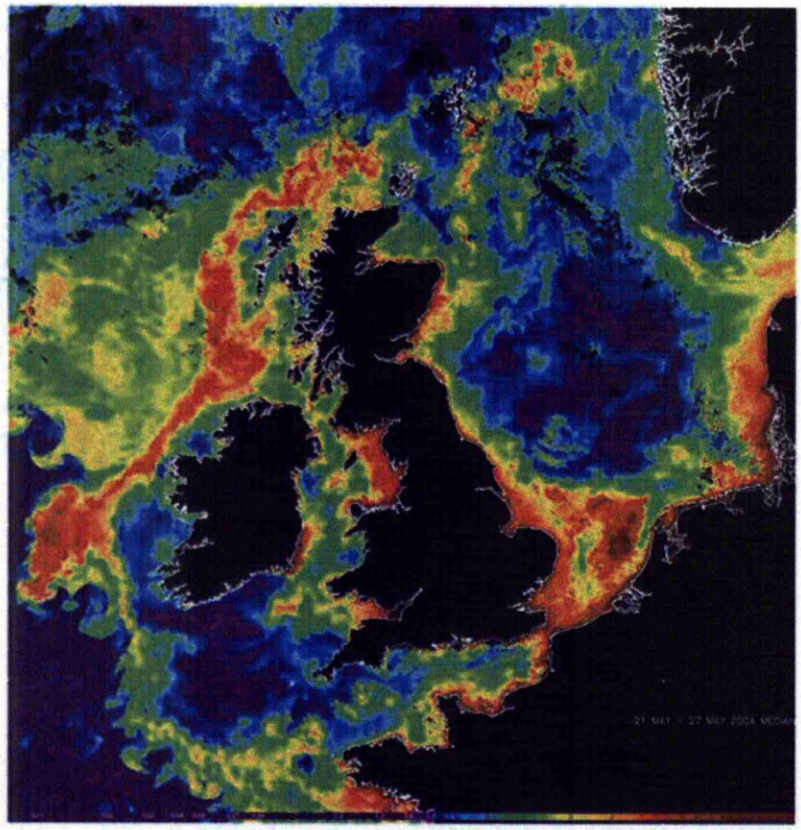

Figure 4.1. An ocean colour satellite image of chlorophyll concentration over the northwest European shelf sea system. Warm colours indicate higher concentrations, while cool blues and purples indicate low concentrations.

Shelf seas are highly productive regions, covering 7% of the global ocean by area but accounting for 16-30 % of ocean primary production (Thomas et al., 2004). Area averaged primary production rates in the temperate Celtic Shelf Sea are 4-times higher than those of the open Atlantic Ocean (Sharples, pers. comm.) with physical mixing processes playing an important role in driving this enhanced productivity (Rippeth, 2005).

Ocean colour satellite images illustrate the importance of physical processes. Satellite ocean-colour observations show bands of high chlorophyll concentrations in regions of strong mixing in the northwest European shelf sea, such as at the shelf edge and the Irish Sea front (Fig. 4.1). Deeper shelf sea regions, such as the Celtic Sea become thermally stratified in the summer and have low chlorophyll concentrations at the surface, except during blooms at the onset and breakdown of stratification (Fig. 4.1).

During summer stratification, the buoyant surface mixed layer (SML) is separated from the nutrient-rich bottom mixed layer (BML) by a thermocline layer of varying thickness. Primary production in the euphotic layer draws down inorganic nutrient concentrations in the SML through biological uptake, leading to the development of a marked nutricline associated with the thermocline (Sharples et al., 2001). The presence of the thermocline restricts the vertical supply of nutrients into the euphotic zone. Thus, during summer stratification, production in the SML becomes nutrient limited shortly after the initial spring bloom. However, there is still some exchange across the base of the thermocline due to turbulent dissipation of shear stress. This drives diapycnal fluxes of nutrient-rich BML water into the lower euphotic zone where it fuels 'new' production.

The observed biological response is an accumulation of phytoplankton biomass associated with the nutricline forming subsurface chlorophyll maxima (SCM; Fig 4.2) within the base of the thermocline. SCM development requires enough turbulent exchange with the BML to supply sufficient new nutrients to support phytoplankton growth, but not sufficient turbulence that phytoplankton biomass is lost to the BML. Throughout summer stratification, SCM-primary production is thought to be an

important component of annual new (i.e. nitrate fuelled) primary production in the Celtic Sea (Rippeth, 2005). As tidal- and wind-driven processes affect shear stress at the base of the thermocline, they play an important role in the magnitude of new nutrient fluxes into the euphotic zone and strongly influence primary production.

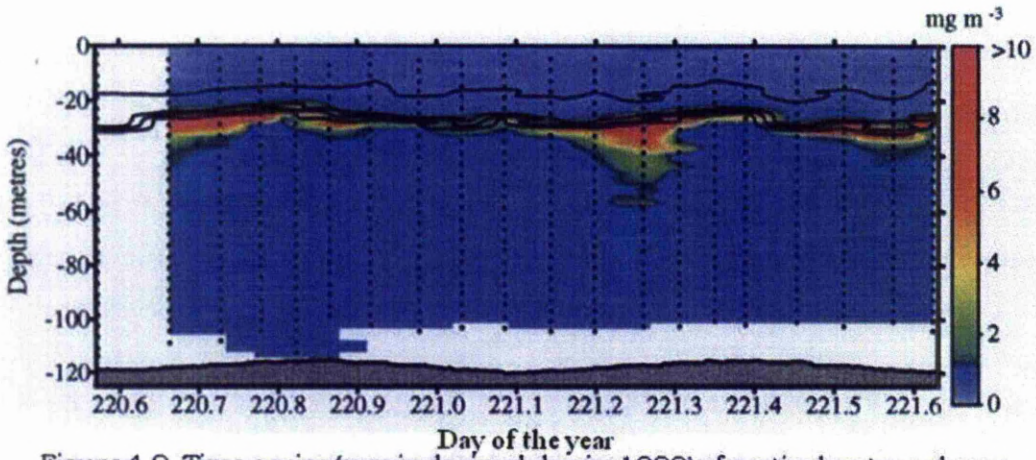

Figure 4.2. Time series (x axis decimal day in 1999) of vertical water column structure in the Celtic Sea, taken from Sharples et al. (2001). Black lines depict isotherms (every 2°C) overlaying contoured chlorophyll *a* concentration (mg m^{-3}, coloured).

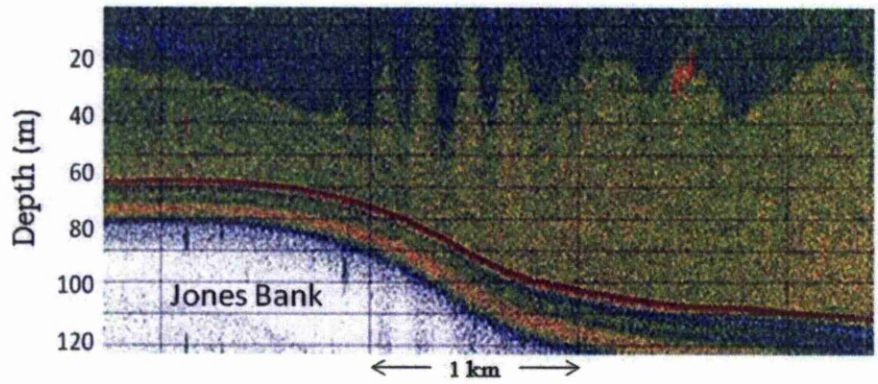

Figure 4.3. EK60 echosounder image of a series of short internal waves triggered by the interaction with the irregular topography of Jones Bank (adapted from Simpson and Sharples, 2012)

There are three primary sources of shear at the thermocline; internal waves, wind driven inertial-oscillations, and tides. When vertically displaced by irregular bathymetry, tidal currents can initiate internal waves which propagate along the thermocline causing turbulent mixing (Fig 4.3;

Simpson and Sharples, 2012). Sudden changes in wind speed or direction can trigger enhanced shear at the thermocline between the wind-driven inertial oscillation of the SML and the tidally-driven oscillations of the BML (Rippeth et al., 2009). Lastly, turbulent dissipation of strong spring tidal currents can propagate through the water column, in some instances to the base of the thermocline (Fig. 4.4). Together, these physical mixing processes drive varying diapycnal nutrient fluxes across the base of the thermocline.

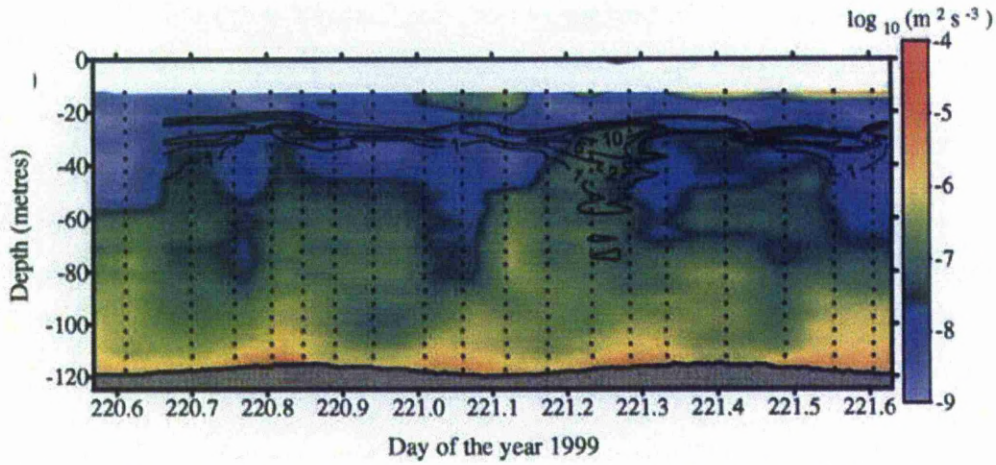

Figure 4.4. A time series (x axis decimal day in 1999) turbulent energy dissipation ($1 \log_{10}(m^2 s^{-3})$; contoured) with chlorophyll *a* concentration (black contour lines marking 1, 2, 5, and 10 mg m^{-3}) taken from Sharples et al. (2001).

In the following chapter, I examine the spatial distribution and dynamics of phosphorus in the Celtic Sea, concentrating on the organic phosphorus pool in particular. Organic nutrients are produced from inorganic nutrients, such as nitrate and phosphate, through biological processes, which include extracellular release from phytoplankton during primary production, release during zooplankton grazing and excretion, and bacterial and viral cell lysis. Organic nutrients typically cannot be directly assimilated by phytoplankton and must first be enzymatically hydrolysed to small labile compounds by alkaline phosphatases and phosphodiesterases. During bloom events, when there is sufficient supply of inorganic nutrients, organic matter production and consumption processes may become decoupled. This leads to a net gain and potential accumulation of organic nutrients, such as dissolved organic phosphorus (DOP). When inorganic nutrients become depleted, many microbes invoke their capacity to synthesise hydrolytic enzymes, allowing

them to access nutrients from the organic pool. Thus, under nutrient limited conditions, organic nutrients can be an alternative source of phosphorus and/or nitrogen supporting primary production.

Particulate and dissolved organic phosphorus is preferentially remineralised before N and C (Kolowith et al., 2001) and much phosphorus is retained in the euphotic zone through microbial degradation processes (Taylor et al., 2009). The DOP pool consists of phosphoesters and phosphonates, the latter being more refractory and less readily utilised by microorganisms (Monaghan and Ruttenberg, 1999). Phosphomonoesters are the most labile fraction of the DOP pool and the microbial community's capacity to hydrolyse this fraction is dependent on the relative abundance of the enzyme alkaline phosphatase. By using fluorogenic substrate addition assays and enzyme-labelled fluorescence (ELF) staining and microscopy, community phosphomonoester hydrolysis rates can be estimated and the microbes contributing to this activity can be identified.

Primary production in the Celtic Sea is nitrogen limited (Pemberton et al., 2004), so inorganic nitrogen is depleted prior to phosphate. With regard to diapycnal nutrient fluxes across the base of the thermocline, the new nitrate supplied will be assimilated at approximately Redfield ratio but will become depleted prior to phosphate. Therefore the dissolved organic nitrogen (DON) pool may be an important alternative source of nitrogen once nitrate becomes depleted. Meanwhile, phytoplankton have sufficient phosphate to meet their phosphorus quota and so during these mixing events, net DOP production is favoured. Assuming this DOP is not mixed into the BML, then DOP could potentially accumulate at the SCM and in the SML.

Through analysis of phosphate, dissolved organic phosphorus (including phosphomonoesters), particulate phosphorus and by measurement of alkaline phosphatase activity, I aim to address the following research questions:

- Does DOP accumulate in the Celtic Sea?
- How labile is this DOP and how rapid is its turnover?

- Is DOP potentially transported laterally to the adjacent P-limited North Atlantic Ocean?

In June 2010, during summertime stratification in the Celtic Sea, a NERC-funded research cruise (D352) was conducted as part of the responsive mode project "a thermocline nutrient pump". The focus of the cruise was to investigate the effects of interactions between wind-induced inertial oscillations and tidal currents, and the resultant shear and pulses of mixing across the thermocline of a seasonally stratified shelf sea. Further, such mixing was investigated in the context of supplying nutrients to the SCM and any possible responsive shifts in phytoplankton community structure.

During the cruise the water column was sampled 59 times in the Celtic and Irish Seas (Fig. 4.5). Biogeochemical sampling in the Irish Sea included casts in Liverpool and Cardigan Bays. Within the Celtic Sea, biogeochemical sampling of the water column included a shelf-shelf break transect consisting of 12 CTD casts (Fig. 4.5b), a time series at "IM1" consisting of 3 biogeochemical sampling CTD casts and a further replicate cast over the shelf slope (CTD 29). This chapter will focus on data from the cross-shelf transect.

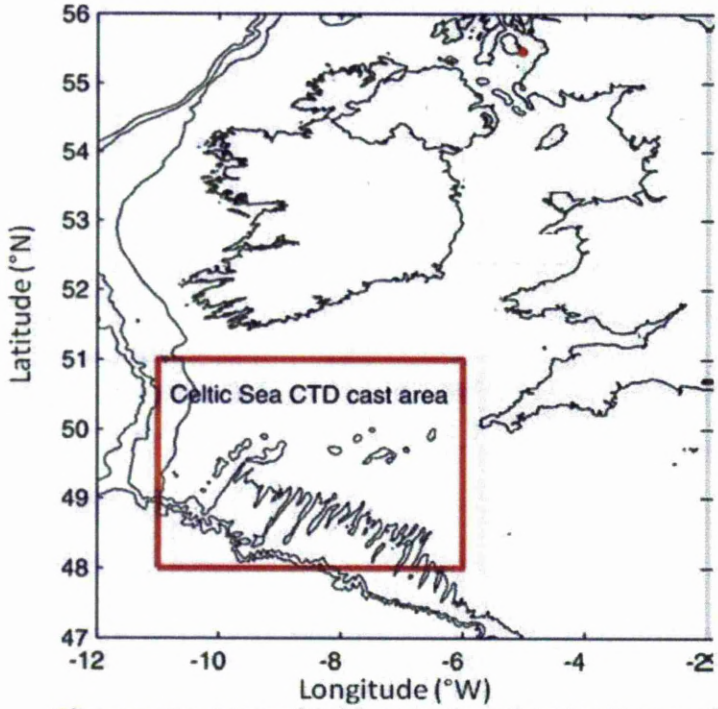

Figure 4.5a. Map of CTD sampling sites in Liverpool Bay (2) and the Irish Sea (58); the red box indicates the region of the Celtic Sea where the majority of sampling was conducted. Black lines depict the 150 m, 500 m and 1000 m isobaths.

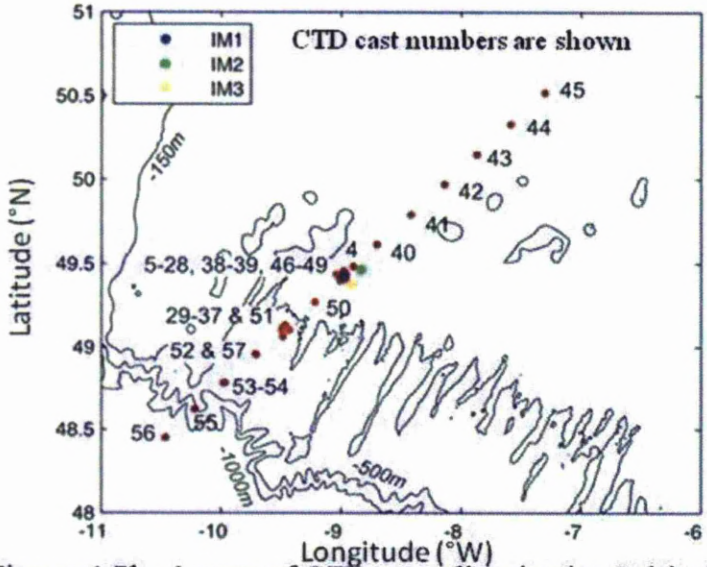

Figure 4.5b. A map of CTD sampling in the Celtic Sea (see inset above). Black lines depict the 150 m, 500 m, and 1000 m isobaths.

4.2. Results

4.2.1. Hydrography of the transect

Temperature

The water column was thermally stratified with strong vertical gradients in temperature at all stations along the transect (Figs 4.6 and 4.7). However, the thermocline gradient (i.e. dT/dz) was weaker at the shelf edge than it was on-shelf and thermocline thickness decreased linearly ($p<0.05$) with distance on-shelf along the transect (Fig. 4.17a). East of CTD 52 (at ~75 km), the temperature difference between the surface mixed layer (SML) and bottom mixed layer (BML) increased and the thermocline and SML became two distinct layers. This suggests that there was stronger vertical mixing over the shelf edge than on-shelf. This may have resulted from greater internal wave activity at the shelf edge, triggered by tidal currents interacting with shelf edge topography.

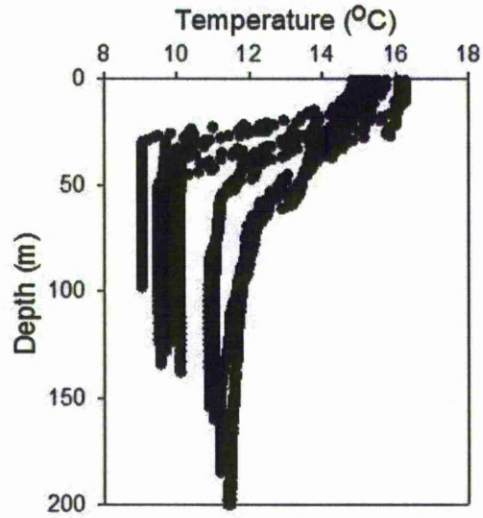

Figure 4.6. Temperature (°C) in the surface 200 m across the transect (CTDs 40-45, 51-53, 55 & 56).

Temperature data revealed a lateral temperature gradient between oceanic and shelf deepwaters, with deepwater (or BML) temperatures being 2.5 °C cooler on the shelf than those at the shelf edge. This results from the shallower shelf seas losing heat more efficiently during winter mixing than

the deep oceanic waters prior to the onset of spring stratification and is a potential indicator of the different water masses below the thermocline. The difference in oceanic/shelf water is also reflected in the lateral gradient in salinity (Fig. 4.8), with more saline waters to the west of the shelf break and fresher waters to the east. This point on the transect also marks the western extent of on-shelf enhanced stratification (Fig. 4.7).

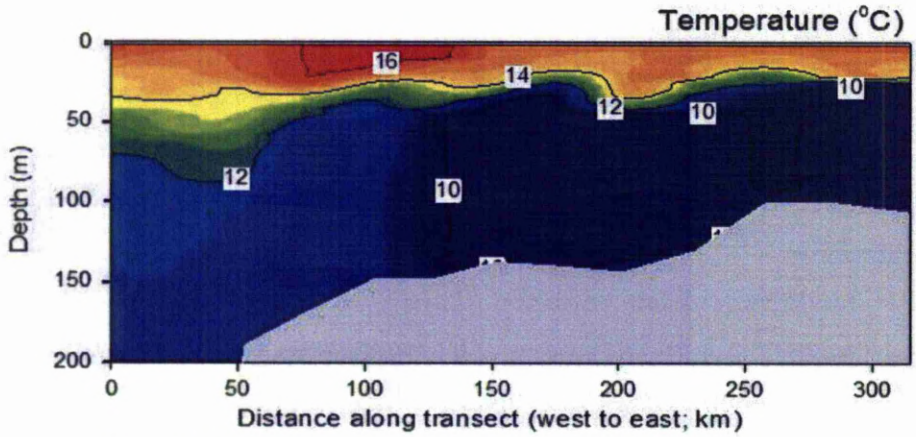

Figure 4.7. Temperature transect (°C, coloured) with crude bottom topography (shaded gray).

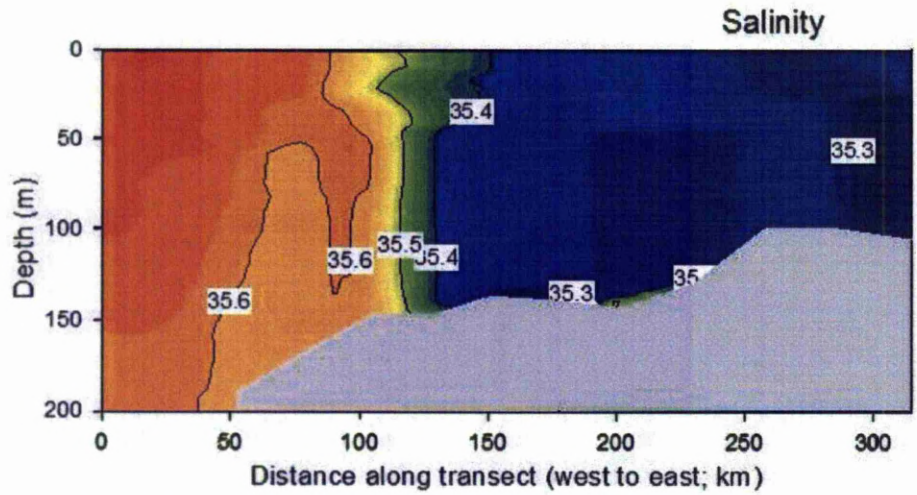

Figure 4.8. Salinity transect (psu, coloured) with crude bottom topography (shaded gray).

4.2.2. Biology

Chlorophyll concentrations varied vertically, generally being higher in the upper 60 m, and horizontally along the transect forming intense subsurface patches on the shelf (Fig. 4.9 and 4.10). At the shelf edge chlorophyll concentrations were highest in the surface layer (<1.5 μg L^{-1}) over a broad depth range (surface to 40 m; Fig. 4.10). Further on-shelf, subsurface chlorophyll maxima (SCM) were observed with concentrations <4 μg L^{-1} over increasingly narrow depth ranges (Fig 4.9 and 4.10). Dissolved oxygen concentrations (Fig. 4.11) were highest at the chlorophyll maxima. To the eastern extreme of the transect, BML dissolved oxygen concentrations were higher than those below the thermocline at other stations.

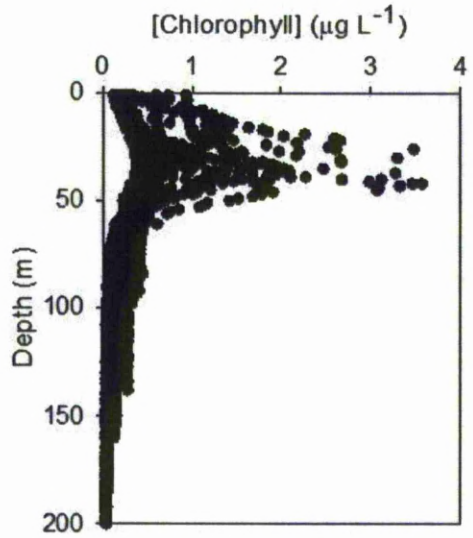

Figure 4.9. Chlorophyll concentration (μg L^{-1}) in the surface 200 m across the transect (CTDs 40-45, 51-53, 55 & 56).

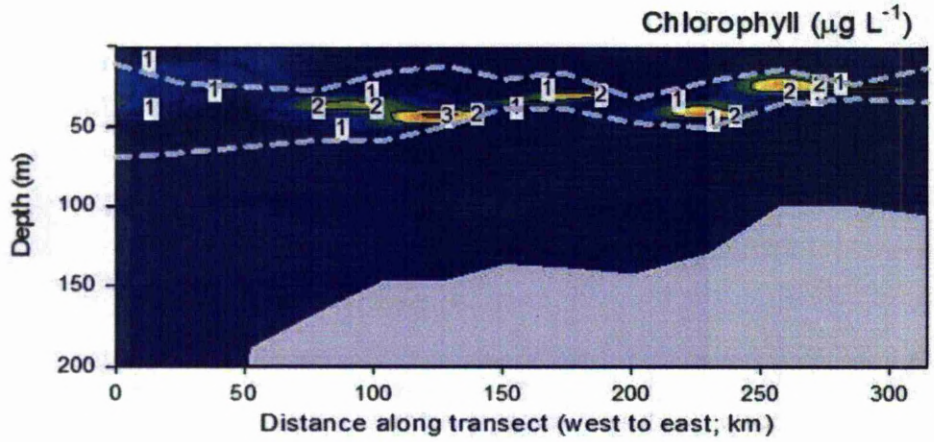

Figure 4.10. Transect of chlorophyll concentration (µg L^{-1}, coloured) with crude bottom topography (shaded gray).

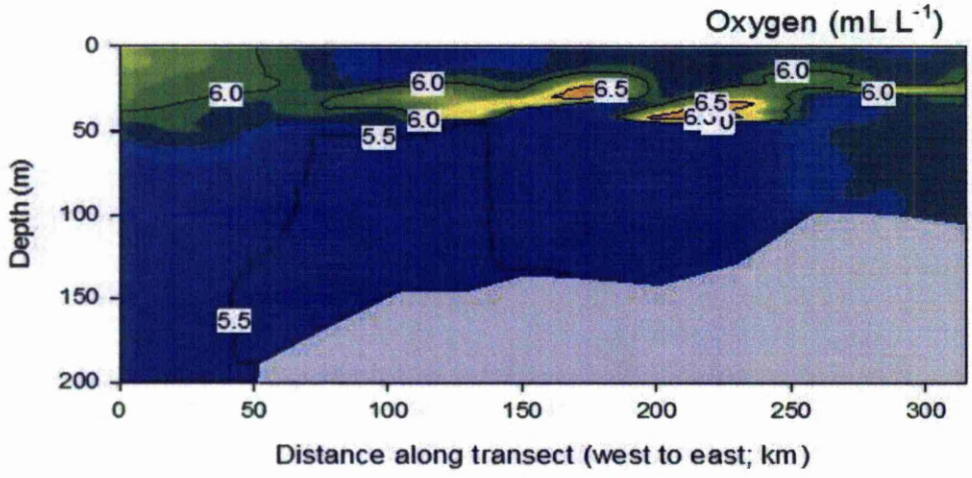

Figure 4.11. Transect of dissolved oxygen concentration (mL L^{-1}, coloured) with crude bottom topography (shaded gray).

4.2.3. Dissolved nutrients

4.2.3.1. Phosphate

Dissolved phosphate concentrations were low in the SML (<0.1 µM) and highest in the BML (~0.6 µM) at all stations (Fig. 4.12). This vertical distribution reflects biological uptake of phosphate in the euphotic zone and remineralisation of organic matter in the BML, which act to maintain winter phosphate concentrations below the thermocline (Hydes et al., 2004). At 200 m depth in the adjacent northwest Atlantic Ocean, phosphate concentrations are also ~ 0.6 µM, and 0.9 µM at 500 m (WOCE, 2011). In the bottom water, the N:P ratio decreased from ~16 at the deepest CTD to

~12 at the furthest on-shelf station. Deepwater phosphate concentrations initially decreased at the shelf edge before becoming relatively constant over the shelf (Fig. 4.13) while bottom water inorganic nitrogen concentrations decreased with distance from the shelf edge (data not shown).

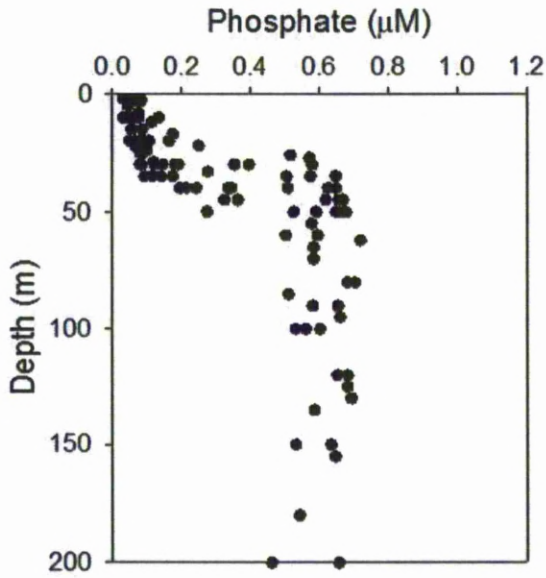

Figure 4.12. Phosphate concentration (µM) for the surface 200 m across the transect (CTDs 40-45, 51-53, 55 & 56).

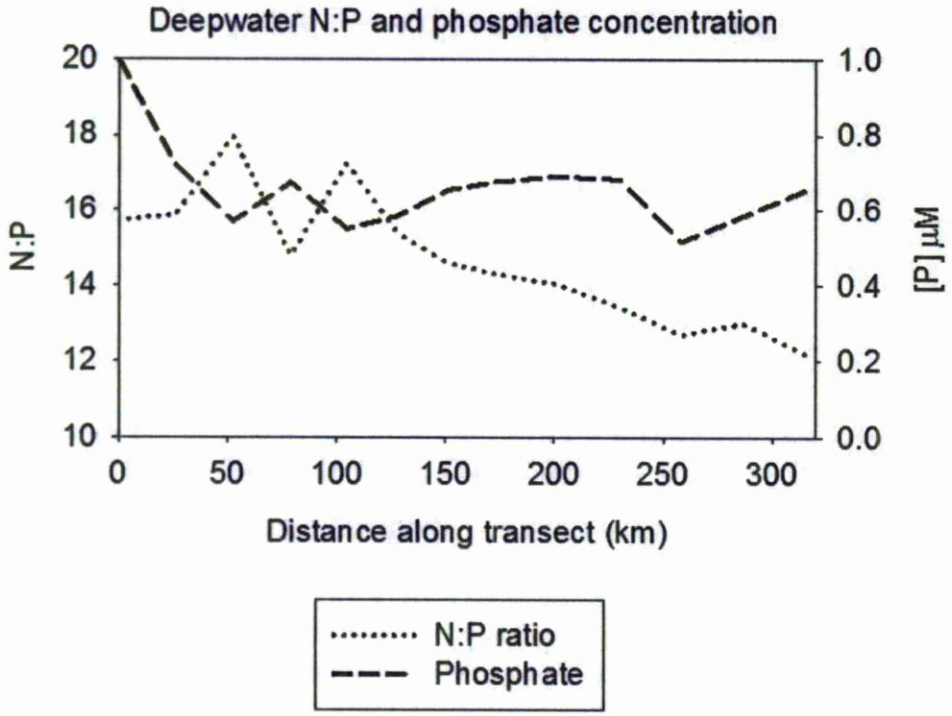

Figure 4.13. Average bottom mixed layer N:P (nitrate plus nitrite to phosphate) ratios and phosphate concentration along the transect.

The deeper limit of the phosphocline (the maximum vertical gradient in phosphorus concentration) corresponded to the base of the thermocline throughout (Fig. 4.14; phosphate in blue), suggesting that physical mixing across the base of the thermocline was the primary control on phosphate fluxes to the euphotic zone. However, there was no linear correlation ($p>0.05$; data not shown) between phosphate and temperature in the thermocline layer. This suggests that the diapycnal dissolved phosphate flux was biologically removed within the thermocline. Chlorophyll and oxygen data (Fig. 4.10 and 4.11) indicated higher phytoplankton biomass at the SCM within the deeper part of the thermocline. Hence the SCM was a potentially significant biological barrier to diapycnal phosphate flux across the base of the thermocline. The efficiency of phosphorus cycling within the SCM is not clear from this data set, but has important implications in terms of water column phosphorus distribution. As the thermocline, phosphocline and SCM were grouped within the water column it is likely that a combination of varying physical mixing and biological removal and remineralisation processes governed phosphate characteristics.

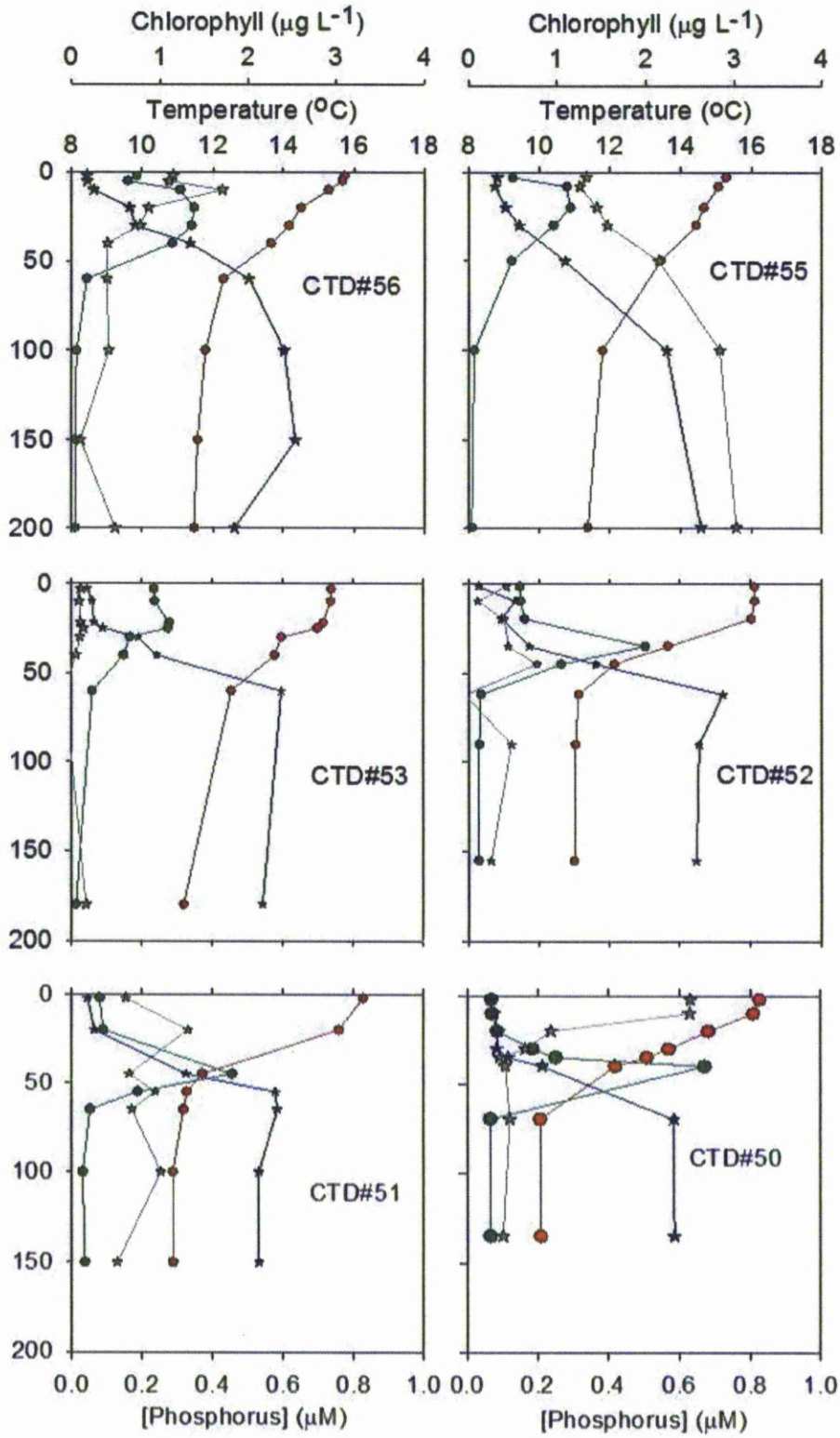

Figure 4.14. Water column profiles in sequential order along the transect, west to east; showing temperature (°C, red circles), chlorophyll (µg L^{-1}, green circles), phosphate (µM, blue stars), and dissolved organic phosphorus (DOP; µM, gray stars).

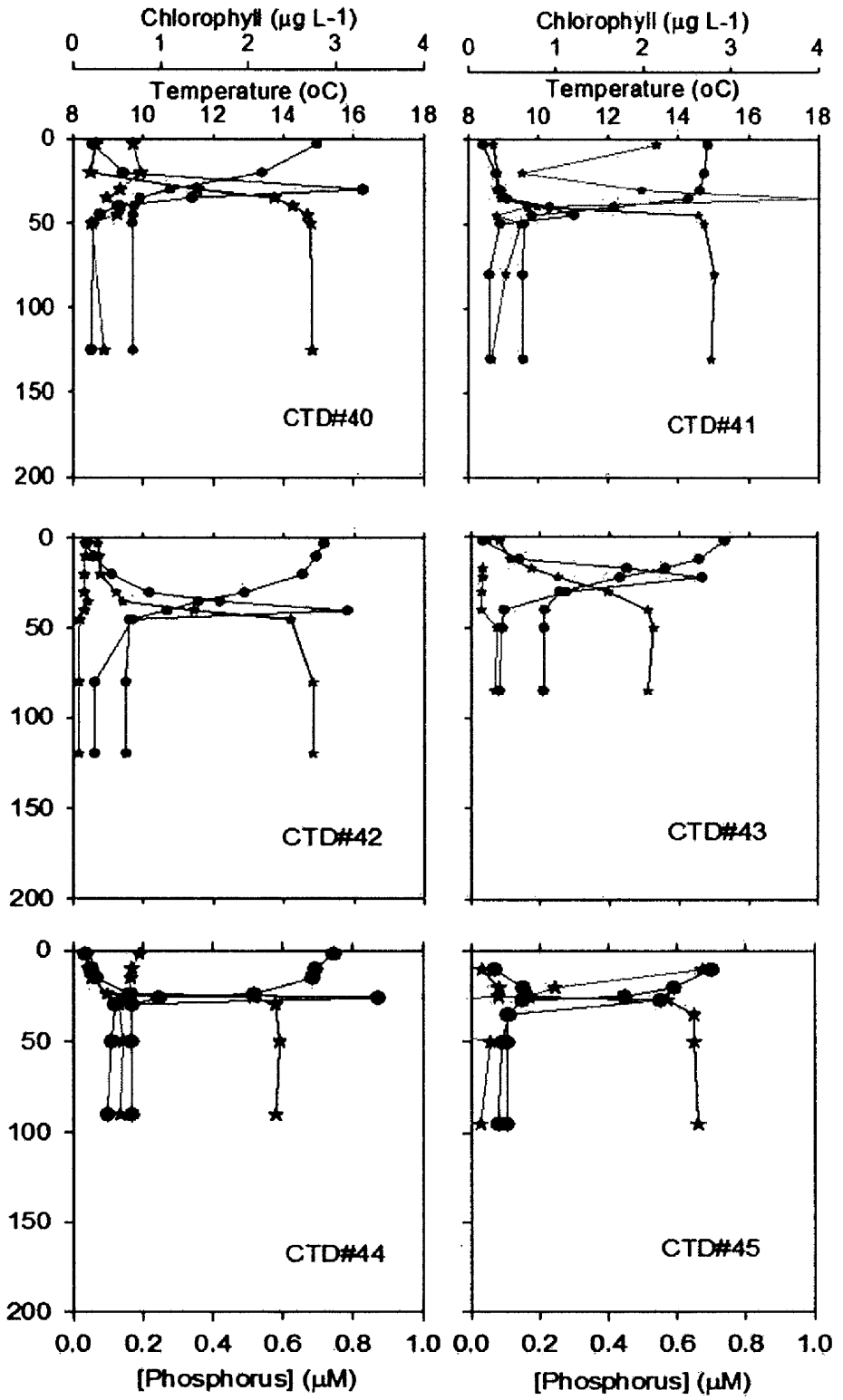

Figure 4.14. continued. Water column profiles in sequential order along the transect, west to east; showing temperature (°C, red circles), chlorophyll (µg L^{-1}, green circles), phosphate (µM, blue stars), and dissolved organic phosphorus (DOP; µM, gray stars).

4.2.3.2. Dissolved organic phosphorus

Dissolved organic phosphorus (DOP) distributions were vertically and horizontally variable, ranging between BLD – 1 μM without a clear spatial trend (Fig. 4.14 and 4.15). Generally, DOP concentrations would be expected to be higher in the euphotic zone than at depth, to reflect the varying balance between DOP production related to primary production and DOP consumption related to remineralisation and heterotrophy, as seen in the stratified open ocean (Karl and Bjorkman, 2002).

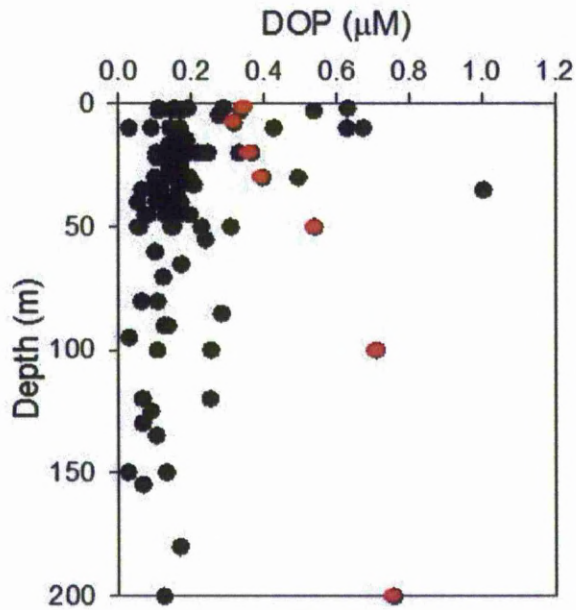

Figure 4.15. Dissolved organic phosphorus (DOP) concentration (μM) for the surface 200 m across the transect (CTDs 40-45, 51-53, 55 & 56). The shelf edge CTD (55) is highlighted in red.

At the oceanic end of the transect, DOP concentrations were elevated in surface waters (0.4 μM at 10 m). Five of the shelf stations (CTDs 50, 40, 41, 44 and 45; Fig. 4.14) exhibited similar DOP distributions. However, DOP was detected in BML water at all stations, in the range of 0.05-0.1 μM (Fig. 4.15), compared with <0.05 μM in the open ocean at station ALOHA, Hawaii (Karl and Bjorkman, 2002) and 0.03 μM at 900 m in the Atlantic Ocean (Kolowith et al., 2001). At four shelf stations (CTDs 53, 52, 51, and 42; Fig

4.14), DOP in the SML was not significantly different ($p>0.05$) from BML concentrations, and at stations 43 and 55 BML-DOP exceeded SML concentrations.

The highest DOP concentration was measured in the on-shelf thermocline at CTD 41 (>1 μM; Fig 4.14). The depth of this DOP-maximum coincided with the upper boundary of the strong thermocline and phosphocline gradients, and the upslope of the SCM (SCM peak 1.2 μg Chl *a* L^{-1}).

Perhaps the most striking feature in DOP distribution was observed at the shelf edge station (CTD 55) where DOP increased with depth from 0.35 μM at the surface to 0.75 μM at 200 m (Fig. 4.14). The only other station where deepwater DOP exceeded euphotic zone concentrations was on-shelf at CTD 43 where concentrations were of the order of 0.1 μM and relatively consistent with depth. At station 55, the thermocline and SML were not as distinct from one another as at other stations (Fig. 4.8), and a relatively weak temperature gradient was observed between the surface and 100 m, similarly above 100 m chlorophyll was seen to increase gradually with a sharp decrease at the surface (Fig. 4.14).

4.2.4. Turnover of the DOP pool – alkaline phosphatase and phosphomonoesters

Alkaline phosphatase activity (APA) rates were low during this study (0.01-1.6 nM P h^{-1}; Table 4.1) compared with the literature. APA was measured at a shelf edge (CTD 53) station, an on-shelf station (CTD17) and at one intermediate station (CTD 29) at four depths. At each cast, APA was observed to increase with depth with lower rates measured at the surface, then at the up-slope of the SCM, the peak of the SCM and finally highest in the BML in both raw (Table 4.1) and biomass normalised APA (normalised to PPhos; Table 4.2).

Table 4.1. Phosphomonoester concentration and alkaline phosphatase activity (MUFP hydrolysis rates). Casts 6, 17 and 29 reflect a time series at IM1 while together casts 17, 29 and 53 represent cross-shelf variations.

Cast	Depth	Latitude	Longitude	PME		APA		Turnover
	(m)	(°N)	(°W)	(µM)	Stdev.	nM P h^{-1}	Stdev	(d)
6	10	49 25.11	008 59.47	0.10	0.00	0.01	0.00	346.4
	38	52 25.11	11 59.47	0.18	0.03	0.39	0.01	19.7
	43	55 25.11	14 59.47	0.15	0.02	0.46	0.01	13.8
	60	57 25.11	16 59.47	0.16	0.02	0.32	0.02	20.6
17	15	50 06.94	9 59.73	0.03	0.01	0.04	0.01	28.3
	40	52 06.94	11 59.73	0.05	0.00	1.05	0.28	1.89
	43	54 06.94	13 59.73	0.03	0.01	1.26	0.34	0.84
	55	56 06.94	15 59.73	0.11	0.01	0.01	0.41	2.92
29	15	50 06.94	10 27.42	0.00	0.02	0.05	0.02	0
	36	52 06.94	12 27.42	0.03	0.01	0.67	0.23	1.9
	45	55 06.94	15 27.42	0.00	0.01	0.85	0.29	0
	65	57 06.94	17 27.42	0.04	0.01	0.70	0.24	2.7
53	10	49 46.98	10 58.00	0.04	0.01	0.28	0.05	5.3
	22	51 46.98	12 58.00	0.04	0.04	0.57	0.11	2.7
	30	53 46.98	14 58.00	0.24	0.02	0.84	0.16	11.8
	60	55 46.98	16 58.00	0.04	0.02	1.02	0.19	1.6
58	15	53 59.96	6 10.96	0.22	0.04	0.40	0.08	23.1

Table 4.2. Alkaline phosphatase activity (nM P μM PPhos^{-1} h^{-1}) normalised to particulate phosphorus (PPhos, μM) as a proxy for biomass.

Cast	Depth	PPhos	APA
	m	μM	nM P μM PPhos^{-1} h^{-1}
6	10	0.063	0.18
	38	0.130	2.99
	48	0.073	6.30
	60	0.041	7.68
17	15	0.068	0.63
	40	0.136	7.72
	43	0.077	16.24
	55	0.074	20.66
29	15	0.069	0.74
	36	0.058	11.67
	45	0.020	43.17
	65	0.017	41.31
53	10	0.041	6.81
	22	0.046	12.40
	30	0.049	17.25
	60	0.012	85.60
56	15	0.078	5.14

The highest APA rate was measured in the BML waters furthest on-shelf (1.54 nM P h^{-1}; Table 4.1), while the lowest APA rates were in the surface at that station (0.04 nM P h^{-1}; Table 4.1). At the mid-shelf station, the highest APA rate was at the SCM but this was not statistically different from those of the SCM upslope or BML. Surface APA was significantly higher at the shelf edge than at the on-shelf stations. This was most likely attributable to an apparent diatom contribution to APA in addition to bacterial APA observed at the shelf edge (Fig. 4.16). Enzyme-labelled fluorescence (ELF) staining revealed that at the two on-shelf stations APA was associated with bacteria and particle surfaces, while at the shelf edge station there was additional staining of pennate diatoms at all depths (Fig. 4.16). This may also have been a response to substrate availability, as surface DOP concentrations were higher at the surface near the shelf edge whereas on-shelf DOP concentrations were higher at the SCM and low in the surface.

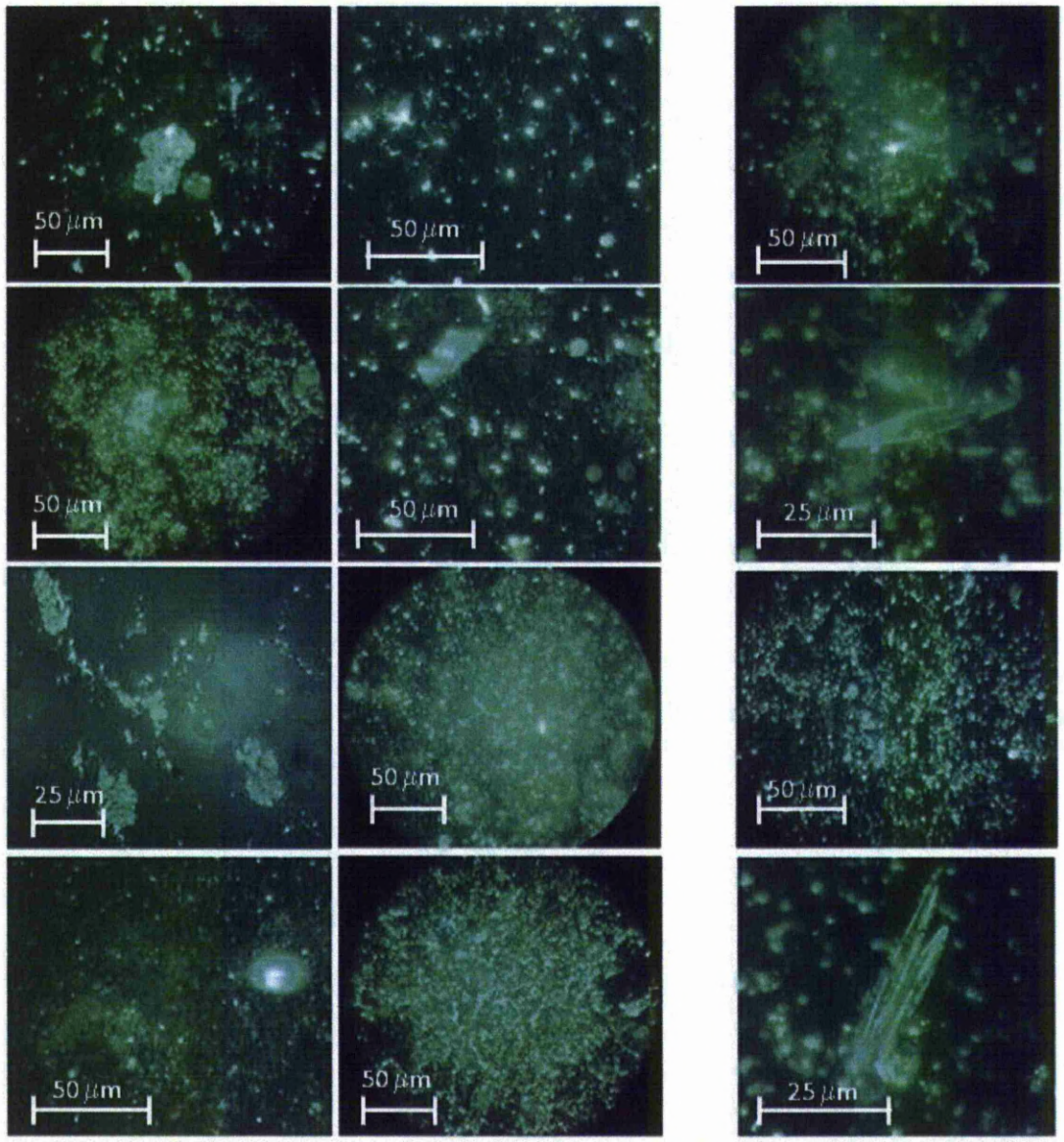

Fig. 4.16. Enzyme Labelled Fluorescence microscope images indicating alkaline phosphatase activity sites in green. Columns (left to right) show samples from CTD 17, 29 and 53. For CTDs 17 and 29, rows show SML, upslope of SCM, peak of SCM and BML samples. For CTD 53, rows show peak of SCM (broad view and close up of pennate diatom) and BML (broad view and close up of pennate diatom).

Phosphomonoesters (PME) are the most labile component of the DOP pool, thus PME concentration was used as a proxy for DOM lability. The presence of PME was assumed to indicate either fresh DOP production with no rapid remineralisation processes, such as APA facilitated hydrolysis, or DOP production at a rate exceeding remineralisation. Measured PME concentrations varied between BLD – 0.24 μM (Table 4.1), with contributions ranging from 0 % to >100 % of the measured bulk DOP pool

(which may have excluded ATP, see Methods, Chapter 2). It is possible that where PME accounted for over 100 % of the total UV-oxidisable DOP pool, that this was the result of ATP compounds being excluded from the bulk DOP measurement but were subject to hydrolysis during the PME determination. ATP can contribute significantly to the total dissolved phosphorus pool. For example at Station ALOHA, Hawaii, where plankton processes are thought to be phosphorus controlled (Karl et al., 2001), ATP concentrations are in the range of 1-60 nM (~25 % of the dissolved organic phase; Björkman and Karl, 2003).

On-shelf at station 17, PME concentrations were low in the euphotic zone (0.03-0.05 μM) but significantly higher in the BML (0.11 μM) where turnover time, calculated from PME concentration and APA hydrolysis rate, was 3 days. The mid-transect station had the lowest PME concentrations. PME was below detection limits at the surface and at the SCM peak, the highest concentration was in the BML (0.04 μM) where turnover times were again 3 days. At the shelf edge station (CTD 53), PME concentrations were similar at all measured depths (0.04 μM) bar the SCM peak (0.24 μM) where turnover was of the order of 12 days.

Nutrient addition incubations were also conducted where phosphate (as $KHPO_4$, 4 μM final concentration), and organic carbon and nitrogen (as glycine, $CH_2NH_2CO_2H$, 10 μM final concentration) were added separately to samples from the BML and SCM at different stations (Table 4.3). Addition of phosphate should indicate whether the APA observed was P-repressible, which would suggest that synthesis of the enzyme had initially been in response to P-stress. Addition of glycine should indicate whether the community present had the capacity to synthesise alkaline phosphatase in response to P-stress. Bottom mixed layer APA did not show a strong response in either treatment compared with the control (Table 4.3). This suggests that APA in the BML was not responsive to P-status and did not appear to be strongly repressible or inducible. At the SCM, APA appeared more responsive to induction and repression. At the SCM at the shelf edge (CTD 53, Table 4.3), the measured APA appeared to be constitutive and non-repressible for the most part. However, the shelf edge SCM samples were very responsive to the +glycine treatment suggesting that the microbial

community had the capacity to induce APA in times of P-stress. However, this increase in SCM-APA in the +glycine may have been related to increased secondary production and bacterial production.

Table 4.3. Summary of alkaline phosphatase activity (nM P h^{-1}) measured during Celtic Sea 2010 nutrient addition experiments with additions of phosphate ($KHPO_4$) and glycine (NH_2CH_2COOH; at 10 µM and 4 µM, respectively).

	APA (nM P h^{-1})			
	T zero	T final		
	CTRL	CTRL	KHPO4 +	Glycine +
BML (CTD 29)	0.70	2.14	1.71	1.99
Base SCM (CTD 38)	0.58	1.46	0.85	7.77
Base SCM (CTD 53)	0.84	4.37	4.17	28.35

4.2.5. Integrated phosphorus cross-shelf trends

Thermocline-integrated phosphate and DOP both decreased linearly from off to on-shelf ($p<0.05$; Fig. 4.17), while SML-integrated phosphate and DOP data showed no significant trend with distance on-shelf ($p>0.05$; Fig. 4.17). As thermocline layer thickness and integrated phosphate/DOP were strongly correlated ($p<0.05$; Fig. 4.18), it is possible that the trends observed in Fig. 4.17 were an artefact of varying thermocline layer thickness rather than concentration.

Therefore, it is arguable that there is an important spatial trend in shelf edge phosphorus distributions. Whether there is more phosphorus held in the euphotic zone due to higher concentrations or due to broader thermocline layer thickness the net result is the same – there is more phosphorus in the euphotic zone at the shelf edge than there is on-shelf. Thus, there is potentially more phosphorus available to support growth and production at the shelf edge than on-shelf.

A simple phosphorus budget was constructed based on euphotic zone integrated primary production (data courtesy of A. Panton, University of Liverpool) assuming the phytoplankton assimilated nutrients at Redfield ratio (106 C: P; Table 4.4). Phosphate assimilation rates were highest at the

shelf edge (CTD 53; 0.40 mmol m^{-2} d^{-1}), and lowest at mid-transect (CTD 27; 0.26 mmol m^{-2} d^{-1}), with an intermediate assimilation rate further on-shelf (CTD 17; 0.34 mmol m^{-2} d^{-1}). As these estimates are derived from carbon fixation data and assumed Redfield uptake proportion, they exclude the bacterial component of phosphorus assimilation. While a potentially significant component (<50 %) of the whole community phosphorus assimilation (Rees et al., 1999), it is difficult to confidently estimate bacterial phosphorus assimilation as the stoichiometry of their nutrient uptake can vary greatly depending on their nutrient status (Church, 2002). In addition, assuming nutrient uptake was in Redfield proportion may not have been representative of the sampled phytoplankton community as uptake ratios can vary with different growth stages (Arrigo, 2005).

The phosphorus budget indicates that there was sufficient phosphorus in the euphotic zone as either phosphate or DOP to meet the phytoplankton community's phosphorus demand for a number of days (6 – 30 days for phosphate, and 8 – 28 days for DOP). Euphotic zone integrated APA rates were highest mid-transect, then on-shelf and lowest at the shelf edge (0.15, 0.36 and 0.31 mmol m^{-2} d^{-1}, respectively; Table 4.3). Assuming hydrolysis of the total DOP pool by alkaline phosphatase was possible, this suggests turnover times of 10 – 25 days (increasing on-shelf). Thus, this simple budget suggests that there was sufficient phosphate, the preferred P-source, to meet the phosphorus demand of the phytoplankton communities across the transect.

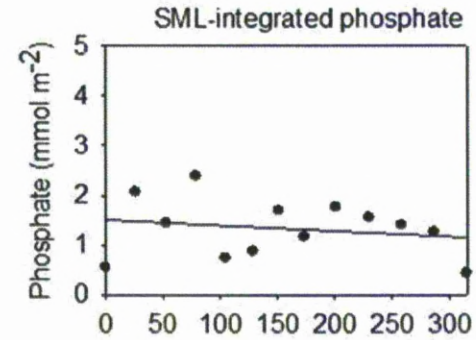

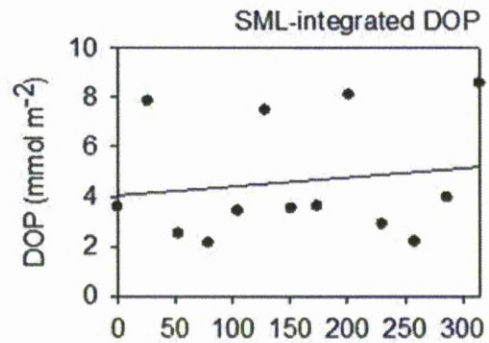

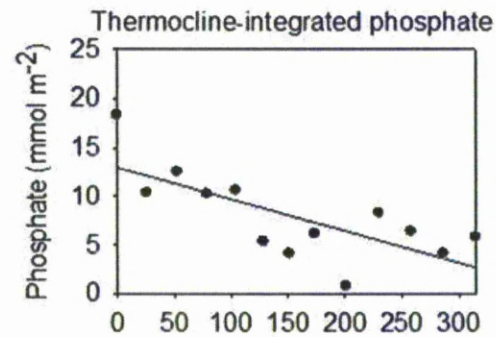

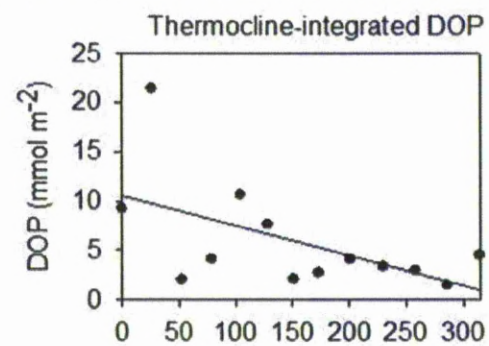

Figure 4.17. Linear regression plots of surface mixed layer (SML)-integrated and thermocline-integrated phosphorus against distance along transect. SML trends are not significant, but thermocline trends are significant ($P<0.05$).

Table 4.4 A simple phosphorus budget based on primary production data (courtesy of A. Panton, University of Liverpool) for 3 stations along the Celtic Sea transect.

CTD	Carbon fixation	P assimilation total	DIP	DOP	APA
	mmol C m^{-2} d^{-1}	mmol P m^{-2} d^{-1}	mmol m^{-2}	mmol m^{-2}	mmol m^{-2} d^{-1}
17	35.53	0.34	6.03	3.89	0.15
29	27.39	0.26	7.70	7.20	0.36
53	42.82	0.40	2.23	3.22	0.31

4.3. Discussion

4.3.1. Does DOP accumulate in the Celtic Sea?

Primary production in the Celtic Sea has previously been shown to be nitrogen limited (e.g. Pemberton et al., 2004; Hydes et al. 2004) so when new macronutrients are supplied to the system nitrate becomes depleted before phosphate. The Celtic Sea is a nitrogen sink via denitrification, with removal rates ranging between 0.23 and 0.6 mmol N m^{-2} d^{-1} (Hydes et al., 1999). Bottom water N:P ratios were seen to decrease off to on with distance from the shelf edge during the present study. The same trend was not observed in phosphate concentrations, therefore it is unlikely to be a dilution effect but instead is more likely attributable to a loss of nitrogen via denitrification. The result of this is that nutrient fluxes across the base of the thermocline will supply inorganic nutrients at lower than Redfield ratios. Therefore regenerated nitrogen sources, such as ammonium and DON, may be important in sustaining microbial production. As inorganic nitrogen becomes deplete before phosphate, there is residual phosphate available, which would favour the accumulation of phosphorus, particularly in the organic phase as a by-product of primary production.

Previously, DOP concentrations in the Celtic Sea were reported to be low throughout the year (0 - 0.2 μM; Hydes et al., 2001). In the present study, DOP concentrations ranged from BLD to 1 μM, with a mean concentration of 0.19 ± 0.17 μM for the whole transect and 0.17 ± 0.16 μM on-shelf. By comparison, Mather et al. (2008) report a mean DOP concentration for the North Atlantic Subtropical Gyre of 0.08 ± 0.01 μM. Therefore the data suggest that relative to the open ocean, the Celtic Sea may be a region of DOP accumulation.

Vertically-resolved DOP distributions suggest that net DOP production may occur at discrete depth horizons rather than ubiquitously throughout the euphotic zone. The link to production within the SCM was quite clear in certain profiles. This may have resulted from direct exudation of organic matter from productive phytoplankton populations, or as release of cellular matter during zooplankton grazing or cell lysis (Carlson, 2002). However, distinct DOP maxima were not present in all profiles. This may relate to

dispersal caused by physical mixing, such as the decoupling of biological signals and physical characteristics in the SML due to atmospheric forcing (Martin et al., 2008). Where exchanges across the thermocline were greater, the signal from net DOP production may have been diluted by deep water. It is possible that during times of mixing across the base of the thermocline, while new nutrients supplied would have fuelled primary production and promoted net DOP production, an influx of bacteria from the BML with higher APA may have enhanced remineralisation rates of freshly formed DOP.

Whether DOP accumulates or not in the Celtic Sea will be dependent on the rates of both production and remineralisation. DOP production rate is dependent on new nutrient supply and phytoplankton community structure. New production favours DOM production and is related to phytoplankton size (Rees et al., 1999). Hence, primary production during the spring and autumn blooms, and at the SCM during stratification favour higher DOP production rates given the supply of new nutrients, which can support larger phytoplankton species. During the stratified summer period, production in the SML is largely regenerated and dominated by smaller phytoplankton species (Pemberton et al., 2004), thus summertime production in the SML would not necessarily favour high DOP production rates.

DOP and PME data suggest that net production of fresh DOP occurred at the shelf edge in the presence of low APA rates (Table 4.1). Enhanced DOP production at the shelf edge was most likely linked to elevated primary production, either directly through phytoplankton exudation or via zooplankton processes such as prey fragmentation, sloppy feeding and excretion (Nagata, 2000). The results of the nutrient addition experiments suggest that production in the SCM at the shelf edge was not phosphorus-stressed as there was the potential for APA-induction by the microbial community. Thus, it is unlikely that more complex fractions of the DOP pool, such as phosphodiesters, were being utilised as these are energetically more demanding to hydrolyse. So the potential for net DOP production and export from the shelf edge region is high.

However, it has previously been reported that in the Celtic Sea summer SML *Synechoccus* and picoplankton dominate the phototrophs (Martin et al., 2008) and are efficiently grazed by microzooplankton (Joint et al., 2001). Bacteria directly utilise the products released by phytoplankton during primary production with a summer heterotrophic carbon requirement that exceeds production (Joint et al., 2001). Therefore, a net production and accumulation of DOM, including DOP, in the Celtic Sea away from the shelf edge would be unlikely outside of bloom events and the SCM.

This study has shown that bacterial remineralisation is an important DOP removal process in the Celtic Sea (Fig. 4.17). Heterotrophic bacteria assimilate organic matter as a principle source of energy and carbon, often synthesising hydrolytic enzymes to access the DOM pool (Church, 2000). In the Celtic Sea, the DOP pool is probably utilised as a relatively labile source of organic carbon, as bacteria are thought to access the more refractory phosphonate pool in response to phosphorus stress (Carlson and Ducklow, 1995; Luo et al., 2011). Vertical profiles in APA obtained during this study suggest that remineralisation of DOP was more rapid below the thermocline despite bacterial production usually being linked to primary production, and therefore being higher in the euphotic zone (Church, 2000). However, APA was higher in the BML. This higher APA may have been associated with bacterial-remineralisation concentrated on particle surfaces of sinking detritus from the SCM. Phosphomonoesters were often most abundant in the BML the higher bacterial APA may have been a response to substrate availability in the water column (Shiah et al., 2000).

4.3.2. How labile is the DOP pool and how rapid is its turnover?

Phosphomonoester concentrations were low, ranging BLD – 0.24 μM (while total DOP concentrations ranged BLD - 1 μM). Despite this, in some instances PME contributed over 100 % of the measured bulk DOP pool. Experimental error during PME determination was low (<0.04 μM) and so the disparity between PME and total DOP may be the result of inefficient ATP recovery during UV oxidation (see Methods 2.3 for further details). However, it is clear that PME was present in the BML as well as the euphotic zone. The labile nature of this fraction of the DOP pool suggests that in the Celtic Sea fresh DOP production rates exceed consumption rates

during summer stratification, otherwise PME would not have been observed. Residence times of 2 years have previously been estimated for the Celtic Sea, through applying the nitrogen deficit, calculated from the predicted Redfield concentration for a given phosphorus content, and denitrification rates (Hydes et al., 2004). In contrast, phosphomonoester turnover times of 0 – 30 days were measured in this study; a residence time of 2 years is more than sufficient for the labile DOP pool to be recycled.

Phosphomonoester concentrations in the BML often exceeded those in the euphotic zone. This is surprising given that bacterial remineralisation rates (in this case referring to measured APA) were higher below the thermocline, and that outside of the euphotic zone DOP production relating to photosynthesis would be expected to be negligible. However, zooplankton processes, such as prey fragmentation, sloppy feeding and excretion, can provide a significant source of DOP (Nagata, 2000). During summer stratification in the Celtic Sea, zooplankton are strongly associated with the SCM (Scrope-Howe and Jones, 1986) which may in part account for the high DOP concentrations at the SCM observed in some profiles. Physical mixing at the base of the thermocline may act to efficiently export DOP produced at the SCM by zooplankton processes to the BML. Diel vertical migration of zooplankton populations may act to drive an additional flux of DOP below the thermocline (Steinberg et al., 2002). Once below the thermocline, this DOP may be metabolised to provide a source of relatively fresh and labile DOP possibly accounting for the observed PME in the BML. PME in the BML may occur as a product of the progressive decomposition and remineralisation of particulate organic matter and DOP of higher molecular weight and complexity exported from the euphotic zone or resuspension of particulates at the sediment-water interface. Alternatively, one might argue that organic nutrients may be mixed down from the SCM into the BML countering the upward diapycnal inorganic nutrient flux. In either case, PME in the BML was typically turned over in 3 days so accumulation would be dependent on the flux of DOM and POM to the BML, with long term accumulation being unlikely given the estimated residence times of Celtic Sea waters.

4.3.2. Is DOP potentially transported laterally to the adjacent P-limited North Atlantic Ocean?

Hydes et al. (2001) reported a mean on-shelf flow in the Celtic Sea, and therefore minimal exchange across the shelf break (Hydes et al., 2001). The discontinuity in horizontal salinity and temperature observed in the present study suggests that horizontal mixing was restricted across the shelf edge. In addition, the residence time on the shelf of 2 years reported by Hydes et al. (2004) is sufficient to suggest that there is no exchange of on-shelf DOP with the Atlantic. However, Huthnance et al. (2001) report that significant mixing exchanges occur at the shelf edge as a result of tides, wind driven flow, ridge associated upwelling, cross-frontal exchange, surface and internal waves, with contributions from eddies and cascading in winter (Huthnance et a al., 2001). Together these studies suggest that on-shelf regions probably do not have exchanges with the North Atlantic but that regions in close proximity to the shelf edge may do.

The present study observed a bloom event at the shelf edge, likely fuelled by nutrients supplied to the euphotic zone by internal tides induced by the interaction between spring tides and the 200 m contour, as recorded by Rees et al. (1999). Natural perturbations such as this favour larger phytoplankton (Pemberton et al., 2004) with an off-shelf progression from a dominance of *Synechococcus* on shelf, to eukaryotes at the shelf break, and *Synechococcus and Prochlorococcus* in the ocean (Sharples et al., 2007). In the present study, ELF staining revealed a diatom contribution to APA at all depths, which was absent at other stations. Thus, at the shelf edge primary production and new production were higher than on shelf.

The highest DOP concentrations observed during this study were associated with this region of high production at the shelf edge. This DOP may have been the direct product enhanced primary production through direct exudation or release during zooplankton grazing (Carlson, 2002). DOP concentrations increased with depth at the shelf edge, which may have arisen from oxidation of particulate organic matter and resuspended sediments, or even perhaps porewater diffusion from sediments (Nedelec et al., 2007).

Through a number of possible exchange pathways, these shelf edge waters with high concentrations of DOP offer the greatest potential for the transfer of DOP to the North Atlantic. Internal tides propagate both on and off shelf (Joint et al., 2001), potentially transporting and mixing DOP within the thermocline. Additional eddy exchange resulting from instabilities in the shelf slope current may also drive sporadic transport of DOP rich waters to the ocean (Hutnance et al., 2001; Liu et al., 2000). Transfer of DOP-rich waters along isopycnals could also occur within the thermocline layer (Hopkins et al., in review).

At the Celtic Sea shelf edge, internal tides can drive resuspension of sediments creating nepheloid layers. Previously, nepheloid layers have been reported to transfer organic matter to the Atlantic Ocean (Nedelec et al. 2007). These layers can detach from the sediment and travel along density surfaces, commonly along water mass boundaries (Nedelec et al., 2007). It is possible that the observed DOP at depth was linked to the resuspension of sediments and oxidation of organic matter. However, there is no evidence from the beam attenuation data (data not shown) to suggest that nepheloid layers were present at density surfaces during this study.

At the western extremity of the transect, beyond the shelf edge bloom, DOP concentrations below 50 m were low. Thus, if the shelf edge is a source of DOP to the Atlantic, then assimilation during lateral transport may be very rapid. Alternatively, latitudinally adjacent Atlantic waters may be isolated from the high DOP water at the shelf edge, which may be contained within the slope current. In this case, the DOP rich waters may be mixed laterally into the North Atlantic further north, through the slope current eddies, or may be lost to the deepwater via the Ekman drain pump (Huthnance, 1995). Across broader slope regions, winds can drive surface water exchange, while at steep and irregular regions of the slope tidal mixing is enhanced (Huthnance et al., 2001). Therefore, it is certainly possible that DOP at the shelf edge region may be transferred to the adjacent ocean.

4.4. Conclusions

Biogeochemical phosphorus signals are spatially patchy in the Celtic Sea, most likely in response to highly dynamic physical mixing processes. The on-shelf region of the Celtic Sea is most probably not a source of phosphorus to the P-limited North Atlantic. However, high productivity within shelf edge blooms may offer a phosphorus source to the ocean via a number of possible transport pathways. Exchange at the shelf edge is predominantly driven by tides and wind mixing (Huthnance et al., 2001) and along-isopycnal transport processes (Hopkins et al., in review). However, whether this feature of higher DOP at the shelf edge compared with adjacent waters is a persistent feature of the Celtic Sea continental margin is not clear from the current study.

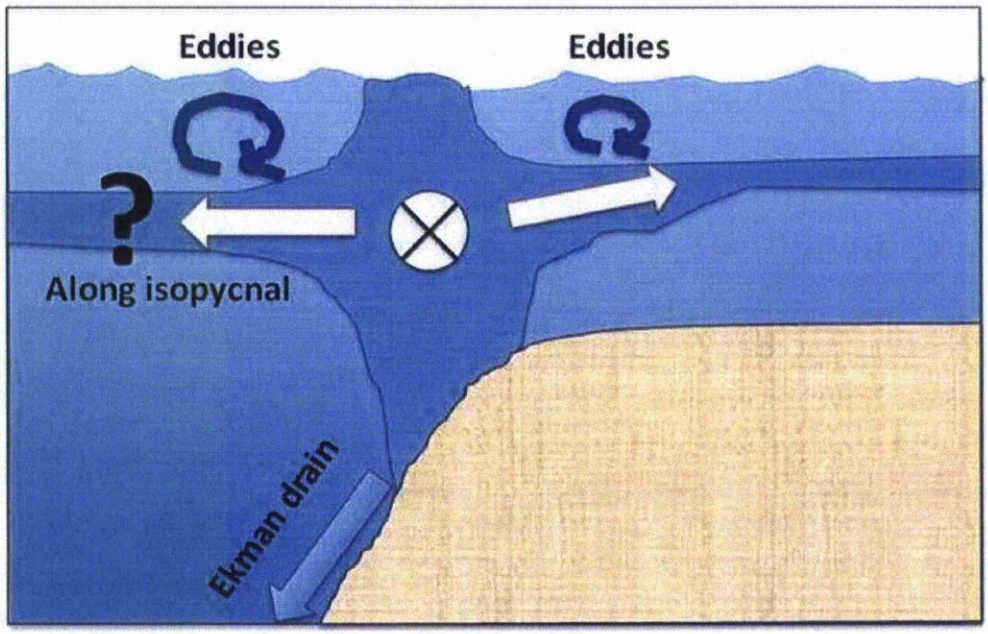

Figure 4.18. A schematic of potential shelf edge exchange via eddies, Ekman drain and along-isopycnal transport

5. CONTINENTAL SHELF EDGE DYNAMICS: A STUDY OF THE PORCUPINE BANK REGION

5. Continental Shelf Edge Nutrient Dynamics: A study of the Porcupine Bank region

Summary

Physical processes at the shelf break drive mixing and water mass exchange between the ocean and shelf. This mixing brings oceanic nutrients to the surface waters, where they fuel primary production. In this chapter, data from a research cruise (*RV Celtic Explorer;* CE911) that sampled 5 cross-slope transects in the region of the Porcupine Bank are presented to reveal the spatial variability of phosphorus partitioning in this physically dynamic shelf edge and shelf slope environment. Cross-slope trends indicated higher inorganic nutrient concentrations at the slope than at the shelf or ocean, and higher organic phosphorus concentrations at the shelf than in the adjacent slope and ocean regions. Latitudinal variations indicated phosphate concentrations increased north of the Porcupine Bank transect at the slope and ocean, while at the shelf they decreased. There was little indication that topographically-induced circulation around the summit of the Porcupine Bank affected measured biogeochemical parameters, but alkaline phosphatase activity rates appeared to be elevated at the thermocline possibly associated with zooplankton grazing and bacterial remineralisation of organic matter.

5.1. Introduction

The Northwest European shelf seas are largely isolated from the adjacent North Eastern Atlantic Ocean by the continental Shelf Edge Current (SEC; Pingree and LeCann, 1990). The SEC flows northwards following the topography of the continental slope, with occasional periods of flow cessation or reversal (Huthnance et al., 2001). The interaction of oceanic currents with topography drives physical mixing processes that deliver oceanic nutrients to the surface at the shelf edge, where they fuel enhanced primary production and chlorophyll concentrations (Joint et al., 2001). The most significant mixing and water exchanges occur because of tides, wind driven flow, ridge associated upwelling, cross-frontal exchange, surface and internal waves, with contributions from eddies and cascading in winter (Huthnance et al., 2001). At the Celtic Sea shelf edge, the topography and slope gradient vary with a steep slope intersected by canyons at La Chapelle

Bank, the large-scale protrusion of Goban Spur briefly diverting flow ocean-ward, before the flow continues north again to the much larger topographic feature of the Porcupine Bank.

The Ocean Margin Exchange (OMEX I) project (sampling 1993-1995) investigated physical and biogeochemical processes and their seasonal variation in the Goban Spur region (see review paper by Joint et al., 2001). A particularly interesting and recurrent feature was the contrast between the shelf, shelf edge and ocean regions. The onset of stratification was earlier at the shallower shelf stations, with shelf sea blooms persisting for longer than those at the slope or in the ocean. In the summer, the shallower regions became net heterotrophic with high mesozooplankton grazing rates, while the ocean remained autotrophic (Joint et al., 2001). Carbon fixation rates increased into shallower water and were highest at the 180 m contour, as was phosphate uptake (Rees et al., 1999). Nitrate assimilation rates were observed to increase with the onset of stratification during the spring bloom, but spatially were highest over the slope showing no clear water depth-trend (Rees et al., 1999). Primary production rates increased from 70 mmol C m^{-2} d^{-1} in winter to 120 mmol C m^{-2} d^{-1} at the spring bloom (Rees et al., 1999), compared with ~20 – 30 mmol C m^{-2} d^{-1} at the on-shelf Jones Bank region of the Celtic Sea during summertime stratification (data courtesy of Dr Linda Gilpin, Napier University). Before the onset of stratification ammonium assimilation rates were comparable to nitrate uptake (*f*-ratio ~ 0.5), but once stratification occurred and the spring bloom developed nitrate assimilation became more important and *f*-ratios increased to >0.8 indicating enhanced new production during the highly productive spring bloom (Rees et al., 1999).

In regions of high primary production where nutrients are replete, such as the shelf edge, one might expect an accumulation of nutrients in the dissolved organic phase to occur associated with phytoplankton exudation, zooplankton grazing and cell lysis etc. (Carlson, 2002) and the particulate organic phase as biomass. However, Hydes et al. (2001) saw no accumulation of organic nutrients at the Goban Spur, except for elevated concentrations of dissolved organic carbon above the thermocline in late summer (Hydes et al., 2001). Dissolved organic phosphorus (DOP) was

undetectable in the surface waters in the winter, increasing to 0.10 μM in the summer in the presence of 0.30 μM phosphate and 0.09 μM particulate phosphorus (Hydes et al., 2001). Despite the elevated DON:DOP ratio relative to Redfield (Redfield et al., 1963), summertime inorganic nutrient ratios were low suggesting a nitrogen deficient system, with N:P ratios of 15.7 in May/June, 1 in July and 11 in August/September (Hydes et al., 2001).

The following questions arise from the OMEX I findings:

- Why are the high primary production rates at the shelf edge not reflected by an accumulation of DOP given that the system is presumed to be nitrogen limited?
- Is the difference between the shelf, shelf edge and ocean a persistent feature along the NW European continental slope or is it confined to the Goban Spur region?

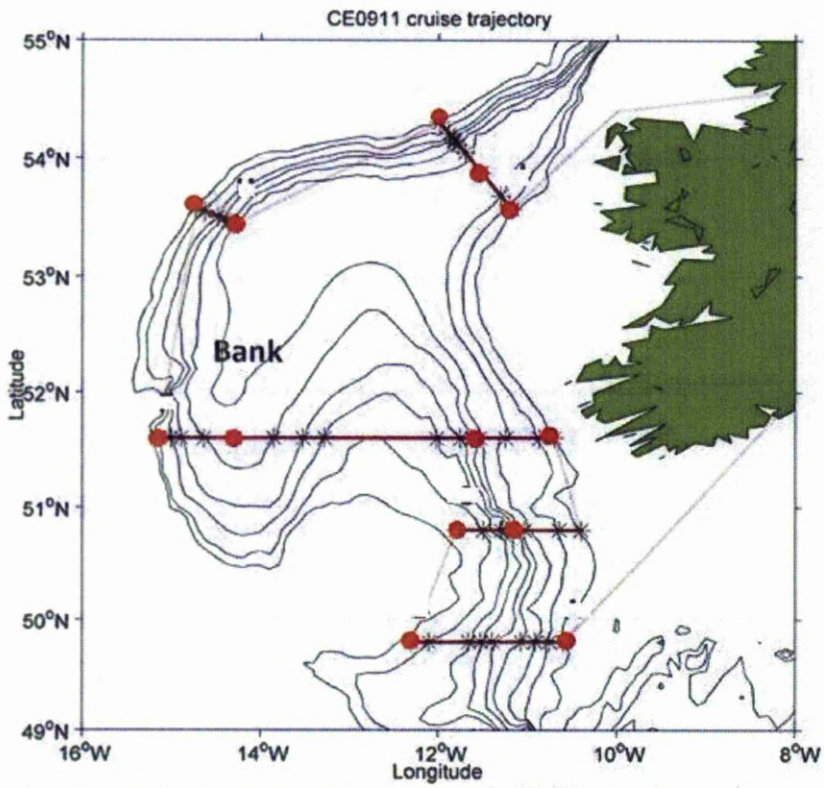

Figure 5.1. Cruise trajectory and CTD locations along transects. See table 5.1 for coordinates of biogeochemical CTD casts.

The Porcupine Bank is a large elliptical submerged bank to the West of Ireland. The bank is strongly asymmetric as the western flank is very steep while the eastern side forms the central plateau. The shallowest point is at 170 m and this western summit is connected to the shelf by a ridge or plateau of approximately 500 m depth (Mohn et al., 2002). A Taylor Column is present over the bank summit. Taylor Columns result from the diversion of geostrophic flow around topographic features to conserve vorticity, giving a relatively isolated water column extended from the bed above the feature. During seasonal stratification the Taylor Column at the Porcupine Bank becomes capped by the thermocline. The result is a doming, or uplifting, of isotherms and isopycnals. Flow around the upper flanks of the bank is anticyclonic and intensifies below the thermocline (Mohn et al., 2002), favouring sediment movement and encouraging nepheloid layer formation on the western flank (Huthnance et al., 2001). The SEC flows southward on the eastern flank before turning northwards to follow the western flank, with tidal rectification being the dominant process maintaining the cold dome feature (Mohn et al., 2002). The nutricline also domes over the Porcupine Bank, and this dome is largely isolated from the surrounding waters, except during storms and spring tides when the Taylor Column is weakened (White et al., 1998).

Table 5.1. CTD cast number, coordinates and nominal depth for each group; shelf edge (SE), slope (S) and ocean (O).

	CTD cast	Latitude	Longitude	Nominal depth
SE (n=3)	1	49.80	10.60	143
	18	51.60	10.70	145
	47	53.60	11.22	165
S (n=6)	5	49.80	11.40	510
	13	50.80	11.24	400
	21	51.60	11.54	350
	30	51.60	14.90	766
	36	53.47	14.37	735
	43	54.11	11.79	500
O (n=6)	9	49.80	12.30	1806
	10	50.80	11.80	1069
	24	51.60	12.02	1002
	32	51.60	15.15	1530
	33	53.58	14.73	1998
	40	54.20	11.89	1480

In this chapter, I assess data collected during a research cruise in the Porcupine Bank region in June 2009 on the *RV Celtic Explorer*. The cruise consisted of 5 transects that crossed the slope 6 times (Fig. 5.1; Table 5.1). The overarching aims of the survey were to map the structure, continuity and water mass characteristics of the SEC and to establish links between shelf edge oceanography, biogeochemical cycling and regional ecosystem dynamics. My contribution was the collection of particulate and dissolved nutrient data and determination of alkaline phosphatase activity rates. In the previous chapter, an accumulation of DOP was observed at the shelf edge relative to the broader shelf environment. Through analysis of data in the present chapter, I aim to address the following broad research questions:

- Is there a significant difference between biogeochemical parameters and rates measured at the shelf edge (SE), slope (S) and ocean (O) regions?
- Are there trends in the data with the progressive move northwards along the shelf edge region and around the Porcupine Bank?

- Does the station at the Porcupine Bank (B) exhibit any notably different characteristics to the other regions sampled (i.e. the SE, S or O)?

5.2. Results

Data are first presented to address whether the shelf edge, slope and ocean regions differ with respect to surface layer dissolved and particulate nutrient concentrations; then in terms of northward trends along the slope current; and finally the parameters measured at Porcupine Bank will be compared with those of the other regions.

5.2.1. Hydrography

Temperature and salinity plots (Fig. 5.2; composite of all data) indicate that the deep water at 49.8 °N is distinct from the deepwater masses further north due to the influence of high salinity Mediterranean Sea Water (MSW) at ~ 8 °C (Hydes et al., 2001). The low temperature, low salinity deepwater found below this and at higher latitudes was Labrador Sea Water, while above the MSW water at ~1000 m were North East Atlantic Water and Sub Polar Mode Waters (Hydes et al., 2001; Huthnance et al., 2001). Surface temperature and salinity decreased gradually northwards, with two distinctly lower surface salinities at the shelf adjacent to the northern Porcupine Sea Bight (51.6 °N 10.7 °W; 14.3 °C, 35.2 psu) and on the Irish Shelf (53.6 °N 11.2 °W; 13.9 °C, 35.3 psu; Fig. 5.2). Surface temperature and density profiles indicated the water column was thermally stratified at all stations (Fig. 5.3).

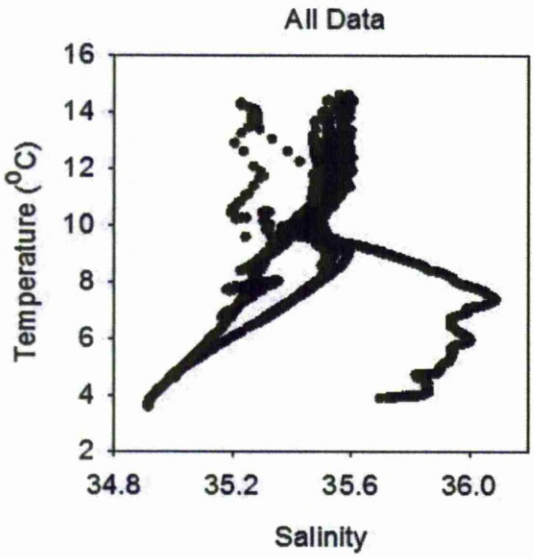

Figure 5.2. Temperature and salinity plots for all stations.

Temperature and density profiles indicate the presence of a surface mixed layer at least 20 m deep at all stations (Fig. 5.3). Herein, surface layer concentrations refer to the mean concentration between 0 – 20 m. The depth of the base of the thermocline varied between ~27 m at one of the northernmost oceanic stations and ~ 60 m at the most southerly slope station. Mohn et al. (2002) used 1027.33 kg m^{-3} as a reference isopycnal to observe the doming of isotherms and isopycnals over the Porcupine Bank (Mohn et al., 2002). In the present study, the 1027.33 kg m^{-3} isopycnal was always situated within the phosphocline and thermocline layer, and was significantly shallower over the shelf than it was over the slope and ocean (50 ± 4 m (95 % CI, n = 3), cf. 63 ± 7 m (95 % CI, n = 6) and 60 ± 4 m (95 % CI, n = 6), respectively; Fig. 5.15).

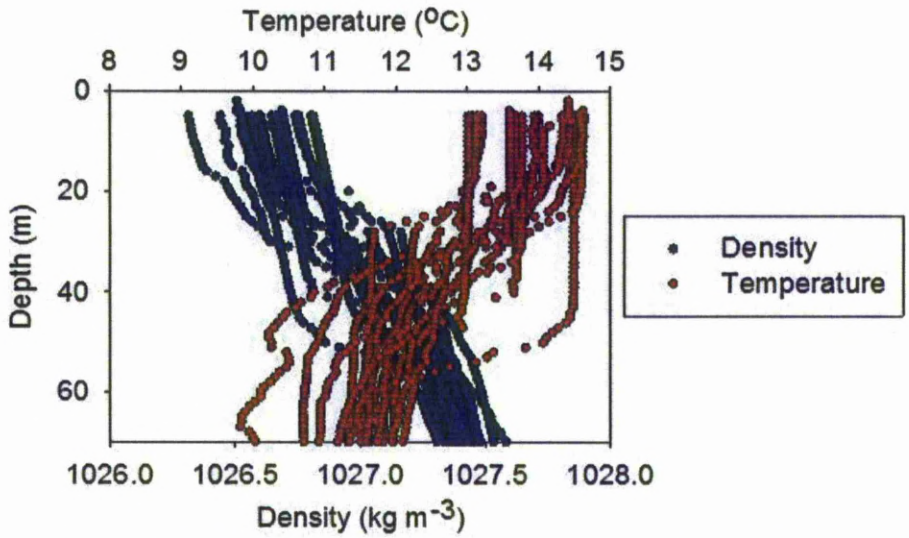

Figure 5.3. Depth profiles of all temperature (°C) and density (kg m^{-3}) data for the upper 70 m of the water column.

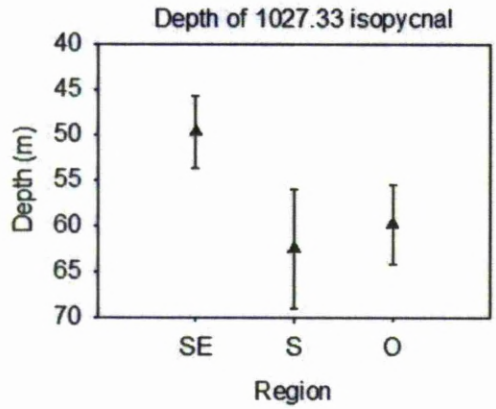

Figure 5.15. Depth of the 1027.33 kg m^{-3} isopycnal (in metres ± 95 % confidence interval) at the shelf edge (SE), slope (S) and ocean (O) stations.

5.2.2. Shelf edge, slope and ocean

Stations were grouped into three categories according to bathymetry and nominal water depth. Stations shallower than 200 m were classed as "shelf edge", those deeper than 1000 m as "ocean", and those between were classed as "slope" (Table 5.1, Fig. 5.1). This categorisation allowed the differences between the shelf edge (SE), slope (S) and oceanic (O) regions at the continental margin could be assessed (Table 5.1).

5.2.2.1. Dissolved nutrients

The highest mean surface layer inorganic nutrient concentrations were found at the slope, with the lowest concentrations at the shelf edge (Figs. 5.4 and 5.5). Mean surface layer phosphate and nitrate (from here on, 'nitrate' refers to nitrate plus nitrite) concentrations were significantly higher at the slope (0.19 ± 0.03 μM PO_4^{3-}; 3.14 ± 0.93 μM NO_3; 95 % CI, n = 12; Tukey test, p = 0.001) than at the shelf edge (0.08 ± 0.04 μM PO_4^{3-}; 0.82 ± 0.94 μM NO_3; 95 % CI, n = 7; Dunn's test, p = 0.03). Oceanic phosphate concentrations (0.14 ± 0.04 μM PO_4^{3-}) were not significantly different from those at the shelf edge (Shapiro-Wilk's test, p = 0.051) but were lower than those at the slope region (Dunn's test, p = 0.015), while oceanic nitrate concentrations (0.14 ± 0.01 μM NO_3^-) were not significantly different to those at the shelf edge or slope (Shapiro-Wilk's test, p = 0.07 and 0.33, respectively). The highest mean surface layer dissolved organic phosphorus

(DOP) concentrations were at the shelf edge (0.15 ± 0.01 μM; 95 % CI, n = 7), but were not significantly higher than concentrations at the slope (0.13 ± 0.01 μM; 95 % CI, n = 12); Shaprio-Wilk's test, p = 0.095; Fig. 5.6). Oceanic surface layer DOP concentrations (0.14 ± 0.01 μM; 95 % CI, n = 10) were not significantly different from the shelf edge or slope regions (Shaprio-Wilk's test, p = 0.091 and 0.596, respectively).

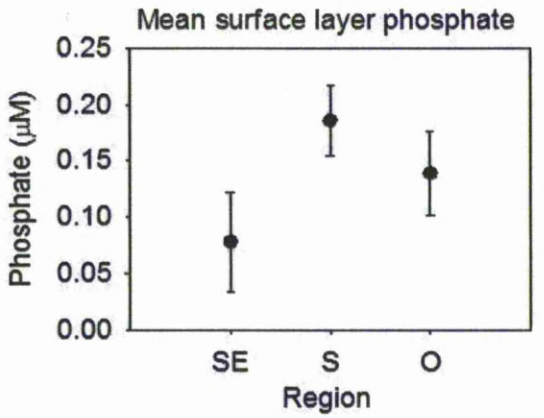

Figure 5.4. Mean surface layer phosphate (μM, ± 95 % confidence interval) at the shelf edge (SE), slope (S) and ocean (O) stations.

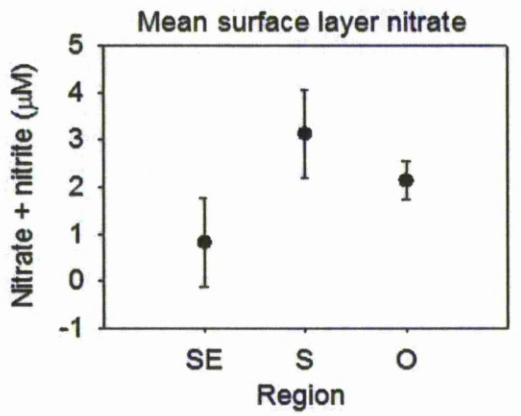

Figure 5.5. Mean surface layer nitrate (N+N in μM, ± 95 % confidence interval) at the shelf edge (SE), slope (S) and ocean (O) stations.

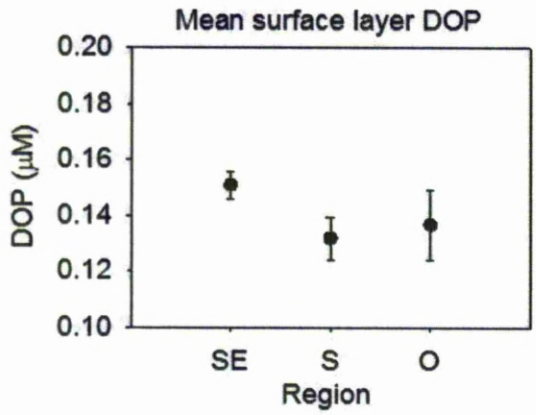

Figure 5.6. Mean surface layer dissolved organic phosphorus (DOP in μM; ± 95 % confidence interval) at the shelf edge (SE), slope (S) and ocean (O) stations.

Nitrate and phosphate trends were decoupled in the deep-water. Nitrate concentrations were higher in the oceanic deep water (10.1 ± 0.9 μM NO_3 at 713 ± 266 m; 95 % CI, n = 6) than at the shelf edge (8.0 ± 1.6 μM NO_3 at 117 ± 59 m; 95 % CI, n = 6; Fig. 5.7), but not significantly (Shapiro-Wilk's test, p = 0.179). This may be the result of nitrate removal on the shelf potentially through denitrification. Although, the highest mean phosphate concentrations were in the oceanic deep water (0.95 ± 0.16 μM; 95 % CI, n = 3), these were not significantly higher than deep-water concentrations at other regions (0.71 ± 0.22 μM at the shelf edge; and 0.75 ± 0.05 μM at the slope; 95 % CI, n = 6; Shaprio-Wilk's test, p = 0.872; Fig. 5.8). The different trends in deep-water nutrient concentrations probably relate to the presence of different deep-water masses subjected to different degrees of remineralisation of organic matter.

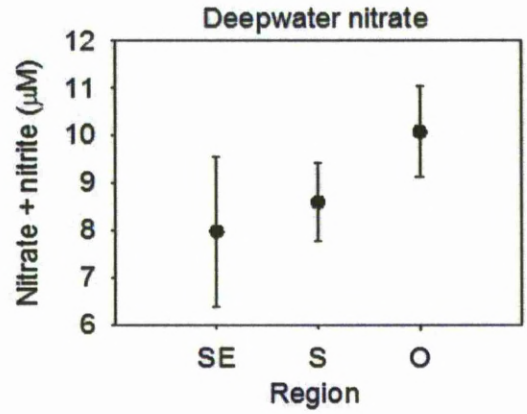

Figure 5.7. Deepwater nitrate (N+N in μM, ± 95 % confidence interval) at the shelf edge (SE), slope (S) and ocean (O) stations.

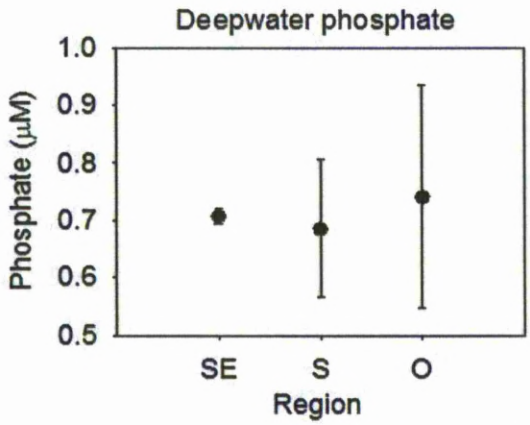

Figure 5.8. Deepwater phosphate (in μM, ± 95 % confidence interval) at the shelf edge (SE), slope (S) and ocean (O) stations.

Phosphate and nitrate were both strongly correlated with temperature ($p<0.001$; data not shown); with low concentrations in the warm surface layer and higher concentrations in the cold deep-water. Temperature had a greater contribution to density than salinity in the upper water column, thus it was possible to correlate phosphate to density across the thermocline layer ($p<0.001$; Fig. 5.9). The phosphocline gradient was then calculated from the change in density across 10 m of the water column, centred at the maximum density gradient. There was no clear trend in the depth of the maximum density gradient between regions (Fig. 5.10) but the phosphocline gradient was significantly sharper at the shelf edge than at the slope or ocean stations (Fig. 5.11).

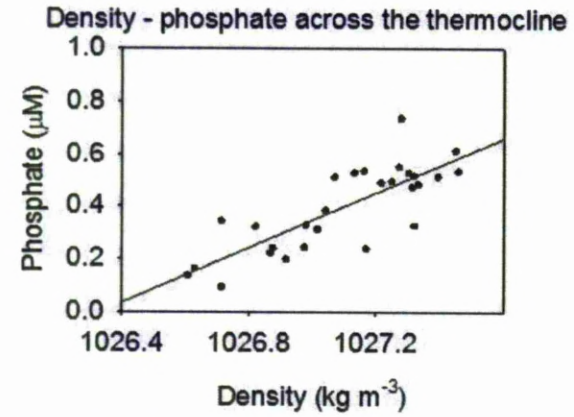

Figure 5.9. Dissolved phosphate (µM) versus density (kg m^{-3}) across the thermocline ($p<0.001$).

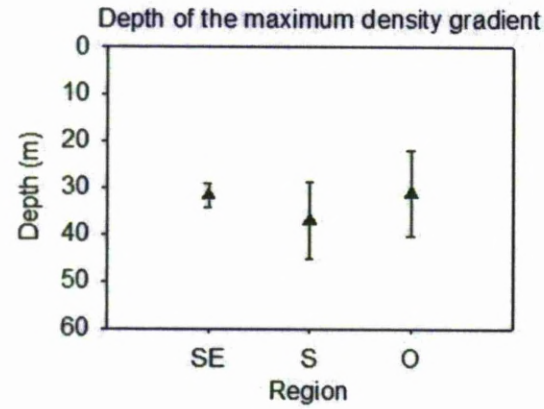

Figure 5.10. Depth of the maximum density gradient (in metres ± 95 % confidence interval) at the shelf edge (SE), slope (S) and ocean (O) stations.

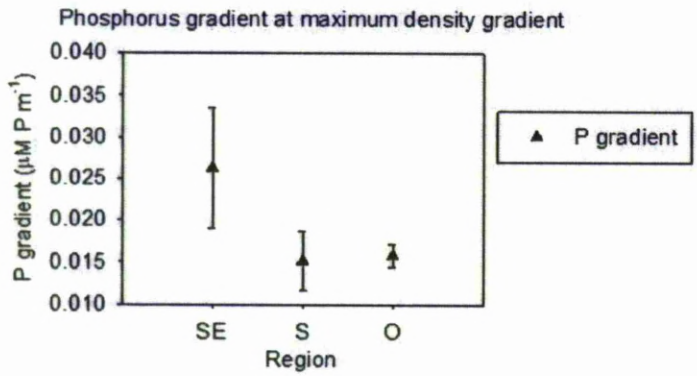

Figure 5.11. Phosphorus gradient (µM P m^{-1}) at the maximum density gradient (± 95 % confidence interval) at the shelf edge (SE), slope (S) and ocean (O) stations.

Surface layer nitrate to phosphate ratios increased from the shelf edge to the ocean (from 6.7 ± 5.9 at the shelf edge, to 16.6 ± 3.8 at the ocean; Fig. 5.12). The oceanic surface N:P ratio was significantly higher than that of the shelf edge and slope regions (Tukey test, p = 0.018 and 0.030, respectively). This trend was also apparent in the deep-water, but was not significant (Shapiro-Wilk's test, p>0.05), with a shelf edge deep-water N:P of 11.9 ± 3.7 and an oceanic N:P of 14.4 ± 1.2 (depths as before; Fig. 5.13). Plotting the linear regression of all nitrate and phosphate data gave a ratio of 13.7 N:P (p<0.001; Fig. 5.14).

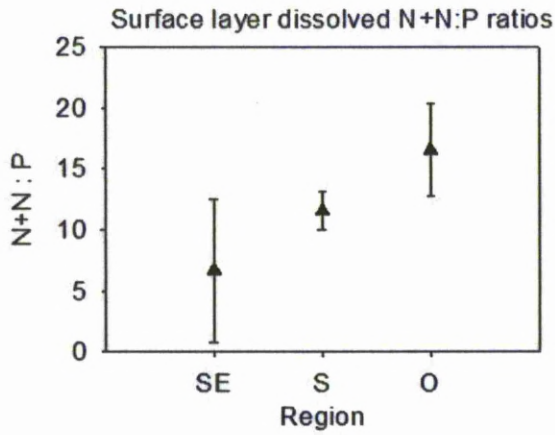

Figure 5.12. Mean surface layer dissolved N:P ratios (± 95 % confidence interval) at the shelf edge (SE), slope (S) and ocean (O) stations.

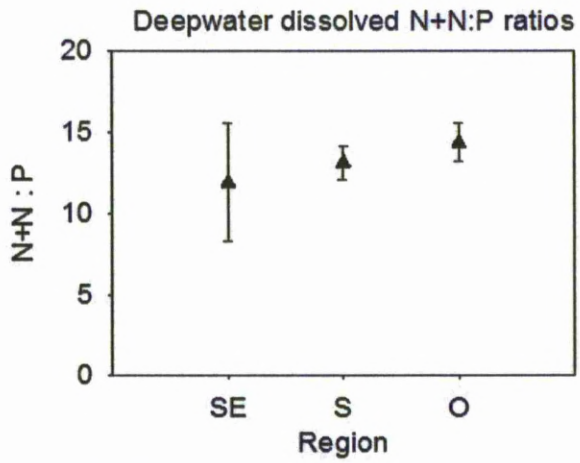

Figure 5.13. Mean deepwater dissolved N:P ratios (± 95 % confidence interval) at the shelf edge (SE), slope (S) and ocean (O) stations.

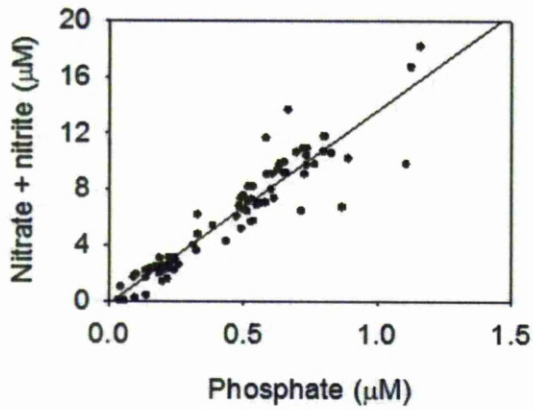

Figure 5.14. Dissolved nitrate (N+N; μM) versus phosphate (μM) for all data; gradient of 13.7 ($p<0.001$).

5.2.2.2. Particulate nutrients

Mean surface layer particulate nutrient concentrations (Figs. 5.16, 5.17 and 5.19) did not vary significantly between the three regions (Shapiro-Wilk's test, $p>0.05$). Shelf edge particulate nutrient concentrations were slightly lower than those at slope and oceanic stations (Table 5.2), but there were no apparent spatial trends in the data (Figs. 5.16, 5.17 and 5.18). PPhos and PON had high variability in the oceanic surface mixed layer, while POC was most variable at the shelf edge.

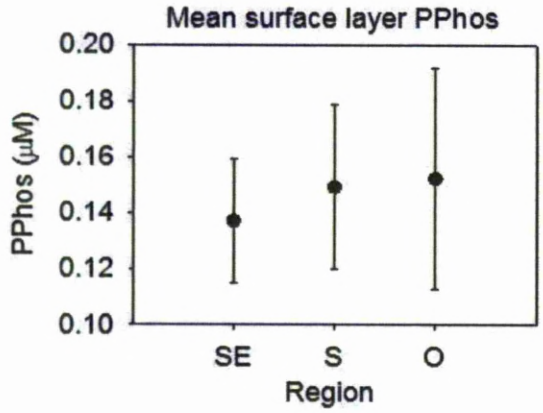

Figure 5.16. Mean surface layer particulate phosphorus (in μM ± 95 % confidence interval) at the shelf edge (SE), slope (S) and ocean (O) stations.

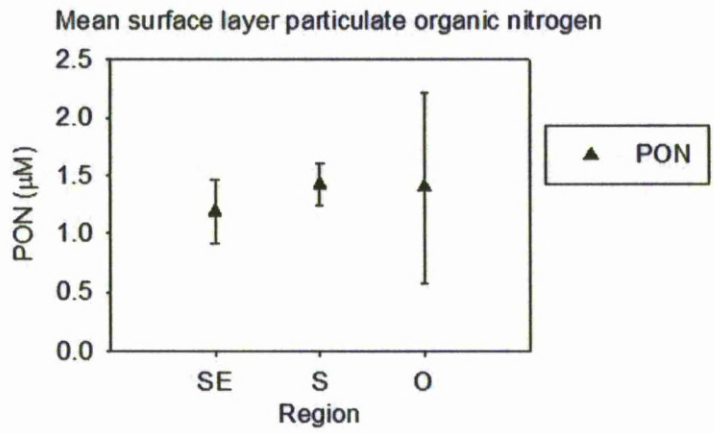

Figure 5.17. Mean surface layer particulate organic nitrogen (in µM ± 95 % confidence interval) at the shelf edge (SE), slope (S) and ocean (O) stations.

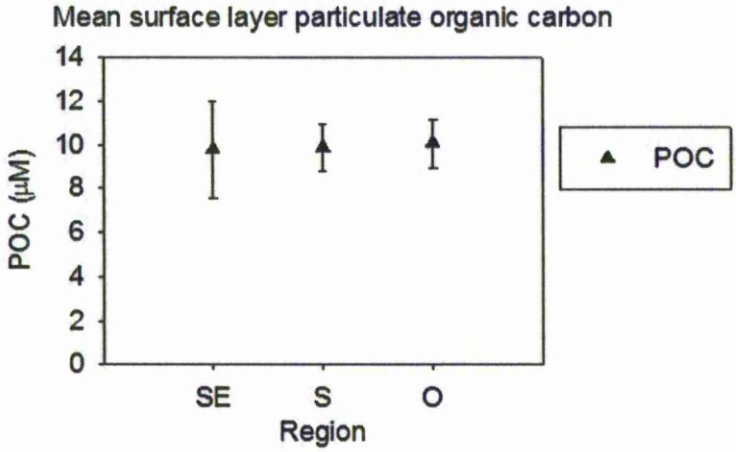

Figure 5.18. Mean surface layer particulate organic carbon (in µM ± 95 % confidence interval) at the shelf edge (SE), slope (S) and ocean (O) stations.

Despite this lack of differences in absolute concentrations between regions, the surface POC to PON ratio was significantly higher at the shelf edge (8.27 ± 0.49, n = 4) than at the slope (6.99 ± 0.21, n = 11; Tukey test, $p < 0.001$) and ocean (7.18 ± 0.34, n = 11; 95 % CI given; Tukey test, $p = 0.003$). Particulate nitrogen to PPhos ratios were higher in the surface layer at the ocean (10.35 ± 2.45, n = 11) than the slope (9.77 ± 1.41, n = 11) and shelf edge (8.3 ± 2.27, n = 4; with 95 % CI given) stations, but this was not significant (Shaprio-Wilk's test, $p > 0.05$; Table 5.3).

Table 5.2. Surface layer mean concentrations (all in μM) for dissolved phosphate (PO4), dissolved nitrate (N+N), dissolved organic phosphorus (DOP), particulate phosphorus (PPhos), particulate organic nitrogen (PON), and particulate organic carbon (POC) at the different regions; shelf edge (SE), slope (S), ocean (O) and Porcupine Bank (B).

		Mean (μM)	Stdev	n	95% conf
PO4	SE	0.08	0.06	7	0.04
	S	0.19	0.08	12	0.03
	O	0.14	0.07	10	0.04
	B	0.22	0.01	1	0.43
N+N	SE	0.82	1.28	7	0.94
	S	3.14	1.65	12	0.93
	O	2.15	0.67	10	0.42
	B	2.57	0.05	1	0.10
DOP	SE	0.15	0.06	7	0.00
	S	0.13	0.12	12	0.01
	O	0.14	0.08	10	0.01
	B	0.12	0.01	1	0.23
PPhos	SE	0.14	0.30	7	0.02
	S	0.15	0.19	12	0.03
	O	0.15	0.06	10	0.04
	B	0.13	0.00	1	0.26
PON	SE	1.19	0.28	4	0.27
	S	1.42	0.30	11	0.18
	O	1.40	1.40	11	0.83
	B	1.18	0.07	1	-
POC	SE	9.78	2.26	4	2.22
	S	9.87	1.82	11	1.08
	O	10.08	1.88	11	1.11
	B	7.97	0.24	1	-

Table 5.3. Particulate nutrient ratios for the surface layer at the different regions; shelf edge (SE), slope (S), ocean (O) and Porcupine Bank (B).

		Mean ratio	Stdev	n	95% conf
N:P	SE	9.83	2.32	4	2.27
	S	9.77	2.39	11	1.41
	O	10.35	4.14	11	2.45
	B	8.04	2.07	2	2.87
C:P	SE	81.34	19.54	4	19.14
	S	68.81	19.72	11	11.65
	O	75.68	33.99	11	20.08
	B	54.88	13.42	2	18.60
C:N	SE	8.27	0.50	4	0.49
	S	6.99	0.35	11	0.21
	O	7.18	0.57	11	0.34
	B	6.84	0.09	2	0.12

5.2.2.3. Alkaline phosphatase activity

Alkaline phosphatase activity (APA) hydrolysis rates showed no distinct trends between regions, with large variability at each site. In the context of this study, exceptionally high APA rates were measured at the shelf edge at 49.8 °N (31.4 nM P h^{-1} in the surface layer and 8.1 nM P h^{-1} in the thermocline; Table 5.4), yet at the shelf edge at 53.6 °N surface layer APA was low both in the surface layer and in the thermocline (0.58 nM P h^{-1} and 1.29 nM P h^{-1}, respectively). The oceanic stations exhibited relatively large variability in measured APA (Table 5.4), while the lowest variability was observed in the surface layer at the slope (1.21-1.26 nM P h^{-1}, n = 2), however this group only included measurements from 2 stations.

Table 5.4. Alkaline phosphatase activity (APA; nM P h^{-1}) measured in the surface layer and thermocline at the shelf edge (SE), shelf (S), ocean (O) and Porcupine Bank (B).

	CTD	APA (nM P h^{-1})	
		Surface	Thermocline
SE	1	31.39	8.09
	47	0.58	1.29
S	21	1.21	1.69
	43	1.26	1.07
O	10	4.83	2.51
	33	0.97	1.39
	40	1.11	1.88
B	28	1.58	6.42

5.2.3. Northward trends

5.2.3.1. Dissolved nutrients in the surface layer

When listed in order of latitude, i.e. south to north (Table 5.5), mean surface layer phosphate concentrations increased in each region (shelf edge, slope and ocean) at 51.6 °N and northward. Further examination of these trends within regions (Table 5.6) indicates that phosphate at the shelf edge was significantly lower north of 51.6 °N (0.06 ± 0.03 μM cf. 0.15 ± 0.01 μM south of 51.6 °N, respectively; 95 % CI, n = 3; Tukey test, $p<0.001$), while phosphate concentrations were higher north of 51.6 °N at the slope (0.23 ± 0.01 μM cf. 0.12 ± 0.06 μM to the south; 95 % CI, n = 6; Tukey test, $p<0.001$) and ocean stations (0.17 ± 0.02 μM cf. 0.07 ± 0.04 μM to the south; 95 % CI, n = 6; Dunn's test, $p = 0.017$). Surface layer nitrate concentrations were higher at the shelf edge south of 51.6 °N (0.09 ± 0.04 μM to the north cf. 2.34 ± 0.39 μM to the south; 95 % CI, n = 6; Tukey test, $p<0.001$) and at the oceanic stations (2.50 ± 0.35 μM to the north cf. 9.44 ± 3.80 μM to the south; 95 % CI, n = 6; Tukey test, $p = 0.043$). However, nitrate concentrations did not vary significantly at the slope (Table 5.6). There was no latitudinal trends in DOP concentration (Shapiro-Wilk's test, $p>0.05$).

Table 5.5. Mean surface layer phosphate (μM),nitrate (N+N; μM) and DOP (μM) concentrations and N:P ratio at all stations; grouped according to shelf edge (SE), slope (S), ocean (O) or Porcupine Bank (B).

	Latitude	Longitude	Phosphate (μM)	Stdev	Nitrate (N+N; μM)	Stdev	N:P	DOP (μM)	Stdev
SE	49.80	10.60	0.15	0.01	0.15	0.01	15.71	0.15	0.01
	51.60	10.70	0.23	0.01	0.12	0.00	12.63	0.15	0.01
	53.60	11.22	0.22	0.01	0.12	0.00	11.78	0.16	0.05
S	49.80	11.40	0.04	0.00	0.15	0.01	3.39	0.14	0.00
	50.80	11.24	0.16	0.01	0.14	0.01	14.63	0.14	0.01
	51.60	11.54	0.24	1.56	0.11	0.01	10.23	0.12	0.00
	51.60	14.90	0.04	0.01	0.15	0.02	25.60	0.11	0.01
	53.47	14.37	0.18	0.00	0.17	0.06	13.51	0.14	0.01
	54.11	11.79	0.19	0.00	0.12	0.00	11.49	0.13	0.05
O	49.80	12.30	0.08	0.05	0.16	0.05	0.95	0.15	0.02
	50.80	11.80	0.09	0.00				0.14	0.02
	51.60	12.02	0.22	0.90	0.14	0.01	9.48	0.13	0.01
	51.60	15.15	0.10	0.01	0.14	0.02	19.02	0.17	0.06
	53.58	14.73	0.14	0.01	0.13	0.01	13.15	0.11	0.02
	54.20	11.89	0.19	0.01	0.11	0.02	16.53	0.12	0.00
B	51.60	14.30	0.21	0.07	0.13	0.05	10.84	0.12	0.00

Table 5.6. Mean nitrate and phosphate concentrations in the surface layer, categorised based on region (SE, S or O) and location north and inclusive of 51.6 °N (the main Porcupine Bank transect) and south of that latitude.

			Mean (μM)	95% CI
Phosphate	SE (n=3)	South of 51.6 N	0.15	0.01
		North of 51.6 N	0.06	0.03
	S (n=6)	South of 51.6 N	0.12	0.06
		North of 51.6 N	0.23	0.01
	O (n=6)	South of 51.6 N	0.07	0.04
		North of 51.6 N	0.17	0.02
Nitrate	SE (n=3)	South of 51.6 N	2.29	0.11
		North of 51.6 N	0.09	0.04
	S (n=6)	South of 51.6 N	2.31	0.09
		North of 51.6 N	2.34	0.39
	O (n=6)	South of 51.6 N	9.44	3.80
		North of 51.6 N	2.50	0.35

5.2.3.2. Particulate nutrients in the surface layer

PON concentrations at the slope were higher north of 51.6 °N (1.40 ± 0.13 μM cf. 0.85 ± 0.05 μM to the south; 95 % CI, n = 6), but this difference was not significant (Shaprio-Wilk's test, p = 0.622). There were no other significant latitudinal trends in PON or PPhos concentrations (Shaprio-Wilk's test, p>0.05; Table 5.7).

Table 5.7. Mean particulate organic nitrogen (PON) and particulate phosphorus (PPhos) concentrations in the surface layer, categorised based on region (SE, S or O) and location north and inclusive of 51.6 °N (the main Porcupine Bank transect) and south of that latitude.

			Mean (μM)	95% conf
PPhos	SE (n=3)	South of 51.6 N	0.17	0.04
		North of 51.6 N	0.12	0.02
	S (n=6)	South of 51.6 N	0.15	0.08
		North of 51.6 N	0.15	0.03
	O (n=6)	South of 51.6 N	0.19	0.03
		North of 51.6 N	0.13	0.05
PON	SE (n=3)	South of 51.6 N	-	-
		North of 51.6 N	1.19	0.29
	S (n=6)	South of 51.6 N	0.85	0.05
		North of 51.6 N	1.40	0.13
	O (n=6)	South of 51.6 N	1.53	0.26
		North of 51.6 N	1.36	0.17

5.2.3.3. Alkaline phosphatase activity (APA)

The highest APA rates were at the southernmost shelf edge station at the surface and thermocline (3.1.4 nM P h^{-1} and 8.1 nM P h^{-1}, respectively). Excluding Porcupine Bank rates, APA at the thermocline decreased northwards (in the range of 0.6 – 1.9 nM P h^{-1}; Table 5.8). However, this trend was not significant due to the high variability in APA rates to the south of 51.6 °N (Table 5.8).

Table 5.8. Alkaline phosphatase activity (APA; nM P h^{-1}) in the surface and thermocline layers listed in sampling order.

	CTD	Latitude	Longitude	APA (nM P h^{-1})	
				Surface	Thermocline
SE	1	49.80	10.60	31.39	8.09
O	10	50.80	11.80	4.83	2.51
S	21	51.60	11.54	1.21	1.69
B	28	51.60	14.30	1.58	6.42
O	33	53.58	14.73	0.97	1.39
O	40	54.20	11.89	1.11	1.88
S	43	54.11	11.79	1.26	1.07

5.2.4. The Porcupine Bank

Previous reports indicated a doming of isotherms above the Porcupine Bank and associated higher inorganic nutrient concentrations than surrounding waters at equivalent depth (e.g. Mohn et al., 2002; White et al., 1999). In the present study, the mean depth of the 1027.33 kg m^{-3} pycnocline was deeper than at the shelf edge, but did not differ significantly from the slope or ocean (Table 5.9).

Table 5.9. Mean depth of the 1027.33 kg m^{-3} pycnocline at the different regions; shelf edge (SE), slope (S), ocean (O) and Porcupine Bank (B).

	Mean (m)	Stdev	95% conf.
SE	49.7	3.5	4.0
S	62.5	8.2	6.5
O	59.8	5.5	4.4
B	62	1	-

Surface layer phosphate and nitrate concentrations were higher on the Bank (0.22 ± 0.4 µM PO_4^{3-} and 2.57 ± 0.10 µM NO_3, respectively; 95 % CI, n = 1) than in the other regions, but not significantly (Tukey test, $p>0.05$; Table 5.2). Conversely, DOP concentrations were lower (0.12 ± 0.23 µM; 95 % CI, n = 1) but this also was not significant (Table 5.2). Surface layer dissolved inorganic nutrient ratios at the Bank (11.8 ± 0.38; 95 % CI, n = 2)

were similar to those at the slope, lower than the ocean and higher than the shelf edge (Table 5.10).

Table 5.10. Dissolved N+N:P ratios for both the surface layer and the deepwater at the different regions; shelf edge (SE), slope (S), ocean (O) and Porcupine Bank (B).

		Mean N:P	Stdev	n	95% conf
Surface layer	SE	6.68	7.91	7	5.86
	S	11.56	2.07	7	1.54
	O	16.55	5.18	7	3.84
	B	11.78	0.28	2	0.38
Deep water	SE	11.89	3.73	4	3.65
	S	13.13	1.95	13	1.06
	O	14.36	2.50	17	1.19
	B	14.07	0.70	3	0.80

Particulate nutrient concentrations were lower in the surface layer at the Bank (0.13 ± 0.00 μM PPhos, 1.18 ± 0.07 μM PON, and 7.97 ±0.24 μM POC; ± 1 s.d.) than they were at the shelf edge, slope or ocean although this was not statistically significant (Shapiro-Wilk's test, $p>0.05$; Table 5.2). Particulate nitrogen to phosphorus, carbon to phosphorus and carbon to nitrogen ratios were all lower at the Bank (8.04 ± 2.1 N:P, 54.9 ± 13.4 C:P, and 6.8 ± 0.1 C:N; ± 1 s.d.; Table 5.3) than elsewhere.

Alkaline phosphatase activities (APA) were higher at the Bank than those measured at similar latitude (Table 5.8). This was most pronounced in the thermocline where APA was 6.42 nM P h^{-1} at the Bank, compared with 1.39 – 1.69 nM P h^{-1} at other stations at similar latitude. In the surface layer, APA at the Bank was 1.58 nM P h^{-1} compared with 0.97 – 1.21 nM P h^{-1}.

5.3. Discussion

The Northwest European continental margin is characterized by a surface water band of low temperature and high chlorophyll concentration that marks the boundary between the shelf sea and the Northeast Atlantic Ocean (Joint et al., 2001). The high productivity at the shelf edge is maintained by oceanic nutrients mixing to the surface by tidal and wind forcing. Such mixing processes are enhanced by the interaction of currents with the irregular bathymetry of the continental slope. Internal tides generated at the 200 m isobath contribute significantly to mixing and exchange at the shelf edge through turbulence and shear dissipation (Joint et al., 2001; Huthnance et al., 2001). In this sense, the shelf edge topography accommodates cross-slope exchange between the ocean and shelf sea. However, for the most part the shelf is insulated by the continental slope current, which is constrained by topography to flow largely poleward (Pingree et al., 1999).

The OMEX I project (e.g. Joint et al., 2001) determined that physical and biogeochemical parameters and features differed between the shelf, slope and ocean in the Goban Spur region of the Northwest European margin (Joint et al., 2001; Rees et al., 1999; Hydes et al., 2001). The present study focused on the Porcupine Bank region with the aim of investigating if the shelf, slope and ocean differences previously observed at Goban Spur were a persistent feature along the Northwest European shelf margin, or whether there was a latitudinal variation to these features. This discussion addresses the following questions:

- Is there a significant difference between biogeochemical parameters and rates measured at the shelf edge (SE), slope (S) and ocean (O) regions during this study?
- Are there any trends in the data with the progressive move northwards along the continental margin and around the Porcupine Bank?
- Does the station at the Porcupine Bank (B) exhibit any notably different characteristics to the other regions sampled (i.e. the SE, S or O)?

5.3.1. Differences between the shelf edge, slope and ocean

The present study found that at the shelf edge inorganic nutrient concentrations were lower with a stronger nutricline gradient compared to the slope and ocean, while organic phosphorus concentrations were higher. This is thought to have resulted from high productivity at the shelf facilitating rapid assimilation of inorganic nutrient fluxes followed by production of organic matter. Similar observations were reported by Hydes et al. (2001) and White et al. (1998). In the former study, off shelf waters had distinct properties relative to those shallower than 200 m, and the latter reported a warm core to the slope current that was relatively insulated from adjacent waters.

The contrast in physical regimes between the shelf edge, slope and ocean may in part explain the observed biogeochemical differences. Shelf waters are relatively stationary compared with the slope current, but are subject to exchanges with off-shelf waters driven by tide and wind mixing (Huthnance et al., 2001). At the slope, on the other hand, there is a continuous, poleward current that is usually barotropic with current speeds of 0.01 – 0.02 ms^{-1}, and a downslope residual current of <0.15 ms^{-1} (Huthnance et al., 2001). Therefore, parameters measured at the slope may reflect biogeochemical signals originating further south. As biomass growth, cell regeneration and induced biological responses (such as alkaline phosphatase induction and repression) are not instantaneous; this may also contribute to differences observed between the slope and adjacent shelf edge.

Turbulent dissipation and shear, which drive mixing, differ between stratified shelf waters and the barotropic slope current. Cross-slope exchange also varies, affecting water column hydrography. For example, the thermocline has been reported to thicken (<80 m) at the slope where cross-slope tidal currents are strongest. Wind forced surface exchange also occurs at regions where the slope is broader (Huthnance et al., 2001). Processes such as this may contribute to the contrasting depth in isopycnals between the shelf edge and deeper regions observed in the present study.

The shallower isopycnals at the shelf edge may be due to "bunching" of density gradients in the shallower water column. This results in a stronger thermocline, which acts as a barrier between the bottom mixed layer and the productive surface waters. The present study observed a stronger phosphocline gradient at the shelf edge compared to the slope and ocean, which may be a reflection of this. In addition, surface layer phosphate concentrations were lower at the shelf edge than at the other stations. With similar concentrations below the thermocline, this provides a greater contrast between bottom and surface water concentrations, encouraging a stronger phosphocline gradient. Biology may therefore also drive the stronger phosphocline, as Rees et al. (1999) report faster phosphate assimilation rates at the shelf edge than over the slope and ocean. The stronger phosphocline gradient at the shelf edge may result from a combination of higher phosphate assimilation rates and a potentially lower vertical mixing rate than at the slope and ocean.

During the present study, the measurement of phosphate and APA suggested that biological assimilation of phosphorus may have been higher at the shelf edge than at the slope and ocean stations (Table 5.4). Rees et al. (1999) reported similar findings for the Goban Spur region, supported by their determination of phosphate assimilation rates. In addition to the lower phosphate concentrations and stronger phosphocline gradient, there were higher DOP concentrations at the shelf edge 'bloom' station than at the other stations. Elevated DOP concentrations may be due to the decoupling of removal and production processes as typically observed during high primary production and bloom events or when production is N-limited (Carlson, 2002) or alternatively . Joint et al. (2001) report higher grazing rates at the shelf edge and slope than at deeper stations at the Goban Spur in the summer. As a result of these different grazing rates, the shelf edge and slope were net heterotrophic in June, while the ocean remained autotrophic (Joint et al., 2001). If a similar grazing distribution were present during the current study, then sloppy zooplankton grazing may have been a significant source of DOP to the water column and may explain the elevated concentrations at the shelf edge.

5.3.2. Northward trends

The results of this study suggest that stations south of 51.6 °N had lower phosphate concentrations at the shelf edge, slope and ocean while nitrate concentrations were higher at the southern shelf edge. South of 51.6 °N Mediterranean Seawater was present in the deep-water, while north of 51.6 °N Labrador Seawater dominated the deep-water T-S signal (Huthnance et al., 2001). This change in the deep-water composition may have affected the availability of nutrients to the surface layer, however the deepwater N:P ratio did not vary greatly between the northern and southern stations suggesting that this was probably not causing the disparity in surface concentrations.

The gradient and topography of the slope varies along the continental margin. The result is that mixing and water exchange with the shelf are likely to be spatially variable. At the Porcupine Bank (~ 51.6 °N) the slope current contorts southwards around the Bank summit, before reverting back to a northly direction. The bottom currents are intensified on the western flank compared to the east (Mohn et al., 2002). The changes in velocity profile may lead to shear in the water column and the current may even overshoot the Bank or form spin-off eddies. A visible effect of the interaction between the Porcupine Bank and the slope current is the development of nepheloid layers on the western flank (Huthnance et al., 2001). It is possible that the variation in slope topography may induce greater turbulence and mixing at 51.6 °N and to the north than at the slope to the south. However, 49.8 °N is only just north of the Goban Spur and the tidally energetic La Chapelle region (Huthnance et al., 2001). Therefore, higher turbulent mixing might be expected across these regions, which may be transferred with the slope current to 49.8 °N.

It seems unlikely that physical processes dominate the northward nutrient trends as phosphate and nitrate concentrations do not vary in a similar manner while deepwater N:P ratios did not vary greatly (N:P ~ 14 ± 2). Therefore, it is presumed unlikely that the differences observed in nutrient concentrations resulted from a change in position of the SEC over the slope and shelf edge. At the southern transect, surface layer N:P ratios were

highest (15.7 – 25.6) and decreased northwards (reaching a minimum of 1.7 at the shelf edge at 53.6 °N). The shelf edge N:P ratio was the same as the winter surface ratio (15.7) reported by Hydes et al. (2001) for the Goban Spur region, but the oceanic surface N:P ratios observed in the present study at 49.8 °N were higher (19.9). The same trend was not seen in deep-water nutrient concentrations, suggesting that this surface layer trend was attributable to biological uptake and assimilation of nutrients, with greater phosphate uptake to the south and greater nitrate uptake further north, or nitrogen was being added to surface waters at lower latitude.

Alkaline phosphatase activity in surface waters at the shelf edge at 49.8 °N was 16-fold higher than the mean APA rate in this study. At this site, phosphate and nitrate concentrations were 0.15 μM and 2.29 μM, respectively, resulting in a surface N:P ratio of 15.7. Surface DOP concentrations were 0.15 μM. It is unclear if the elevated APA is associated with rapid bacterial turnover of labile DOP, or associated with zooplankton grazing, or assimilation of PME by phytoplankton exposed to phosphorus limitation. Although the N:P ratio would not suggest the latter.

There are clear gradients in phytoplankton community composition in shelf seas, with *Prochlorococcus* and *Synechococcus* species dominating in stratified shelf waters and diatoms dominating at the shelf edge (Sharples et al., 2007). Genomic studies have revealed that both *Prochlorococcus* and *Synechococcus* have the genes that code for alkaline phosphatase (Kathuria and Martiny, 2011; Li et al., 1998), but ELF studies in Chapter 4 (Fig. 4.16) show that diatoms also have the potential to contribute to alkaline phosphatase activity at the shelf edge. Furthermore, Rees et al. (1999) observed during the early spring bloom that phosphate uptake is elevated at the shelf edge whereas nitrate uptake is not, implying that phytoplankton are assimilating ammonium as their principle source of nitrogen. Thus, APA may be produced to supplement phosphorus demands in this productive region.

Zooplankton can also contribute significantly to total community APA (Gambin et al., 1999). Joint et al. (2001) report higher grazing over the shelf edge and slope than in the ocean, thus APA should be higher at these

stations if APA is associated with zooplankton. In stratified regions, zooplankton grazing may be focused on the subsurface chlorophyll maximum associated with the thermocline (Hobson and Lorenzen, 1972), so thermocline APA would likely exceed surface APA if it was attributable to zooplankton. Neither of these trends were apparent from the APA data obtained during this study, and so zooplankton grazing is unlikely to have been the dominant source of APA in these regions.

Bacterial communities have previously been reported to contribute to APA at ocean margin environments, such as the northwest African Upwelling region (Sebastian et al., 2004). APA has also been assumed to increase with bacterial growth, reflecting its dependence on organic matter to alleviate carbon limitation (Hoppe and Ullrich, 1999). Bacteria associated with particles have also been found to express high levels of ectoenzymes such as alkaline phosphatase, releasing dissolved nutrients from particulate organic matter (Smyth et al., 1992). Thus, when bacteria access the DOP pool as a labile source of DOC, there is not always a link between APA and phosphate concentrations (Kolowith et al., 2001). Bacterially associated APA probably made an important contribution to total community APA during this study as observed at the shelf edge in Chapter 4.

Alkaline phosphatase hydrolysis rates were much lower at stations north of 49.8 °N (~ 2.0 ± 1.6 nM P h^{-1}). White et al. (1998) and Raine et al. (2002) both report a dominance of dinoflagellates in the Porcupine Bank region during summertime. Dyhrman and Ruttenberg (2006) observed a high percentage of dinoflagellate cells exhibiting APA (via ELF staining) in a coastal ocean environment, which did not appear to be repressible and so was probably constitutive (Dyhrman and Ruttenberg, 2006). As the N:P ratio determined in this study appears to be lower at higher latitudes, there is the suggestion that nitrogen limitation increased northwards. This would support the idea that the observed APA may be constitutive. So it is possible that the APA observed across the Porcupine Bank region was in part attributable to dinoflagellate assemblages.

Alkaline phosphatase data therefore support the idea that biological phosphorus demand was higher at the southern extent of the study region.

5.3.3. The Porcupine Bank

Previous studies have reported doming of isotherms over the Porcupine Bank, due to rectification of tidal currents (Mohn et al., 2001). Physical data collected at higher spatial resolution during the present study (data courtesy of Heather Cannaby, University Institute Galway) indicates a similar feature over the Bank, with enhanced stratification and warmer sea surface temperatures. This may have indicated the presence of a capped Taylor Column over the Bank (Mohn et al., 2002).

Over the Bank, surface layer inorganic nutrient concentrations were higher and DOP and particulate nutrient concentrations were lower than the shelf edge, slope and ocean. This is similar to the observations of White et al. (1998) and is thought to relate to doming of isotherms over the Bank. APA was relatively high, at the Bank with higher activity at the thermocline than at the surface. This may reflect a longer residence time of water within the Taylor Cap, resulting in greater remineralisation. However, apparent oxygen utilisation below the thermocline at the Bank did not vary greatly from other stations of similar depth (data not shown), suggesting that perhaps remineralisation was comparable. In this case, higher APA may have resulted from more efficient zooplankton grazing within the relatively low turbulence Taylor Cap, or an accumulation of microbial biomass (autotrophic and heterotrophic). However, sampling resolution at the Bank was not sufficient to make significant comparisons with the other regions and infer topographical influences on biogeochemical cycling.

5.4. Conclusions

The shelf edge was found to be a region of higher DOP concentrations than the slope and ocean. The lower phosphate found in this region suggests a conversion of phosphate to DOP. Low N:P ratios in surface waters suggest that microbial communities relied largely on regenerated nitrogen to sustain production. Latitudinal variations in alkaline phosphatase activity suggest that the microbial community composition and nutritional status varied from phosphorus-stressed communities at the shelf edge at 49.8 °N to nitrogen-limited communities at 53.6 °N. Despite these latitudinal variations, the shelf edge stations had higher DOP concentrations than the adjacent slope and ocean.

In regions where the continental slope is broad, wind mixing may drive exchange of surface waters between the shelf and deeper waters. As the shelf edge was found to have higher DOP concentrations than the adjacent slope, it is possible that some of the high DOP surface waters are transferred to the phosphorus-limited North Atlantic. The strongest process driving exchange at the continental margin is tidal mixing. The nature of internal wave driven turbulence at thermocline is more likely to export DOP from the surface layer to the thermocline, where it will be more likely to be remineralised. The mechanisms for the potential export of phosphorus from the shelf sea are still not fully understood. However, rivers provide a significant source of nitrogen and phosphorus to the shelf sea environment. Although this is generally at a high N:P ratio where rivers are relatively unpolluted, it is delivered to a nitrogen limited region via the estuarine buffer system. In the marine N-limited shelf sea the riverine fluxes of nitrogen are quickly assimilated while the phosphorus fluxes have a longer residence time and contribute to the shelf sea phosphorus pool. This pool is replenished further by oceanic waters during winter mixing with oceanic waters. Why then was a strong accumulation of phosphorus appear to be absent in shelf seas? To answer this question a greater understanding of sediment interactions and organic matter transfers with the overlying water column is needed. However, the present study suggests that a possible candidate for phosphorus loss from the shelf occurs through export of dissolved organic phosphorus through surface layer exchange across broad slope regions. Over steep bathymetry, the topography acts to constrain this

region as slope currents are narrowed and enhanced, and internal tides trigger turbulence at the thermocline encouraging export of organic matter to below the bottom waters.

6. SYNTHESIS

6. Synthesis

"Understanding the water column biogeochemical cycling of all nutrients and trace metals is essential for elucidating the current and future effects of both natural and anthropogenically induced changes in nutrient composition on the plankton productivity and speciation of the world's oceans." (Benitez-Nelson, 2000).

Shelf seas are highly productive regions of the world's ocean. Dynamic physical mixing processes drive enhanced nutrient fluxes to the euphotic layer, enabling shelf seas to make a disproportionately large contribution to global ocean carbon fixation given their relatively small size. In addition, their role as a buffer between terrestrial and ocean systems means it is important that we have a greater understanding of the sources, sinks, cycling and transfer of nutrients, such as nitrogen and phosphorus, within shelf sea environments. Often operating under very different nutrient regimes to adjacent ocean regions, shelf seas can potentially provide an important source of nutrients to the open ocean, while conversely also potentially acting as a sink of oceanic nutrients, for example through processes such as denitrification.

In the present study we addressed the following research questions:

- Is there a net accumulation of phosphorus in the dissolved organic phase, and therefore a net gain of DOM in the euphotic layer of the Celtic Sea during summer stratification?
- Does the Celtic Sea act as a sink or source of phosphorus to the P-limited North Atlantic?
- How might climate change and the associated increase in nitrogen in the ocean and meteorological changes, i.e. increase storm frequency, affect phosphorus and DOM dynamics in the Celtic Sea?

We found an accumulation of DOP above the thermocline during summer stratification in the Celtic Sea, and at the shelf edge where physical mixing processes drove enhanced primary production. The greatest net DOP production coincided with times of elevated diatom abundance, mostly associated with short post-storm bloom events and the more sustained

shelf edge bloom. ELF-staining showed that some fraction of labile DOP was lost from the euphotic zone through remineralisation by alkaline phosphatase associated with small cells and bacteria, and additionally through utilisation as a nutrient source for diatoms at the shelf edge. Physical mixing of fresh DOP below the thermocline was evident in phosphomonoester concentrations during the storm event in Chapter 3 and the presence of DOP in the bottom water in all studies (Fig. 6.1). Thus physical mixing processes acted as a strong feedback mechanism, with enhanced mixing diluting DOP in the euphotic layer but also supplying inorganic nutrients. This in turn enhanced production and exudation of DOP in the euphotic layer. The timescales of this feedback loop require further investigation, but observations reported in Chapter 3 suggest that it was within 20 days (i.e. comparable to the inter-spring tidal cycle). The presence of phosphomonoesters in both surface and bottom waters at various stations indicates that this newly generated DOP pool is relatively labile and not rapidly remineralised. As the Celtic Sea is predominantly nitrogen limited, the DOM pool would likely have DON:DOP ratios lower than Redfield (Redfield et al., 1963), i.e. the DOM pool is enriched in DOP (Conan et al., 2007). In the Celtic Sea, DOP is an important component of the DOC pool as the molecular composition involves carbon and therefore there is potential for the accumulation of carbon within the DOP pool.

We also addressed whether the Celtic Sea may potentially act as a source of phosphorus to adjacent regions, specifically the North Atlantic where production is considered phosphorus-limited (Mather et al., 2008) and allochthonous DOP may add 'new' phosphorus to the pool. Observations in Chapters 4 and 5 indicate an accumulation of DOP on the shelf and at the shelf edge relative to the adjacent slope and ocean. This DOP was of relatively labile nature but not rapidly remineralised, hence export of DOP is dependent on physical mixing processes and water mass exchange across the shelf edge. On shorter timescales, ocean-shelf water exchange in this region is dominated by wind-driven cross-shelf exchange of surface water, internal tidal mixing at the thermocline, and drainage in the bottom Ekman layer (Huthnance et al. 2009), and on-shelf transport of lenses of shelf edge water along isopycnals within the thermocline layer (Hopkins et al., 2012). Despite there being no evidence of whether the latter exchange process also

acts in an off-shelf direction, but it is physically possible. Seasonal mixing such as deep winter mixing and cascading over the shelf edge provide an important export mechanism for both 'fresh' DOM produced during the summer, and residual DOM produced during previous seasons that escaped winter remineralisation (Carlson et al., 1994; Hopkinson et al., 2005). Therefore, there are a number of physical exchange processes that could potentially transfer DOP produced in the Celtic Sea to the North Atlantic (Fig. 6.1).

Future changes to phosphorus dynamics in the Celtic Sea are difficult to predict. Policy, regulation and changes in land management practice will undoubtedly act to influence riverine fluxes of nutrients to coastal regions. Meanwhile, meteorological events driven by climate change such as storms of increased frequency and intensity, will act to enhance run off and riverine inputs to the coastal ocean. In addition, the influence of storm-driven shelf sea mixing on phosphorus cycling has been observed to some extent in the present study. Meanwhile countering this is the predicted increase in sea surface temperature which may enhance stratification and act to reduce nutrient fluxes vertically across the thermocline and horizontally across the shelf. In order to assess shelf sea phosphorus dynamics more fully further studies would be required. For example, detailed investigations into the composition of the dissolved organic pool, interactions between the sediment and the water column, and cross shelf transfers of phosphorus including within benthic boundary layers. Investigating shelf edge exchanges would be a crucial part of improving our understanding of shelf sea nutrient dynamics. Firstly, with respect to assessing whether the shelf provides a source of organic nutrients during and after summer stratification. And secondly, with respect to the dynamics of winter recharge and oceanic-shelf exchanges during periods when the shelf sea water column is fully mixed. Comparison of these two components of shelf edge exchange would give useful insight as to whether the shelf is a net source or sink of nutrients to the northeast Atlantic. In addition, further investigation and monitoring of terrestrial inputs of inorganic and organic nutrients and fluxes from the coastal and estuarine environment would also be an important step towards understanding shelf sea phosphorus dynamics more fully.

The picture is much clearer on a global scale. Climate change is predicted to increase nitrogen fluxes to the marine environment through enhanced atmospheric deposition (Duce et al., 2008) and enhanced nitrogen fixation as a result of increasing sea surface temperatures and enhanced stratification (Boyd and Doney, 2002). Therefore, the increase in nitrogen in the system will drive the world oceans toward P-limitation. Considering this, there are frighteningly few studies on phosphorus fluxes and cycling in the marine environment (Slomp, 2011).

There are evolving ideas about N:P stoichiometry and how DOP plays an uncertain role. In a review article, Arrigo (2005) discussed how growth strategies of microbes resulted in varying non-Redfield behaviour. Three different growth strategies were identified: a) the survivalist, which required high N:P for resource acquisition machinery; b) the bloomer, which had a low N:P demand due to a high proportion of growth machinery such as RNA; and c) the generalist, which had an N:P of near Redfield. Results from the present study suggest the presence of 'bloomers' at the shelf edge region where surface layer dissolved inorganic N:P ratios were relatively high, and there was evidence of the DOP pool being accessed as a nutrient source by diatoms. Meanwhile, in the surface layer on-shelf N:P ratios were low and hydrolysis of the DOP pool was predominantly via bacterial remineralisation, suggesting 'survivalist' phytoplankton communities. It is important to understand the net effect of phytoplankton community structure and their various nutritional strategies on the magnitude and stoichiometry of nutrients, including organic nutrients, in shelf seas.

This study has revealed that phosphorus accumulates in the dissolved organic phase in the surface waters during periods of enhanced stratification to a background level that appears to be in the order of ~0.2-0.3 μM. When mixing is enhanced, for example when spring tidal currents cause mixing over topography or during wind mixing events, this relatively fresh DOP may be mixed below the thermocline as observed in Chapter 3. Remineralisation of DOP in the Celtic Sea appears to be largely associated with bacteria and small cells and in some instances relatively slow calculated turnover rates (up to 30 days). Therefore, the DOP pool in the

Celtic Sea may represent an important temporary storage mechanism of atmospheric carbon. More information would be required to construct a detailed phosphorus budget to determine the ultimate fate of the DOP pool. Cross-shelf fluxes of the various phosphorus pools at pertinent times of the year, DOP production rates and responsiveness to changes in physical mixing, and characterisation of the DOP pool and how it ages would all give essential detail on internal cycling and therefore the form of phosphorus exported from the shelf.

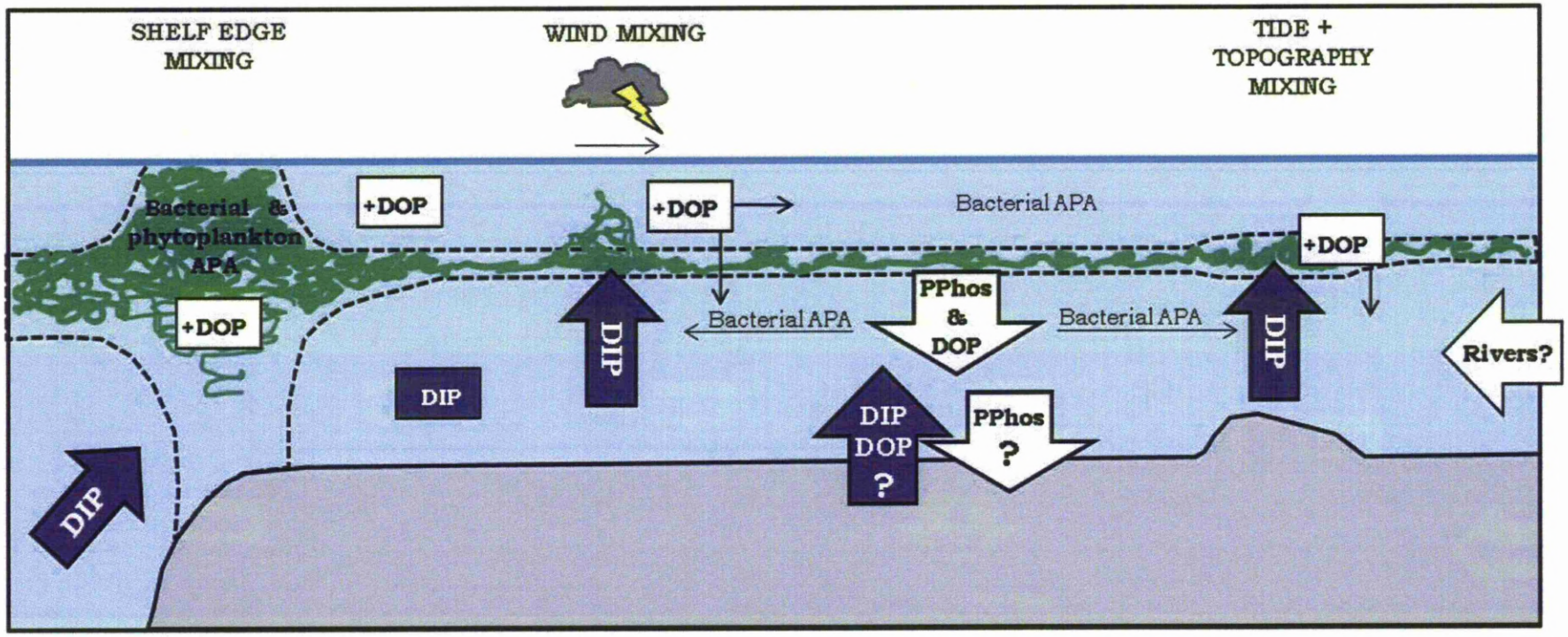

Figure 6.1. Schematic illustrating the physical and meteorological processes controlling water column structure and biological processes within a shelf sea. Shelf edge upwelling of phosphate (DIP) fuels enhanced primary production and net DOP production. Wind mixing and the interaction of tidal currents with topography enhance phosphate fluxes across the thermocline resulting in the development of subsurface chlorophyll maxima (SCM) and net DOP production in the surface layer on the shelf. On-shelf DOP removal processes include bacterial remineralisation and mixing below the thermocline. At the shelf edge DOP is utilised as a nutrient source by diatoms.

7. REFERENCES

References

Abell, J., Emerson, S., and Renaud, P. (2000). Distributions of TOP, TON and TOC in the North Pacific subtropical gyre: implications for nutrient supply in the surface ocean and remineralisation in the upper thermocline. Journal of Marine Research 58, 203-222.

Alvarez-Salgado, X. A., Doval, M. D. and Perez, F. F. (1999). Dissolved organic matter in shelf waters off the Ria de Vigo (NW Iberian upwelling system). Journal of Marine Systems 18 (4), 383-394.

Ammerman, J.W. (1993). Chapter 76: Microbial cycling of inorganic and organic phosphorus in the water column. In Handbook of methods in aquatic microbial ecology.

Amon, R. M. W. and Benner, R. (1996). Bacterial utilization of different size classes of dissolved organic matter. Limnology and Oceanography 41 (1), 41-51.

Armstrong, F.A.J., Williams, P.M., and Strickland, J.D.H. (1966). Photo-oxidation of organic matter in sea water by ultra-violet radiation, analytical and other applications. Nature 211, 481 – 483.

Arrigo, K.R. (2005). Marine microorganisms and global nutrient cycles. Nature 437, 349-355.

Azam, F., Fenchel, T., Field, J. G., Gray, J. S., Meyer-Reil, L. A. and Thingstad, F. (1983). The ecological role of water-column microbes in the sea*. Marine Ecology – Progress Series 10, 257-263.

Behrenfeld MJ, Boss E, Siegal DA, Shea DM (2005). "Carbon-based ocean productivity and phytoplankton physiology from space". Global Biogeochemical Cycles 19 (1): Art No. GB1006.

Benitez-Nelson, C. R. (2000). The biogeochemical cycling of phosphorus in marine systems. Earth-Science Reviews 51 (1-4), 109-135.

Benitez-Nelson, C. R., and Buesseler, K. O. (1999). Variability of inorganic and organic phosphorus turnover in the coastal ocean. Nature 398, 502-505.

Benitez-Nelson, C. R., O'Neill, L., Kolowith, L. C., Pellechia, P., and Thunell, R. (2004). Phosphonates and particulate organic phosphorus cycling in an anoxic marine basin. Limnology and Oceanography 49 (5), 1593-1604.

Benitez-Nelson, C. R., O'Neill Madden, L. P., Styles, R. M., Thunell, R. C., and Astor, Y. (2007). Inorganic and organic sinking particulate phosphorus fluxes across the oxic/anoxic water column of Cariaco Basin, Venezuela. Marine Chemistry 105 (1-2), 90-100. doi:10.1016/j.marchem.2007.01.007

Benner, R. (2003). Molecular Indicators of Bioavailability of Dissolved Organic Matter. In: Aquatic Ecosystems: interactivity of dissolved organic matter (eds Findlay, S., Sinsabaugh, R. L.), pp. 121–135. Academic Press, San Diego.

Benner, R. and Biddanda, B. (1998). Photochemical transformations of surface and deep marine dissolved organic matter: effects on bacterial growth. Limnology and Oceanography 43 (6), 1373-1378.

Bianchi, T. S., Lambert, C. D., Santschi, P. H., and Guo, L. (1997). Sources and transport of land-derived particulate and dissolved organic matter in the Gulf of Mexico (Texas shelf/slope): the use of lignin-phenols and loliolides as biomarkers. Organic Geochemistry 27 (1-2), 65-78.

Björkman, K., Thomson-Bulldis, A. L., Karl, D. M. (2000). Phosphorus dynamics in the North Pacific subtropical gyre. Aquatic Microbial Ecology 22, 185-198.

Björkman, K., Karl, D. M. (2003). Bioavailability of dissolved organic phosphorus in the euphotic zone at Station ALOHA, North Pacific Subtropical Gyre. Limnology and Oceanography 48 (3), 1049-1057.

Boschker, H. T. S., Kromkamp, J. C., and Middelburg, J. J. (2005). Biomarker and carbon isotopic constraints on bacterial and algal community structure and functioning in a turbid, tidal estuary. Limnology and Oceanography 50 (1), 70-80.

Boschker, H. T. S., and Middelburg, J. J. (2002). Stable isotopes and biomarkers in microbial ecology. FEMS Microbiology Ecology 40, 85-95.

Brainard J, Bateman IJ, Lovett AA (2005). The social value of carbon sequestered in Great Britain's woodlands. CSERGE Working Paper EDM 05-03.

Carlson, C. A., Ducklow, H. W., and Michaels, A. F. (1994). Annual flux of dissolved organic carbon from the euphotic zone in the northwestern Sargasso Sea. Nature letters 371, 405-408.

Carlson, C. A. and Ducklow, H. W. (1995). Dissolved organic carbon in the upper ocean of the central equatorial Pacific Ocean, 1992: Daily and finescale vertical variations. Deep-Sea Research II 42 (2-3), 639-656.

Carlson, C. A., Hansell, D. A., Peltzer, E. T., Smith Jr, W. O. (2000). Stocks and dynamics of dissolved and particulate organic matter in the southern Ross Sea, Antarctica. Deep-Sea research II 47, 3201-3225.

Carlson, C. A. (2002) Production and Removal Processes. In: Biogeochemistry of Marine Dissolved Organic Matter (Ed.s Hansell, D. A., and Carlson, C. A.). pp. 91-151.Academic Press, Santa Barbara.

Carlson, C. A., and Ducklow, H. W. (1996). Growth of bacterioplankton and consumption of dissolved organic carbon in the Sargasso Sea. Aquatic Microbial Ecology 10, 69-85.

Cembella, A. D., Antia, N. J., and Harrison, P. J. (1984). The utilization of inorganic and organic phosphorus compounds as nutrients by eukaryotic microalgae: a multidisciplinary perspective: part 2. Critical Reviews in Microbiology 11 (1), 13-81.

Chrost, R. J., Siuda, W., Albrecht, D., and Overbeck, J. (1986). A method for determining enzymatically hydrolysable phosphate (EHP) in natural waters. Limnology and Oceanography 31 (3), 662-667.

Church, M. (2000) Resource control of bacterial dynamics in the sea. Chapter 10 in Advances in microbial ecology of the oceans (Kirchman, Eds). Wiley.

Clark, L. L., Ingall, E. D., and Benner, R. (1998). Marine phosphorus is selectively remineralised. Scientific correspondence in Nature 393, 426.

Conan, P., Sondergaard, M., Kragh, T., Thingstad, F., Puji-Pay, M., Williams, P. J. B., Markager, S., Cauwet, G., Borch, N. H., Evans, D., Riemann, B.

(2007). Partitioning of organic production in marine plankton communities: the effects of inorganic nutrient ratios and community composition on new dissolved organic matter. Limnology and Oceanography 52 (2), 753-765.

Copin-Montegut, G., and Avril, B. (1993). Vertical distribution and temporal variation of dissolved organic carbon in the North-Wester Mediterranean Sea. Deep-Sea Research I 40 (10), 1963-1972.

Cotner, J. B., Ammerman, J. W., Peele, E. R., and Bentzen, E. (1997). Phosphorus-limited bacterioplankton growth in the Sargasso Sea. Aquatic Microbial Ecology 13, 141-149.

Dafner, E. V., Mallin, M. A., Souza, J. J., Wells, H. A., Parsons, D.C. (2007). Nitrogen and phosphorus species in the coastal and shelf waters of Southeastern North Carolina, Mid-Atlantic U.S. Coast. Marine Chemistry 103, 289-303.

Diaz, J., Ingall, E., Benitez-Nelson, C., Paterson, D., de Jonge, M. D., McNulty, I., and Brandes, J. A. (2008). Marine polyphosphate: a key player in geologic phosphorus sequestration. Science 320, 652-655.

Downing, J. A. (1997). Marine nitrogen: phosphorus stoichiometry and the global N:P cycle. Biogeochemistry 37 (3), 237-252.

Ducklow, H. W. (2000). Bacterial production and biomass in the oceans. In: Microbial Ecology of the Oceans (ed. Kirchman, D. L.), pp. 85-120. Wiley-Liss, New York.

Dugdale, R.C., and Goering, J.J. (1967). Uptake of new and regenerated forms of nitrogen in primary productivity. Limnology and Oceanography 12, 196-206.

Duhamel, S., Dyhrman, S. T., and Karl, D. M. (2010). Alkaline phosphatase activity and regulation in the North Pacific Subtropical gyre. Limnology and Oceanography 55 (3), 1414-1425.

Dyhrman, S. T., Ammerman, J. W., and Van Mooy, B. A. S. (2007). Microbes and the marine phosphorus cycle. Oceanography 20 (2), 110-116.

Dyhrman, S. T., Benitez-Nelson, C. R., Orchard, E. D., Haley, S. T., and Pellechia, P. J. (2009). A microbial source of phosphonates in oligotrophic marine systems. Nature Geosciences Letters 2, 696-699.

Dyhrman, S. T., Chappel, P. D., Haley, S. T., Moffet, J. W., Orchard, E. D., Waterbury, J. B., and Webb, E. A. (2006). Phosphonate utilization by the globally important marine diazotroph *Trichodesmium*. Nature 439, 68-71.

Dyhrman, S. T., and Palenik, B. (1999). Phosphate stress in cultures and field populations of the dinoflagellates *Prorocentrum minimum* detected by a single-cell alkaline phosphatase assay. Applied and Environmental Microbiology 65 (7), 3205-3212.

Dyhrman, S. T., and Ruttenberg, K. C. (2006). Presence and regulation of alkaline phosphatase activity in eukaryotic phytoplankton from the coastal ocean: implications for dissolved organic phosphorus remineralisation. Limnology and Oceanography 51 (3), 1381-1390.

Eppley, R.W.; Peterson, B.J. (1979). "Particulate organic matter flux and planktonic new production in the deep ocean". Nature 282 (5740): 677–680. doi:10.1038/282677a0

Espinosa, L. F., Pantoja, S., Pinto, L. A., and Rullkotter, J. (2008). Water column distribution of phospholipid-derived fatty acids of marine microorganisms in the Humboldt Current system off northern Chile. Deep-Sea Research II, doi:10.1016/j.dsr2.2008.09.008.

Falkowski PG, Barber RT, Smetacek V (1998). Biogeochemical controls and feedbacks on ocean primary productivity. *Science* 281, 200-206.

Fankhauser S (1994). Evaluating the social costs of greenhouse gas emissions. CSERGE working paper GEC-94-01.

Fennel, K., and Boss, E. (2003). Subsurface maxima of phytoplankton and chlorophyll: steady-state solutions from a simple model. Limnology and Oceanography 48 (4), 1521-1534.

Froelich, P. N., Bender, M. L., Luedtke, N. A., Heath, G. R., and DeVries, T. (1982). The marine phosphorus cycle. American Journal of Science 282, 474-511.

Gambin, F., Boge, G., and Jamet, D. (1999). Alkaline phosphatase in a littoral Mediterranean marine ecosystem: role of the main plankton size classes. Marine Environmental research 47, 441-456.

Garde, K., and Gustavson, K. (1999). The impact of UV-B radiation on alkaline phosphatase activity in phosphorus-depleted marine ecosystems. Journal of Experimental Marine Biology and Ecology, 238, 93-105.

Gilbert , J. A., Thomas, S., Cooley, N. A., Kulakova, A., Field, D., Booth, T., McGrath, J. W., Quinn, J. P. And Joint, I (2009). Potential for phosphonoacetate utilisation by marine bacteria in temperate coastal waters. Environmental Microbiology 11 (1), 111-125.

Gonzalez-Gill, S., Keafer, B. A., Jovine, R. V. M., Aguilera, A., Lu, S., and Anderson, D. M. (1998). Detection and quantification of alkaline phosphatase in single cells of phosphorus-starved marine phytoplankton. Marine Ecology Progress Series 164, 21-35.

Gowen, R.J., Tett, P., Kennington, K., Mills, D.K., Shammon, T.M., Stewart, B.M., Greenwood, N., Flanagan, C., Devlin, M., Wither, A. (2008). The Irish Sea: is it eutrophic? Estuarine, Coastal and Shelf Science 76 (2), 239-254.

Gruber, N. (2008). Marine nitrogen cycle: overview and challenges *in* Nitrogen in the marine environment, 2nd edition. (Eds. Capone, D.G., Bronk, D.A., Mulholland, M.R., Carpenter, E.J.). Elsevier.

Guildford, S. J., and Hecky, R. E. (2000). Total nitrogen, total phosphorus, and nutrient limitation in lakes and oceans: is there a common relationship? Limnology and Oceanography 45 (6), 1213-1223.

Hickman, A. E., Holligan, P. M., Moore, C. M., Sharples, J., Krivtsov, V., and Palmer, M. R. (2009). Distribution and chromatic adaptation of phytoplankton within a shelf sea thermocline. Limnology and Oceanography 54 (2), 525-536.

Hino, S. (1989). Characterization of orthophosphate release from dissolved organic phosphorus by gel filtration and several hydrolytic enzymes. Hydrobiologia 174, 49-55.

Hobson, L. A., and Lorenzen, C. J. (1972). Relationships of chlorophyll maxima to density structure in the Atlantic Ocean and Gulf of Mexico. Deep-Sea Research 19, 297-306.

Hopkinson, C. S., Fry, B., and Nolin, A. L. (1997). Stoichiometry of dissolved organic matter dynamics on the continental shelf of the northeastern U.S.A. Continental Shelf Research 17 (5), 473-489.

Hopkinson, C. S., and Vallino, J. J. (2005). Efficient export of carbon to the deep ocean through dissolved organic matter. Nature 433, 142-145.

Hoppe, H. G. (2003). Phosphatase activity in the sea. Hydrobiologia 493, 187-200.

Hoppe, H. G., and Ullrich, S. (1999). Profiles of ectoenzymes in the Indian Ocean: phenomena of phosphatase activity in the mesopelagic zone. Aquatic Microbial Ecology 19, 139-148.

Howarth, R. W. (1988). Nutrient limitation of net primary production in marine ecosystems. Annual Review of Ecology and Systematics 19, 89-110.

Hung, J-J, Chen, C. H., Gong, G. C., Sheu, D. D., and Shiah, F. K. (2003). Distributions, stoichiometric patterns and cross-shelf exports of dissolved organic matter in the East China Sea. Deep-Sea Research II 50, 1127-1145.

Huang, B., Ou, L., Wang, X., Huo, W., Li, R., Hong, H., Zhu, M., Qi, Y. (2007). Alkaline phosphatase activity of phytoplankton in East China Sea coastal waters with frequent harmful algal bloom occurrences. Aquatic Microbial Ecology 49, 195-206.

Huang, B., and Hong, H. (1999). Alkaline phosphatase activity and utilization of dissolved organic phosphorus by algae in subtropical coastal waters. Marine Pollution Bulletin 39 (1-12), 205-211.

Huthnance, J.M. (1995). Circulation, exchange and water masses at the ocean margin: the role of physical processes at the shelf edge. Progress In Oceanography, Volume 35 (4), 353-431.

Huthnance, J.M., Coelho, H., Griffiths, C.R., Knight, P.J., Rees, A.P., Sinha, B., Vangriesheim, A., White, M., Chatwin, P.G. (2001). Physical

structures, advection and mixing in the region of Goban spur. Deep Sea Research Part II: Topical Studies in Oceanography, Volume 48 (14-15), 2979-3021.

Hydes, D.J., Kelly-Gerreyn, B.A., Le Gall, A.C., Proctor, R., 1999. Supply of nutrients balanced with the demands of biological production and denitrification in a temperate latitude shelf sea - a treatment of the southern North Sea as an extended estuary. Marine Chemistry 68, 117–131.

Hydes, D.J., LeGall, A.C., Miller, A.E.J., Brockmann, U., Raabe, T., Holley, S., Alvarez- Salgado, X., Antia, A., Balzer, W., Chou, L.,Elskens, M., Helder, W., Joint,I., Orren, M. (2001). Supply and demand of nutrients and dissolved organic matter at and across the NW European shelf break in relation to hydrography and biogeochemical activity. Deep Sea Research II 48, 3023–3047.

Hydes, D. J., Gowen, R. J., Holliday, N. P. et al. (2004) External and internal control of winter concentrations of nutrients (N, P and Si) in north-west European shelf seas. Estuarine Coastal Shelf Sci., 59, 151–161.

Hynes, A. M., Chappell, P. D., Dyhrman, S. T., Doney, S. C., and Webb, E. A. (2009). Cross-basin comparison of phosphorus stress and nitrogen fixation in *Trichodesmium*. Limnology and Oceanography 54 (5), 1438-1448.

Jansson, M., Olsson, H., and Pettersson, K. (1988). Phosphoatases; origin, characteristics and function in lakes. Hydrobiologia 170, 157-175.

Jones, S.E., Jago, C.F., Bale, A.J., Chapman, D., Howland, R.J.M., Jackson, J. (1998). Aggregation and resuspension of suspended particulate matter at a seasonally stratified site in the southern North Sea: physical and biological controls. Continental Shelf Research 18 (11), 1283-1309.

Kaiser, K., and Benner, R. (2009). Biochemical composition and size distribution of organic matter at the Pacific and Atlantic time-series stations. Marine Chemistry 113, 63-77.

Karl, D.M., Dore, J.E., Hebel, D.V., Winn, C.D. (1991). Procedures for particulate carbon, nitrogen, phosphorus and total mass analyses used in the US-JGOFS Hawaii Ocean Timeseries program. In: Hurd DC, Spencer

DW (eds) Marine particles: analysis and characterization. American Geophysical Union, Washington, DC, p 71–77.

Karl, D. M., Beversdorf, L., Bjorkman, K. M., Church, M. J., Martinez, A., and DeLong, E.F. (2008). Aerobic production of methane in the sea. Nature Geosciences 1, 473-478.

Karl, D. M., and Bjorkman, K. M. (2002). Dynamics of DOP. In: Biogeochemistry of Marine Dissolved Organic Matter (Ed.s Hansell, D. A., and Carlson, C. A.). pp. 250-348.Academic Press, Santa Barbara.

Karl, D. M., Bjorkman, K. M., Dore, J. E., Fujieki, L., Hebel, D. V., Houlihan, T., Letelier, R. M., Tupas, L. M. (2001). Ecological nitrogen-to-phosphorus stoichiometry at station ALOHA. Deep-Sea Research II (48), 1529-1566.

Karl, D.M., Tien, G., 1992. MAGIC: a sensitive and precise method for measuring dissolved phosphorus in aquatic environments. Limnology and Oceanography 37, 105–116.

Karl, D. M., and Yanagi, K. (1997). Partial characterization of the dissolved organic phosphorus pool in the oligotrophic North Pacific Ocean. Limnology and Oceanography 42 (6), 1398-1405.

Karner, M., and Herndl, G. J. (1992). Extracellular enzymatic activity and secondary production in free-living and marine-snow-associated bacteria. Marine Biology 113, 341-347.

Kepkay, P. E. (1994). Particle aggregation and the biological reactivity of colloids. Marine Ecology Progress Series 109, 293-304.

Kiorboe, T. (1993). Turbulence, Phytoplankton cell size and the structure of pelagic food webs. Advances in marine biology 29, ISBN 0-12-026129-4. Academic Press Ltd.

Kirchman, D. L., Keil, R. G., Wheeler, P. A. (1990). Carbon limitation of ammonium uptake by heterotrophic bacteria in the subarctic Pacific. Limnology and Oceanography 35, 1267-1278.

Kolowith, L. C., Ingall, E. D., and Benner, R. (2001). Composition and cycling of marine organic phosphorus. Limnology and Oceanography 46 (2), 309-320.

Krishnamurthy, A., Moore, J. K., Mahowald, N., Luo, C., Zender, C. S. (2010). Impacts of atmospheric nutrient inputs on marine biogeochemistry. Journal of Geophysical Research 115, G01006 doi: 10.1029/2009JG001115.

Kustka, A. B., Sanudo-Wilhelmy, A., and Carpenter, E. J. (2003). Iron requirements for dinitrogen- and ammonium-supported growth in cultures of *Trichodesmium* (IMS 101): Comparison with nitrogen fixation rates and iron: carbon ratios of field populations. Limnology and Oceanography 48 (5), 1869-1884.

Joint I., Groom S.B. (2000). Estimation of phytoplankton production from space: current status and future potential of satellite remote sensing. Journal of Experimental Marine Biology and Ecology 250: 233-255.

Joint, I., Wollast, R., Chou, L., Batten, S., Elskens, M., Edwards, E., Hirst, A., Burkill, P., Groom, S., Gibb, S., Miller, A., Hydes, D., Dehairs, F., Antia, A., Barlow, R., Rees, A., Pomroy, A., Brockmann, U., Cummings, D., Lampitt, R., Loijens, M., Mantoura, F., Miller, P., Raabe, T., Alvarez-Salgado, X., Stelfox, C., Woolfenden, J. (2001). Pelagic production at the Celtic Sea shelf break. Deep Sea Research Part II: Topical Studies in Oceanography, Volume 48 (14-15), Pages 3049-3081.

Labry, C., Herbland, A., and Delmas, D. (2002). The role of phosphorus on planktonic productions of the the Gironde plume waters in the Bay of Biscay. Journal of Plankton Research 24 (2), 97-117.

Labry, c., Delmas, D., and Herbland, A. (2005). Phytoplankton and bacterial alkaline phosphatase activities in relation to phosphate and DOP availability within the Gironde plume waters (Bay of Biscay). Journal of Experimental Marine Biology and Ecology 318, 213-225.

Li, W. K. W. (1983). Consideration of errors in estimating kinetic parameters based on Michaelis-Menten formalism in microbial ecology. Limnology and Oceanography 28 (1), 185-190.

Li, B., and Kuang, Y. (2007). Heteroclinic bifurcation in the Michaelis-Menten-type ratio-dependent predator-prey system. Society for Industrial and Applied Mathematics 67 (5), 1453-1464.

Li, H., Veldhuis, M. J. W., and Post, A. F. (1998). Alkaline phosphatase activities among planktonic communities in the northern Red Sea. Marine Ecology Progress Series 173, 107-115.

Liu, W., Linning, K.D., Nakamura, K., Mino, T., Matsuo, T., and Forney, L.J. (2000). Microbial community changes in biological phosphate-removal systems on altering sludge phosphorus content. Microbiology 146, 1099 - 1107.

Lohse, L., Helder, W., Epping, E. H. P., and Balzer, W. (1998). Recycling of organic matter along a shelf-slope transect across the N.W. European continental margin (Goban Spur). Progress in Oceanography 42, 77-110.

Lomas, M. W., Swain, A., Shelton, R., and Ammerman, J. W. (2004). Taxonomic variability of phosphorus stress in Sargasso Sea phytoplankton. Limnology and Oceanography 49 (6), 2303-2310.

Lomas, M. W., Burke, A. L., Lomas, D. A., Bell, D. W., Shen, C., Dyhrman, S. T., Ammerman, J. W. (2010). Sargasso Sea phosphorus biogeochemistry: an important role for dissolved organic phosphorus (DOP). Biogeosciences 7 (2010): 695-710, doi: 10.5194/bg-7-695-2010

Longnecker, K., Lomas, M. W., Van Mooy, B. A. S. (2010). Abundance and diversity of heterotrophic bacterial cells assimilating phosphate in the subtropical North Atlantic Ocean. Environmental Microbioogy 12 (10), 2773-2782.

Lugtenberg, B. (1987). The Pho Regulon in *Escherichia-coli*. In: Phosphate metabolism and cellular regulation in microorganisms; symposium, Concarneau, France (Ed.s Torriani-Gorini, A., et al.) American Society for Microbiology: Washington DC.

Luo, H., Zhang, H., Long, R. A., Benner, R. (2011). Depth distributions of Alkaline phosphatase and phosphonate utilisation genes in the North Pacific Subtropical Gyre. Aquatic Microbial Ecology 62, 61-69.

Mackey, K. R. M., Labiosa, R. G., Calhoun, M., Street, J. H., Post, A. F., and Paytan, A. (2007). Phosphorus availability, phytoplankton community dynamics, and taxon-specific phosphorus status in the Gulf of Aqaba, Red Sea. Limnology and Oceanography 52 (2), 873-885.

Mahaffey, C., Williams, R.G., Wolff, G.A., Anderson, W.T. (2004). Physical supply of nitrogen to phytoplankton in the Atlantic Ocean. Global Biogeochemical Cycles 18, GB1034, doi: 10.1029/ 2003GB002129.

Mari, X., Rochelle-Newall, E., Torreton, J. P., Pringault, O., Jouon, A. (2007). Water residence time: a regulatory factor of the DOM to POM transfer efficiency. Limnology and Oceanography 52 (2), 808-819.

Martin, A.P., Zubkov, M.V., Fasham, M.J., Burkill, P.H., Holland, R.J. (2008). Microbial spatial variability: An example from the Celtic Sea, Progress In Oceanography, Volume 76 (4), Pages 443-465.

Martiny, A. C., Huang, Y., Li, W. (2009). Occurrence of phosphate acquisition genes in *Prochlorococcus* cells from different ocean regions. Environmental Microbiology 11 (6), 1340-1347.

Mather, R. L., Reynolds, S. R., Wolff, G. A., Williams, R. G., Torres-Valdes, S., Woodward, M. S., Landolfi, A., Pan, X., Sanders, R., Achterberg, E. P. (2008). Phosphorus cycling in the North and South Atlantic Ocean subtropical gyres. Nature Geoscience 1, 439-443.

McNeil BI, Matear RJ (2007). Climate change feedbacks on future oceanic acidification. Tellus Series B – chemical and physical meteorology 59 (2): 191-198.

Michaelis, L., and Menten, M. L. (1913). Kinetics of invertase action. Biochemistry 49, 333-369.

Miller LA, Chierica M, Johannessen T, Noji TT, Rey F, Skjelvan I (1999). Seasonal dissolved inorganic carbon variations in the Greenland Sea and implication for atmospheric CO_2 exchange. Deep-sea research part II – topical studies in oceanography 46 (6-7): 1473-1496.

Miller, J. N., Miller, J. C. (2005). Statistics and chemometrics for analytical chemistry. Fifth edition. Pearson Education Ltd, London.

Miller, W. L., and Moran, M. A. (1997). Interaction of photochemical and microbial processes in the degradation of refractory dissolved organic matter from a coastal marine environment. Limnology and Oceanography 42 (6), 1317-1324.

Millero FJ, Sohn ML (1992). Chemical Oceanography. CRC Press Inc. 531 pages.

Misic, C., and Harriague, A. C. (2008). Organic matter recycling in a shallow coastal zone (NW Mediterranean): the influence of local and global climatic forcing on organic matter lability on hydrolytic enzyme activity. Continental Shelf Research 28, 2725-2735.

Monaghan, E. J., and Ruttenberg, K. C. (1999). Dissolved organic phosphorus in the coastal ocean: reassessment of available methods and seasonal phosphorus profiles from the Eel River Shelf. Limnology and Oceanography 44 (7), 1702-1714.

Monbet, P., McKelvie, I. D., Worsfold, P. J. (2009). Dissolved organic phosphorus speciation in the waters of the Tamar estuary (SW England). Geochimica et Cosmochimica Acta 73, 1027-1038.

Moore, L. R., Post, A. F., Rocap, G., Chisholm, S. W. (2002). Utilisation of different nitrogen sources by the marine cyanobacteria *Prochlorococcus* and *Synechococcus*. Limnology and Oceanography 47 (4), 989-996.

Moore, C. M., Sugget, D. J., Hickman, A. E., Kim, Y. N., Tweddle, J. F., Sharples, J., Geider, R. J., Holligan, P. M. (2006). Phytoplankton photoacclimation and photoadaptation in response to environment gradients in a shelf sea. Limnology and Oceanography 51 (2), 936-949.

Moore, C. M., Mills, M. M., Achterberg, E. P., Geider, R. J., LaRoche, J., Lucas, M. I., McDonagh, E. L., Pan, X., Poulton, A. J., Rijkenberg, M. J. A., Suggett, D. J., Ussher, S. J., and Woodward, M. S. (2009). Large-scale distribution of Atlantic nitrogen fixation controlled by iron availability. Nature Geoscience 2, 867-871.

Monbet, P., McKelvie, I. D., Saefumillah, A., and Worsfold, P. J. (2007). A Protocol to Assess the Enzymatic Release of Dissolved Organic Phosphorus Species in Waters under Environmentally Relevant Conditions. Environmental Science & Technology 41 (21), 7479-7485.

Monbet, P., McKelvie, I. D., Worsfold, P. J. (2009). Dissolved organic phosphorus speciation in the waters of the Tamar estuary (SW England). Geochimica et Cosmochimica Acta 73, 1027-1038.

Moran, M. A., Pomeroy, L. R., Sheppard, E. S., Atkinson, L. P., Hodson, R. E. (1991). Distribution of terrestrially derived dissolved organic matter on the southeastern U.S. continental shelf. Limnology and Oceanography 36 (6), 1134-1149.

Moran, M. A., and Zepp, R. G. (1997). Role of photoreaction in the formation of biologically labile compounds from dissolved organic matter. Limnology and Oceanography 42 (6), 1307-1316.

Moutin, T., Karl, D. M., Duhamel, S., Rimmelin, P., Raimbault, P., Van Mooy, B. A. S., and Claustre, H. (2008). Phosphate availability and the ultimate control of new nitrogen input by nitrogen fixation in the tropical Pacific Ocean. Biogeosciences 5, 95-109.

Murphy, J., Riley, J.P. (1962). A modified single solution method for the determination of phosphate in natural waters. Anal. Chim. Acta 27:31-36.

Nagata, T. (2000). Production mechanisms of dissolved organic matter. In: Microbial ecology of the oceans. (Ed. Kirchmann, D.L.). pp. 121-152Wiley Series in Ecological and Applied Microbiology.

Nausch, M. (2000). Experimental evidence for interactions between bacterial peptidase and alkaline phosphatase activity in the Baltic Sea. Aquatic Ecology 34, 331-343.

Nédélec, F., Statham, P.J., Mowlem, M. (2007). Processes influencing dissolved iron distributions below the surface at the Atlantic Ocean–Celtic Sea shelf edge. Marine Chemistry, Volume 104 (3-4), 156-170.

Nicholson, D., Dyhrman, S., Chavez, F., and Paytan, A. (2006). Alkaline phosphatase activity in the phytoplankton communities of Monterey Bay and San Francisco Bay. Limnology and Oceanography 51, 874-883.

Nielsen, T., Kiorboe, T. (1991). Effects of a storm event on the structure of the pelagic food web with special emphasis on planktonic ciliates. Journal of Plankton Research 13 (1), 35-51.

Nowack, B. (2003). Environmental chemistry of phosphonates. Water Research 37, 2533-2546.

Ogawa, H., Amagai, Y., Koike, I., Kaiser, K., and Benner, R. (2001). Production of refractory dissolved organic matter by bacteria. Science 292, 917-920.

Opsahl, S., and Benner, R. (1997). Distribution and cycling of terrigenous dissolved organic matter in the ocean. Nature, 386, 480-482.

Orchard, E.D. (2010). Phosphorus physiology of the marine cyanobacterium *Trichodesmium*. Department of Biology, Woods Hole Oceanographic Institute, Massachusetts Institute of Technology.

Ormaza-Gonzalez, F. I., Statham, P. J. (1996). A comparison of methods for the determination of dissolved and particulate phosphorus in natural waters, Water Research 30 (11), 2739-2747.

Ou, L., Huang, B., Lin, L., Hong, H., Zhang, F., and Chen, Z. (2006). Phosphorus stress of phytoplankton in the Taiwan Strait determined by bulk and single-cell alkaline phosphatase activity assays. Marine Ecology Progress Series 327, 95-106.

Pauly, D., Christensen, V., Guenette, S., Pitcher, T. J., Sumaila, R., Walters, C. J., Watson, R., and Zeller, D. (2002). Towards sustainability in world fisheries. Nature 418, 689-695.

Paytan, A., and McLaughlin, K. (2007). The oceanic phosphorus cycle. Chemical Reviews 107, 563-576.

Paytan, A., Cade-Menum, B. J., McLaughlin, K., and Faul, K. L. (2003). Selective phosphorus regeneration of sinking marine particles: evidence from ^{31}P-NMR. Marine Chemistry 82 (1-2), 55-70.

Pemberton, K., Rees, A. P., Miller, P. I., Raine, R., Joint, I. (2004). The influence of water body characteristics on phytoplankton diversity and production in the Celtic Sea. Continental Shelf Research 24 (17), 2011-2028.

Pettine, M., Patrolecco, L., Manganelli, M., Capri, S., and Farrace, M. G. (1999). Seasonal variations of dissolved organic matter in the northern Adriatic Sea. Marine Chemistry 64, 153-169.

Pingree, R. D., Holligan, P. M., Mardell, G. T., and Head, R.N. (1976). The influence of physical stability on spring, summer and autumn

phytoplankton blooms in the Celtic Sea. Journal of marine biological association UK 56, 845-873.

Pingree, R. D., and Mardell, G. T. (1985). Solitary Internal Waves in the Celtic Sea. Prog. Oceanog. 14, 431-441.

Pomeroy, L. (1974). The ocean's food web, a changing paradigm. Bioscience 24 (9), 499-504.

Probyn, T.A., Michell-Innes, B.A., Searson, S. (1995). Primary productivity and nitrogen uptake in the subsurface chlorophyll maximum on the Eastern Agulhas Bank. Continental Shelf Research 15 (15), 1903-1920.

Redfield, A. C., Ketchum, B. H., and Richards, F. A. (1963). The influence of organicsms on the composition of sea-water. In: The sea (Ed. Hill, M. N.), pp. 26-77. Wiley.

Rees, A. P., Joint, I., and Donald, K. M. (1999). Early spring bloom phytoplankton-nutrient dynamics at the Celtic Sea Shelf Edge. Deep-Sea Research I 46, 483-510.

Rees, A. P., Hope, S. B., Widdicombe, C. E., Dixon, J. L., Woodward, E. M. S., and Fitzimons, M. F. (2009) Alkaline phosphatase activity in the western English Channel: Elevations induced by high summertime rainfall. Estuarine, Coastal and Shelf Science 81, 569-574.

Ridal, J. J., Moore, R. M. (1992). Dissolved organic phosphorus concentrations in the northeast subarctic Pacific Ocean. Notes in Limnology and Oceanography 37 (5), 1067-1075.

Rippeth, T. (2005). Mixing in the seasonally stratified shelf seas: a shifting paradigm. Philosophical Transactions of the Royal Society 363, 2837-2854.

Rippeth, T. P., Palmer, M. R., Tweddle, J. F., Sharples, J., Inall, M., Holligan, P. M., Moore, M., and Simpson, J. H. (2007). Diapycnal nutrient fluxes in seasonally stratified shelf seas. Geophysical research abstracts, vol. 9, 01807. SRef-ID: 1607-7962/gra/EGU2007-A-01807.

Rippeth, T., Wiles, P., Palmer, M. R., Sharples, J., and Tweddle, J. (2009). The diapycnal nutrient flux and shear-induced diapycnal mixing in the

seasonally stratified western Irish Sea. Continental Shelf Research 29, 1580-1587.

Rivkin, R. B., and Swift, E. (1979). Diel and vertical patterns of alkaline phosphatase activity in the oceanic dinoflagellate *Pyrocystis noctiluca*. Limnology and Oceanography 24, 107-116.

Rivkin, R. B., and Swift, E. (1980). Characterization of alkaline phosphatase and organic phosphorus utilization in the ocenic dinoflagellate *Pyrocystis noctiluca*. Marine Biology 61, 1-8.

Rontani, J. F., Zabeti, N., and Wakeham, S. G. (2009). The fate of marine lipids: biotic vs. Abiotic degradation of particulate sterols and alkenones in the Northwestern Mediterranean Sea. Marine Chemistry 113, 9-18.

Rose, C., and Axler, R. P. (1998). Uses of alkaline phosphatase activity in evaluating phytoplankton community phosphorus deficiency. Hydrobiologia 361, 145-156.

Ross, O. N., and Sharples, J. (2007). Phytoplankton motility and the competition for nutrient in the thermocline. Marine Ecology Progress Series 347, 21-38.

Rueter, J.G. (1986). Alkaline phosphatase inhibition by copper: implications to phosphorus nutrition and use as a biochemical marker of toxicity. Limnology and Oceanography 28, 743-748.

Ruttenberg, K. C., and Dyhrman, S. T. (2005). Temporal and spatial variability of dissolved organic and inorganic phosphorus, and metrics of phosphorus bioavailability in an upwelling-dominated coastal system. Journal of Geophysical Research 110, C10S13, doi:10.1029/2004JC002837.

Sarmiento, J.L., Gruber, N. (2006). Chapter 5: Export and Remineralisation *in* Ocean Biogeochemical Dynamics. Princeton University Press.

Scrope-Howe, S., and Jones, D. A. (1986). The vertical distribution of zooplankton in the Western Irish Sea. Estuarine, Coastal and Shelf Science 22, 785-802.

Sebastian, M., and Neill, F. X. (2004). Alkaline phosphatase activity in marine oligotrophic environments: implications of single-substrate

addition assays for potential activity estimates. Marine Ecology Progress Series 277, 285-290.

Sebastian, M., Aristegui, J., Montero, M. F., Escanez, J., Niell, F. X. (2004). Alkaline phosphatase activity and its relationship to inorganic phosphorus in the transition zone of the North-wester African upwelling system. Progress in Oceanography 62, 131-150.

Shaked, Y., Xu, Y., Leblanc, K., Morel, F. M. M. (2006). Zinc availability and alkaline phosphatase activity in *Emiliania huxleyi*: implications for Zn-P co-limitation in the ocean. Limnology and Oceanography 51 (1), 299-309.

Sharples, J. (2008). Potential impacts of the spring-neap tidal cycle on shelf seas primary production. Journal of Plankton Research 30, 183-197.

Sharples, J., Moore, C. M. and Abraham, E. R. (2001). Internal tide dissipation, mixing, and vertical nitrate flux at the shelf edge of NE New Zealand. Journal of Geophysical Research 106, 14069-14081.

Sharples, J., Moore, C. M., Rippeth, T. P., Holligan, P. M., Hydes, D. J., Fisher, N. R., and Simpson, J. H. (2001). Phytoplankton distribution and survival in the thermocline. Limnology and Oceanography 46 (3), 486-496.

Sharples, J., Tweddle, J. F., Green, J. A. M., Palmer, M. R., Kim, N-Y, Hickman, A. E., Holligan, P. M., Moore, C. M., Rippeth, T. P., Simpson, J. H., and Krivtsov, V. (2007). Spring–neap modulation of internal tide mixing and vertical nitrate fluxes at a shelf edge in summer. Limnology Oceanography, 52(5), 2007, 1735–1747.

Sharples, J., and Tett, P. (1994). Modelling the effect of physical variability on the midwater chlorophyll maximum. Journal of Marine Research 52, 219-238.

Shiah, F. K., Liu, K. K., Kao, S. J., Gong, G. C. (2000). The coupling of bacterial production and hydrography in the southeastern East China Sea: Spatial patterns in spring and fall. Continental Shelf Research 20 (4-5), 459-477.

Shum, K. T., and Sundby, B. (1996). Organic matter processing in continental shelf sediments – the subtidal pump revisited. Marine Chemistry 53, 81-87.

Simpson, J.H., Crawford, W.R., Rippeth, T.P., Campbell, A.R., and Choak J.V.S. (1996). Vertical Structure of turbulent dissipation in shelf seas. Journal of Physical Oceanography, 26(8), 1580-1590.

Simpson, J., Sharples, J. (2012). Introduction to the physical and biological oceanography of shelf seas. 424 pages. Cambridge University Press.

Smith,W.H.F., Sandwell, D.T., 1997. Global seafloor topography from satellite altimetry and ship soundings. Science 277, 1956–1962.

Smith, R. E. H., Harrison, W.G., and Harris, L. (1985). Phosphorus exchange in marine microplankton communities near Hawaii. Marine Biology 86, 75-84.

Smyth T., Tilstone G.H., Groom S.B. (2005). Integration of radiative transfer into satellite models of ocean primary production. Journal of Geophysical Research 110: C10014.

Steinberg, D.K., Goldthwait, S.A., Hansell, D.A. (2002). Zooplankton vertical migration and the active transport of dissolved organic and inorganic nitrogen in the Sargasso Sea. Deep-Sea Res I 49,1445–1461.

Strickland, J. D., and Parsons, T. R. (1972). A practical handbook of seawater analysis. Second edition. Bulletin of the Fisheries Research Board of Canada 167.

Strickland, J.D.H., and Solorzano, L.(1966). Determination of monoesterase hydrolysable phosphate and phosphomonoesterase activity in sea water. In: Some Contemporary Studies in Marine Science (Ed. Barnes, H.), pp 665-674. G. Allen and Unwin, London.

Suttle, C. A., Fuhrman, J. A., Capone, D. G. (1990). Rapid ammonium recycling and concentration-dependent partitioning of ammonium and phosphate: implications for carbon transfer in planktonic communities. Limnology and Oceanography 35 (2), 424-433.

Suzumura, M. (2005). Phospholipids in marine environments: a review. Talanta 66, 422-434.

Suzumura, M., Ishikawa, K., and Ogawa, H. (1998). Characterization of dissolved organic phosphorus in coastal seawater using ultrafiltration and

phosphohydrolytic enzymes. Limnology and Oceanography 43 (7), 1553-1564.

Taft, J. L., Loftus, M. E., and Taylor, W. R. (1977). Phosphate uptake from phosphomonoesters by phytoplankton in the Chesapeake Bay. Limnology and Oceanography 22 (6), 1012-1021.

Tambi, H., Flaten, G. A. F., Egge, J. K., Bodtker, G., Jacobsen, A., and Thingstad, T.F. (2009). Relationship between phosphate affinities and cell size and shape in various bacteria and phytoplankton. Aquatic Microbial Ecology 57, 311-320.

Tanaka, T., Rassoulzadegan, F., Thingstad, T. F. (2005) Analysing the trophic link between the mesopelagic microbial loop and zooplankton from observed depth profiles of bacteria and protozoa. Biogeosciences 2 (1), 9-13.

Taylor, G. T., Thunell, R., Varela, R., Benitez-Nelson, C., and Scranton, M. I. (2009). Hydrolytic ectoenzyme activity associated with suspended and sinking organic particles within the anoxic Cariaco Basin. Deep-Sea Research I, doi:10.1016/j.dsr.2009.02.006.

Thingstad, T. F., Zweifel, U. L., and Rassoulzadegan, F. (1998). P limitation of heterotrophic bacteria and phytoplankton in the northwest Mediterranean. Limnology and Oceanography 43 (1), 88-94.

Thomas, H., Bozec, Y., Elkalay, K., de Baar, H. J. W. (2004). Enhanced open ocean storage of CO_2 from shelf sea pumping. Science 304, 1005-1008.

Thomson-Bulldis, A. and Karl, D. (1998). Application of a Novel Method for Phosphorus Determinations in the Oligotrophic North Pacific Ocean. Limnology and Oceanography , Vol. 43 (7), pp. 1565-1577

Torres-Valdes, S., Roussenov, V.M., Sanders, R., Reynolds, S., Pan, X., Mather, R., Landolfi, A., Wolff, G.A., Achterberg, E.P., and Williams, R.G. (2009). Distribution of dissolved organic nutrients and their effect on export production over the Atlantic Ocean. Global Biogeochemical Cycles, vol. 23, SRef-ID: 1607-7962/gra/EGU2007-A-01807.

Townsend, D. W., Cucci, T. L., and Berman, T. (1984). Subsurface chlorophyll maxima and vertical distribution of zooplankton in the Gulf of Maine. Journal of Plankton Research 6 (5), 793-802.

Tweddle, J.F. (2007). Nutrient fluxes into the seasonal thermocline of the Celtic Sea. PhD thesis, University of Southampton, School of Ocean and Earth Sciences. 249 pages.

Tyrrell, T. (1999). The relative influence of nitrogen and phosphorus on oceanic primary production. Nature 400, 525-531.

Vidal, M., Duarte, C. M., Agusti, S.(1999). Dissolved organic nitrogen and phosphorus pools and fluxes in the central Atlantic Ocean. Limnology and Oceanography 44 (1), 106-115.

Vidal, M., Duarte, C. M., Agusti, S., Gasol, J. M., and Vaque, D. (2003). Alkaline phosphatase activities in the central Atlantic Ocean indicate large areas with phosphorus deficiency. Marine Ecology Progress Series 262, 43-53.

Weber, T. S., Deutsch, C. (2010). Ocean nutrient ratios governed by plankton biogeography. Nature 467, 550-553.

Xu, J., Yin, K., He, L., Yuan, X., Ho, A. Y.T., and Harrison, P. J. (2008). Phosphorus limitation in the northern South China Sea during late summer: Influence of the Pearl River. Deep-Sea Research II 55, 1330-1342.

Yin, K. D., Harrison, P. J., Pond, S. et al. (1995) Entrainment of nitrate in the Fraser River Estuary and its biological implications, 3: effects of winds. Estuarine Coastal Shelf Science, 40, 545–558.

Yoshimura, T., Nishioka, J., Saito, H., Takeda, S., Tsuda, A., and Wells, M. L. (2007). Distributions of particulate and dissolved organic and inorganic phosphorus in North Pacific surface waters. Marine Chemistry 103 (1-2), 112-121.

Zweifel, U. L., Wikner, J., Hagstrom, A., Lundberg, E., and Norrman, B. (1995). Dynamics of dissolved organic carbon in a coastal ecosystem. Limnology and Oceanography 40 (2), 299-305.